Appendix C

EXAMPLES, PROBLEMS AND EXERCISES

We hope the examples presented in this appendix will provide some pedagogical illustrations and applications of the "qualitative" theory developed in this book. The range of instances varies from phenomenological problems to applications. Since very few nonlinear systems can be analyzed without computers, we will perform numerical computations where necessary. At some points, our *de facto* presentation will bear a descriptive character, avoiding technical details of computations. The two packages which have been used in the preparation of this appendix are Content [182] and Dstool [164].

C.1 Qualitative integration

C.1.#1. Classify the trajectories shown in Figs. 1.3.1, 1.3.2 and C.1.1 in the following terms: non-wandering, Poisson-stable, periodic, and homoclinic. What are the corresponding α- and ω-limit sets of these trajectories? □

C.1.#2. For different parameter values of a, construct the phase portraits for the following planar systems

(a) $$\dot r = r(a - r^2), \quad \dot\varphi = 1\,;$$

(b) $$\begin{cases} \dot y = x - (y^2-1)\left(\dfrac{x^2}{2} - y + \dfrac{y^3}{3} - \dfrac{2}{3}\right), \\ \dot x = 1 - y^2 - x\left(\dfrac{x^2}{2} - y + \dfrac{y^3}{3} - \dfrac{2}{3}\right); \end{cases}$$

(c) $$\dot x = y, \quad \dot y = 1 - ax^2 + y(x-2)\,;$$

(d) the van der Pol equation:

$$\ddot{x} + a(x^2 - 1)\dot{x} + x = 0\,;$$

(e) the Duffing equation:

$$\ddot{x} + a\dot{x} + x - x^3 = 0;$$

(f) the Bogdanov-Takens normal form:

$$\dot{x} = y, \quad \dot{y} = -x + ay + x^2\,;$$

(g) the Khorozov-Takens normal form:

$$\dot{x} = y, \quad \dot{y} = -x + ay + x^3\,. \qquad \square$$

C.1.#3. Discuss the phase portraits of the cells shown in Fig. C.1.1. What are the special trajectories here? $\square$

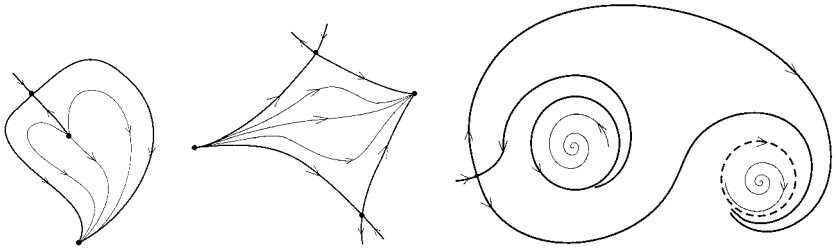

(a) (b) (c)

Fig. C.1.1. Examples of cells.

C.2 Rough equilibrium states and stability boundaries

C.2.1 *Routh-Hurwitz criterion*

Here we will formulate the rule that allows one to determine the structural stability of an equilibrium state and its topological type without solving explicitly the characteristic equation.

The problem in question is how many roots of the characteristic equation

$$\Xi(\lambda) = a_0\lambda^n + a_1\lambda^{n-1} + \cdots + a_n$$

lie to the left or to the right of the imaginary axis and how many roots lie on that axis. The number of zero roots is determined easily: there are s zero roots if and only if $a_n = \cdots = a_{n-s+1} = 0$ and $a_{n-s} \neq 0$. So, if we have a zero root of algebraic multiplicity s, we can just divide the characteristic equation by λ^s and proceed to the case where the last coefficient of the characteristic equation is non-zero, as we will assume to be the case. The next step is to compose the following Routh-Hurwitz matrix:

$$\begin{pmatrix} a_0; & a_2; & a_4; & \cdots \\ a_1; & a_3; & a_5; & \cdots \\ \dfrac{a_1a_2 - a_0a_3}{a_1}; & \dfrac{a_1a_4 - a_0a_5}{a_1}; & \cdots & \cdots \\ \dfrac{\dfrac{a_1a_2 - a_0a_3}{a_1}a_3 - \dfrac{a_1a_4 - a_0a_5}{a_1}a_1}{\dfrac{a_1a_2 - a_0a_3}{a_1}}; & \cdots & \cdots & \cdots \\ & \cdots & \cdots & \cdots \end{pmatrix} \tag{C.2.1}$$

Let us describe the algorithm for constructing the above matrix in detail. The entries of the first two rows are the coefficients of $\Xi(\lambda)$ with even and odd subscripts, respectively. The k-th row is built as follows: the entry r_{kj} at the j-th column is equal to the fraction

$$r_{kj} = \frac{r_{k-1,1}r_{k-2,j+1} - r_{k-2,1}r_{k-1,j+1}}{r_{k-1,1}}$$

whose numerator is taken with opposite sign of the determinant of the (2×2)-matrix at the intersection of the two previous rows with the first column and the $(j+1)$-th column, whereas the denominator is the entry located in the first column of the previous row. The algorithm is subsequently applied until the overall number of the rows in the matrix becomes equal to $(n + 1)$.

Such a construction for the matrix becomes possible only if all entries of the first column do not vanish. This is the *regular* case. Here, the number of the roots of $\Xi(\lambda)$ (including multiplicity) with positive real parts, is equal to the number q of sign changes of the entries in the first column. The polynomial $\Xi(\lambda)$ has no purely imaginary roots in the regular case. Therefore, the corresponding equilibrium state O is structurally stable in the regular case, and its topological type is given by $(n - q, q)$.

One can verify that the first column in (C.2.1) can be expressed through the main minors Δ_i of the Routh-Hurwitz matrix (2.1.10) as follows

$$a_0, \quad \Delta_1, \quad \frac{\Delta_2}{\Delta_1}, \quad \frac{\Delta_3}{\Delta_2}, \ldots, \frac{\Delta_n}{\Delta_{n-1}}\,.$$

In particular, if $a_0 > 0$ and $\Delta_i > 0$ $(i = 1, 2, \ldots, n)$, then the Routh-Hurwitz conditions hold (see Sec. 2.1).

While constructing the matrix (C.2.1) it may turn out that some entry $r_{m+1,1}$ $(1 \le m \le n)$ of the first column vanishes. In this *irregular* case one should find the first non-zero entry $r_{m+1,k+1}$ in the $(m+1)$-th row, as well as the last non-zero entries $r_{m,p}$ and $r_{m+1,s}$ in the m-th and $(m+1)$-th rows, respectively. Compute the deficiency number S_{m+1} by the following rule:

$$S_{m+1} = \begin{cases} k & \text{if } k \le s-p \\ s-p & \text{if } k > s-p \text{ and } (-1)^{s-p} r_{m,p} r_{m+1,s} < 0 \\ s-p+1 & \text{if } k > s-p \text{ and } (-1)^{s-p} r_{m,p} r_{m+1,s} > 0\,. \end{cases}$$

Then, shift the $(m+1)$-th row to the left over k positions, so that the element $r_{m+1,k+1}$ becomes the first one in the line, and multiply all other entries of this row through by $(-1)^k$. Since the first entry is now non-zero, one proceeds as in the regular case. Eventually, the number of roots of $\Xi(\lambda)$ with positive real parts will be equal to the number of sign changes in the first column added to the sum of deficiency numbers over all irregular rows.

There still remains a special case where for some m the entire $(m+1)$-th row of the matrix consists of zeros, i.e. $r_{m+1,j} = 0$ at all j. This is the only situation when pure imaginary roots are possible. If this case is encountered, we should replace the $(m+1)$-th row by a row consisting of the following numbers

$$(p-1)\, r_{m,1}; \quad (p-2)\, r_{m,2}; \quad (p-3)\, r_{m,3}; \quad \cdots\,,$$

where p is the number of the last non-zero entry in the m-th row, and proceed as before. Upon completing the construction (there may be other vanishing rows that should be replaced too) we count the number of sign changes in the first column plus the sum of deficiency numbers (if some irregular rows have appeared). The result equals the number of roots with positive real parts. The number of purely imaginary roots here is equal to $2(p-1-l)$, where p is the ordinal number of the last non-zero entry in the row which precedes the first

vanishing one, and l is the number of sign changes in the first column plus the sum of deficiency numbers computed after this row. The corresponding equilibrium state will be structurally stable only if $p = l + 1$.

C.2.#4. Determine the stability and the topological type of an equilibrium state whose characteristic equation is given below:

$$\Xi(\lambda) = \lambda^4 + 2\lambda^3 + \lambda^2 - 8\lambda - 20 = 0\,.$$

Solution. The corresponding Rough-Hurwitz matrix is given by

$$\begin{array}{rrl} 1 & 1 & -20 \\ 2 & -8 & \\ 5 & -20 & (p=2) \\ 5 & & (\text{zero entry replaced by } (p-1)r_{m,1}=5) \\ -20 & & \end{array}$$

Here there is one sign change in the first column, i.e. $\Xi(\xi)$ has one root in the right open half-plane. Let us count the number of purely imaginary roots: $2(p-1-l) = 2(2-1-1) = 0$. Thus, the equilibrium state O is structurally stable, and its topological type is saddle (3,1). □

C.2.2 *3D case*

Consider a three-dimensional system

$$\begin{aligned} \dot{y}_1 &= a_1^{(1)} y_1 + a_2^{(1)} y_2 + a_3^{(1)} y_3 + P_1(y_1, y_2, y_3), \\ \dot{y}_2 &= a_1^{(2)} y_1 + a_2^{(2)} y_2 + a_3^{(2)} y_3 + P_2(y_1, y_2, y_3), \\ \dot{y}_3 &= a_1^{(3)} y_1 + a_2^{(3)} y_2 + a_3^{(3)} y_3 + P_3(y_1, y_2, y_3)\,. \end{aligned} \tag{C.2.2}$$

Here, the functions P_i contain no linear terms. The characteristic equation of the system (C.2.2) is given by

$$\Xi(\lambda) = \begin{vmatrix} a_1^{(1)} - \lambda & a_2^{(1)} & a_3^{(1)} \\ a_1^{(2)} & a_2^{(2)} - \lambda & a_3^{(2)} \\ a_1^{(3)} & a_2^{(3)} & a_3^{(3)} - \lambda \end{vmatrix} = 0\,. \tag{C.2.3}$$

Equation (C.2.3) can be rewritten in the form of a cubic polynomial:

$$\lambda^3 + p\lambda^2 + q\lambda + r = 0\,, \tag{C.2.4}$$

where

$$
\begin{aligned}
p &= -(a_1^{(1)} + a_2^{(2)} + a_3^{(3)})\,, \\
q &= \begin{vmatrix} a_1^{(1)} & a_2^{(1)} \\ a_1^{(2)} & a_2^{(2)} \end{vmatrix} + \begin{vmatrix} a_1^{(1)} & a_3^{(1)} \\ a_1^{(3)} & a_3^{(3)} \end{vmatrix} + \begin{vmatrix} a_2^{(2)} & a_3^{(2)} \\ a_2^{(3)} & a_3^{(3)} \end{vmatrix}\,, \\
r &= -\begin{vmatrix} a_1^{(1)} & a_2^{(1)} & a_3^{(1)} \\ a_1^{(2)} & a_2^{(2)} & a_3^{(2)} \\ a_1^{(3)} & a_2^{(3)} & a_3^{(3)} \end{vmatrix}\,.
\end{aligned}
\tag{C.2.5}
$$

Here, the Routh-Hurwitz stability condition reduces to the following relation:

$$
p > 0, \quad q > 0, \quad r > 0, \quad \text{and} \quad R \equiv pq - r > 0\,. \tag{C.2.6}
$$

The boundaries of the stability region are two surfaces given by ($r = 0$, $p > 0, q > 0$) and ($R = 0, p > 0, q > 0$). The characteristic equation has at least one zero root on the surface $r = 0$, and a pair of purely imaginary roots on the surface ($R = 0, q > 0$).

C.2.#5. Show that the characteristic exponents of the equilibrium state on the bifurcation surface $R = 0$ are $(-p,\, i\sqrt{q}, -i\sqrt{q})$. □

The number of real roots of Eq. (C.2.4) depends on the sign of the discriminant of the cubic equation:

$$
\Delta = -p^2q^2 + 4p^3r + 4q^3 - 18pqr + 27r^2\,. \tag{C.2.7}
$$

(1) If $\Delta > O$, the cubic equation has one real root and two complex-conjugate ones;
(2) If $\Delta < O$, the cubic equation has three distinct real roots;
(3) When $\Delta = 0$, the equation has one real root of multiplicity 3 if $q = \frac{1}{3}p^2$ and $r = \frac{1}{27}p^3$, or two real roots (one of multiplicity 2).

The equation $\Delta = 0$ can be resolved as follows:

$$
r = \frac{1}{3}pq - \frac{2}{27}p^3 \pm \frac{2}{27}(p^2 - 3q)^{3/2}, \qquad q \le \frac{p^2}{3}\,.
$$

Hence, the characteristic equation has all the three roots real if and only if

$$
q \le \frac{p^2}{3} \quad \text{and} \quad r^-(p,q) \le r \le r^+(p,q)\,, \tag{C.2.8}
$$

where we denote

$$r^{\pm} = \frac{1}{3}pq - \frac{2}{27}p^3 \pm \frac{2}{27}(p^2 - 3q)^{3/2}\,.$$

When the equilibrium state is topologically saddle, condition (C.2.8) distinguishes between the cases of a simple saddle and a saddle-focus. However, when the equilibrium is stable or completely unstable, the presence of complex characteristic roots does not necessarily imply that it is a focus. Indeed, if the nearest to the imaginary axis (i.e. the leading) characteristic root is real, the stable (or completely unstable) equilibrium state is a node independently of what other characteristic roots are.

The boundary between real and complex leading characteristic roots is formed by a part of the surface $\Delta = 0$ which corresponds to the double roots and by the surface

$$r = \frac{p}{3}\left(q - \frac{2p^2}{9}\right), \qquad q \geq \frac{p^2}{3}\,, \tag{C.2.9}$$

which joins the surface $\Delta = 0$ along the line of triple roots. This surface corresponds to the existence of a pair of complex-conjugate roots whose real part is equal to the third root. When we cross this surface towards decreasing $|r|$ this pair is moved farther from the imaginary axis than the real root, so the equilibrium state becomes a node. To the other side of this surface the complex-conjugate pair becomes closer to the imaginary axis than the real root, so that the equilibrium state becomes a focus.

When studying homoclinic bifurcations, an important characteristic of saddle equilibria is the sign of the *saddle value* σ defined as the sum of the real parts of the two leading characteristic exponents nearest to the imaginary axis from the left and from the right.

In the case of a saddle, when both leading exponents $\lambda_{1,2}$ are real, the condition $\sigma = 0$ is a resonance relation $\lambda_1 + \lambda_2 = 0$. In terms of the coefficients of the cubic characteristic equation, this condition recasts as

$$R \equiv pq - r = 0, \qquad -p^2 < q < 0\,. \tag{C.2.10}$$

Observe that when $q > 0$, the surface $R = 0$, corresponds to the Andronov-Hopf bifurcation, whereas the part of the surface where $q < -p^2$, corresponds to the vanishing of the sum of one leading exponent and a non-leading one of opposite sign.

In the case of a saddle-focus of a three-dimensional system the condition $\sigma = 0$ reads as $\lambda_1 + \mathrm{Re}\lambda_2 = 0$ where λ_1 is a real root and $\lambda_{2,3}$ are the pair of complex-conjugate roots. This can be written as

$$r = -p(q + 2p^2), \qquad -p^2 < q\,. \tag{C.2.11}$$

When crossing this surface towards increasing r, the saddle value becomes positive.

Another important characteristic of saddle equilibria of three-dimensional systems is the *divergence* of the vector field at the equilibrium state. It is equal to the sum of the characteristic roots, i.e. to $-p$.

Summarizing, we can classify the rough equilibrium states in $\mathbb{R}^3$ as follows:

(1) The case $p > 0$ (div < 0) (See Table C.1).
(2) The case $p < 0$ (div > 0) (See Table C.2).
(3) The case $p = 0$ (div $= 0$) (See Table C.3).

C.2.#6. Draw the corresponding bifurcation diagrams on the (q, r)-plane with fixed p. □

Let us consider next a few examples. We will focus our consideration on the Lorenz equation, the Chua's circuit, the Shimizu-Morioka model and some others.

The Chua's circuit [179] is given by

$$\begin{aligned} \dot{x} &= a(y - f(x))\,, \\ \dot{y} &= x - y + z\,, \\ \dot{z} &= -by\,, \end{aligned} \tag{C.2.12}$$

with cubic nonlinearity $f(x) = -x/6 + x^3/6$. Here, a and b are some positive parameters. System (C.2.12) is invariant under the transformation $(x, y, z) \leftrightarrow (-x, -y, -z)$.

Let us find the equilibrium states in (C.2.12) by solving the following system:

$$\begin{aligned} 0 &= a(y + x/6 - x^3/6), \\ 0 &= x - y + z, \\ 0 &= -by\,. \end{aligned}$$

Table C.1

Parameter regions	Types of equilibria	σ	Eigenvalues $\lambda_i,\ i=1,2,3$
$0 < r < \begin{cases} r^+(p,q) & \text{for } 0 < q \le \dfrac{p^2}{3} \\ \dfrac{p}{3}\left(q - \dfrac{2p^2}{9}\right) & \text{for } q \ge \dfrac{p^2}{3} \end{cases}$	Stable node $\dim W^s = 3$ $\dim W^u = 0$	—	$0 > \lambda_1 > \mathrm{Re}\lambda_i$ $(i = 2, 3)$
$pq > r > \begin{cases} r^+(p,q) & \text{for } 0 < q \le \dfrac{p^2}{3} \\ \dfrac{p}{3}\left(q - \dfrac{2p^2}{9}\right) & \text{for } q \ge \dfrac{p^2}{3} \end{cases}$	Stable focus $\dim W^s = 3$ $\dim W^u = 0$	—	$0 > \mathrm{Re}\lambda_{1,2} > \lambda_3$
$r > \begin{cases} r^+(p,q) & \text{for } q \le 0 \\ pq & \text{for } q \ge 0 \end{cases}$	Saddle-focus (1,2)	$\sigma < 0$	$\mathrm{Re}\lambda_{2,3} > 0 > \lambda_1$
$0 < r < r^+(p,q),\ q < 0$	Saddle $\dim W^s = 1$ $\dim W^u = 2$	$\sigma < 0$	$\lambda_1 < 0 < \lambda_2 < \lambda_3$
$0 > r > \begin{cases} r^-(p,q) & \text{for } q \le -p^2 \\ pq & \text{for } -p^2 \le q < 0 \end{cases}$	Saddle $\dim W^s = 2$ $\dim W^u = 1$	$\sigma > 0$	$\lambda_1 > 0 > \lambda_2 > \lambda_3$
$r^-(p,q) < r < \begin{cases} pq & \text{for } -p^2 < q \le 0 \\ 0 & \text{for } 0 \le q < \dfrac{p^2}{4} \end{cases}$	Saddle $\dim W^s = 2$ $\dim W^u = 1$	$\sigma < 0$	$\lambda_1 > 0 > \lambda_2 > \lambda_3$
$-p(q+2p^2) < r < \begin{cases} r^-(p,q) & \text{for } -p^2 < q \le \dfrac{p^2}{4} \\ 0 & \text{for } q \ge \dfrac{p^2}{4} \end{cases}$	Saddle-focus (2,1)	$\sigma < 0$	$\lambda_1 > 0 > \mathrm{Re}\lambda_{2,3}$
$r < \begin{cases} r^-(p,q) & \text{for } q \le -p^2 \\ -p(q+2p^2) & \text{for } q \ge -p^2 \end{cases}$	Saddle-focus (2,1)	$\sigma > 0$	$\lambda_1 > 0 > \mathrm{Re}\lambda_{2,3}$

Table C.2

Parameter regions	Types of equilibria	σ	Eigenvalues $\lambda_i,\ i=1,2,3$
$0 > r > \begin{cases} r^-(p,q) & \text{for } 0 < q \le \dfrac{p^2}{3} \\ \dfrac{p}{3}\left(q - \dfrac{2p^2}{9}\right) & \text{for } q \ge \dfrac{p^2}{3} \end{cases}$	Repelling node $\dim W^s = 0$ $\dim W^u = 3$	—	$0 < \lambda_1 < \mathrm{Re}\lambda_i$ $(i = 2, 3)$
$pq < r < \begin{cases} r^-(p,q) & \text{for } 0 < q \le \dfrac{p^2}{3} \\ \dfrac{p}{3}\left(q - \dfrac{2p^2}{9}\right) & \text{for } q \ge \dfrac{p^2}{3} \end{cases}$	Repelling focus $\dim W^s = 0$ $\dim W^u = 3$	—	$0 < \mathrm{Re}\lambda_{1,2} < \lambda_3$
$r < \begin{cases} r^-(p,q) & \text{for } q \le 0 \\ pq & \text{for } q \ge 0 \end{cases}$	Saddle-focus (2,1)	$\sigma > 0$	$\mathrm{Re}\lambda_{2,3} < 0 < \lambda_1$
$0 > r > r^-(p,q),\ q < 0$	Saddle $\dim W^s = 2$ $\dim W^u = 1$	$\sigma > 0$	$\lambda_1 > 0 > \lambda_2 > \lambda_3$
$0 < r < \begin{cases} r^+(p,q) & \text{for } q \le -p^2 \\ pq & \text{for } -p^2 \le q < 0 \end{cases}$	Saddle $\dim W^s = 1$ $\dim W^u = 2$	$\sigma < 0$	$\lambda_1 < 0 < \lambda_2 < \lambda_3$
$r^+(p,q) > r > \begin{cases} pq & \text{for } -p^2 < q \le 0 \\ 0 & \text{for } 0 \le q < \dfrac{p^2}{4} \end{cases}$	Saddle $\dim W^s = 1$ $\dim W^u = 2$	$\sigma > 0$	$\lambda_1 < 0 < \lambda_2 < \lambda_3$
$-p(q+2p^2) > r > \begin{cases} r^+(p,q) & \text{at } q \in \left(-p^2, \dfrac{p^2}{4}\right) \\ 0 & \text{at } q \ge \dfrac{p^2}{4} \end{cases}$	Saddle-focus (1,2)	$\sigma > 0$	$\lambda_1 < 0 < \mathrm{Re}\lambda_{2,3}$
$r > \begin{cases} r^+(p,q) & \text{for } q \le -p^2 \\ -p(q+2p^2) & \text{for } q \ge -p^2 \end{cases}$	Saddle-focus (1,2)	$\sigma < 0$	$\lambda_1 < 0 < \mathrm{Re}\lambda_{2,3}$

Table C.3

Parameter regions	Types of equilibria	Eigenvalues $\lambda_i,\ i=1,2,3$	Dimensions of W^s and W^u
$0 < r < \frac{2}{9}\sqrt{3}\|q\|^{3/2},\ q<0$	Saddle	$\lambda_1 < 0 < \lambda_2 < \lambda_3$	$\dim W^s = 1$ $\dim W^u = 2$
$r > \begin{cases} \frac{2}{9}\sqrt{3}\|q\|^{3/2} & \text{for } q \le 0 \\ 0 & \text{for } q \ge 0 \end{cases}$	Saddle-focus (1,2)	$\lambda_1 < 0 < \mathrm{Re}\lambda_{2,3}$	$\dim W^s = 1$ $\dim W^u = 2$
$r < \begin{cases} -\frac{2}{9}\sqrt{3}\|q\|^{3/2} & \text{for } q \le 0 \\ 0 & \text{for } q \ge 0 \end{cases}$	Saddle-focus (2,1)	$\mathrm{Re}\lambda_{2,3} < 0 < \lambda_1$	$\dim W^s = 2$ $\dim W^u = 1$
$0 > r > -\frac{2}{9}\sqrt{3}\|q\|^{3/2},\ q<0$	Saddle	$\lambda_1 > 0 > \lambda_2 > \lambda_3$	$\dim W^s = 2$ $\dim W^u = 1$

□

From these equilibrium equations, we find that $y=0$, $x=-z$ and $x(1-x^2)=0$. Thus, there are always three equilibria: $O(0,0,0)$ and $O_{1,2}(\pm 1,0,\mp 1)$. The Jacobian matrix at the origin is given by

$$\begin{bmatrix} a/6 & a & 0 \\ 1 & -1 & 1 \\ 0 & -b & 0 \end{bmatrix}.$$

The characteristic equation at $O(0,0,0)$ is

$$\det \begin{bmatrix} a/6-\lambda & a & 0 \\ 1 & -1-\lambda & 1 \\ 0 & -b & -\lambda \end{bmatrix} = 0,$$

or

$$\lambda^3 + (1-a/6)\lambda^2 + (b-7a/6)\lambda - ab/6 = 0. \tag{C.2.13}$$

One can see that since the constant term is negative, it follows immediately from the Routh-Hurwitz criterion that the origin is an unstable equilibrium state. Furthermore, it may have no zero characteristic roots when a and b are positive. The codimension-2 point ($a=b=0$) requires special considerations. We postpone its analysis to the last section, where we discuss the bifurcation of double zeros in systems with symmetry.

The condition $R \equiv pq - r = 0$ reads here as

$$b = 7a/6 - 7a^2/36\,.$$

We have $q = -7a^2/36 < 0$ at $R = 0$. This means that the point at the origin cannot have a pair of purely imaginary eigenvalues. Thus, it is always structurally stable when $(a, b) \neq 0$. In accordance to the above classification table, its topological type is a saddle with a two-dimensional stable manifold, and a one-dimensional unstable manifold.

C.2.#7. In the (a, b)-parameter plane, find the transition boundary: saddle $\to$ saddle-focus for the origin, and equations for its linear stable and unstable subspaces. Detect the curves in the parameter plane that correspond to the vanishing of the saddle value σ of the equilibrium state at the origin. Find where the divergence of the vector field at the saddle-focus vanishes. Plot the curves found in the $(a\,b)$-plane. □

Let us examine next the stability of the non-trivial equilibria $O_{1,2}(\pm 1, 0, \mp 1)$. First, we linearize the system at either O_1 or O_2. The associated Jacobian matrix is given by

$$\begin{bmatrix} -a/3 & a & 0 \\ 1 & -1 & 1 \\ 0 & -b & 0 \end{bmatrix}.$$

The characteristic polynomial is given by

$$\lambda^3 + (1 + a/3)\lambda^2 + (b - 2a/3)\lambda + ab/3 = 0\,. \qquad \text{(C.2.14)}$$

Like O, the equilibria $O_{1,2}$ cannot have a zero characteristic exponent for $ab \neq 0$. The condition $R = 0$ reads here as

$$b = \frac{2}{9}a(3 + a)\,.$$

This bifurcation boundary is plotted in Fig. C.2.1. The corresponding expression for q is $q = 2a^2/9 > 0$. Therefore, at $R = 0$, the equilibria $O_{1,2}$ have a pair of pure imaginary characteristic exponents, namely,

$$\lambda_{1,2} = \pm i\frac{a\sqrt{2}}{3} \quad \text{and} \quad \lambda_3 = -(1 + a/3)\,.$$

This corresponds to the Andronov-Hopf bifurcation. When $R > 0$ the equilibria $O_{1,2}$ are stable foci, and when $R < 0$, they are saddle-foci (1,2). The

stability of $O_{1,2}$ in the critical case depends on whether the corresponding Andronov-Hopf bifurcation is sub- or super-critical (see Secs. 9.3 and 11.5), i.e. whether the point $O_{1,2}$ is a stable or unstable weak focus. To find out what occurs here we will need to determine the sign of the first Lyapunov value L_1. When $L_1 < 0$, $O_{1,2}$ are stable, and they are unstable if $L_1 > 0$. If the Lyapunov value vanishes on the Andronov-Hopf bifurcation curve, the sign of the next Lyapunov value L_2 must be computed, etc.

Consider the Lorenz equation [87]

$$\begin{aligned} \dot{x} &= -\sigma(x-y)\,, \\ \dot{y} &= rx - y - xz\,, \\ \dot{z} &= -bz + xy\,, \end{aligned} \tag{C.2.15}$$

where σ, r and b are positive parameters; we will assume, moreover, that $\sigma > b+1$. Notice that this equation is invariant under the involution $(x,y,z) \leftrightarrow (-x,-y,z)$.

Let us find the equilibrium states of this equation by solving the following system:

$$\begin{aligned} 0 &= -\sigma(x-y)\,, \\ 0 &= rx - y - xz\,, \\ 0 &= -bz + xy\,, \end{aligned}$$

We find that $x = y$, $x(r-1-z) = 0$ and $bz = x^2$. Plugging the last relation into the middle one, we arrive at the equation for the coordinates of equilibria:

$$x(b(r-1) - x^2) = 0\,. \tag{C.2.16}$$

One can see that the Lorenz equation always has one equilibrium state O at the origin. When $r > 1$, along with O there are two more equilibrium states $O_{1,2}(x_{1,2} = y_{1,2} = \pm b^{1/2}(r-1)^{1/2}, z_{1,2} = r-1)$.

The Jacobian matrix at the origin is given by

$$\begin{pmatrix} -\sigma & \sigma & 0 \\ r & -1 & 0 \\ 0 & 0 & -b \end{pmatrix}.$$

The characteristic equation

$$\det \begin{bmatrix} -\sigma-\lambda & \sigma & 0 \\ r & -1-\lambda & 0 \\ 0 & 0 & -b-\lambda \end{bmatrix} = 0$$

has three real roots:

$$\lambda_1 = -b \quad \text{and} \quad \lambda_{2,3} = \frac{-(\sigma+1) \pm \sqrt{(\sigma+1)^2 + 4\sigma(r-1)}}{2}\,.$$

Thus, when $r < 1$, the origin is a stable equilibrium state. When $r = 1$, the equilibrium state has one zero root. When $r > 1$, the origin becomes a saddle with a one-dimensional unstable manifold, and its stability is inherited by the stable equilibria $O_{1,2}$.

The unstable manifold W^u_O is composed of the saddle point itself and two trajectories $\Gamma_{1,2}$ that come from O as $t \to +\infty$. The stable manifold W^s_0 is two-dimensional. The leading stable direction in W^s_0 is given by the eigenvector corresponding to the smallest negative characteristic root. In our case, this is $\lambda_1 = -b$, and the corresponding eigenvector is $(0, 0, 1)$. Note that there is an invariant line $x = y = 0$ in W^s_O.

C.2.#8. Find the equations of $\mathcal{E}^u_O$ and $\mathcal{E}^{ss}_O$ at the origin. □

Let us carry out the stability analysis for $O_{1,2}$. We can choose either one; let it be O_1. The Jacobian matrix at O_1 is given by

$$\begin{bmatrix} -\sigma & \sigma & 0 \\ r - z_1 & -1 & -x_1 \\ x_1 & y_1 & -b \end{bmatrix}.$$

The corresponding characteristic equation is given by

$$\lambda^3 + (\sigma + b + 1)\lambda^2 + b(\sigma + r)\lambda + 2b\sigma(r-1) = 0\,.$$

The stability boundary of the equilibria $O_{1,2}$ is determined by the condition:

$$R \equiv b(\sigma + r)(\sigma + b + 1) - 2b\sigma(r-1) = 0\,. \qquad \text{(C.2.17)}$$

Thus, provided $\sigma > b + 1$, the equilibrium states $O_{1,2}$ are stable when

$$1 < r < \frac{\sigma(\sigma + b + 3)}{\sigma + b - 1}\,.$$

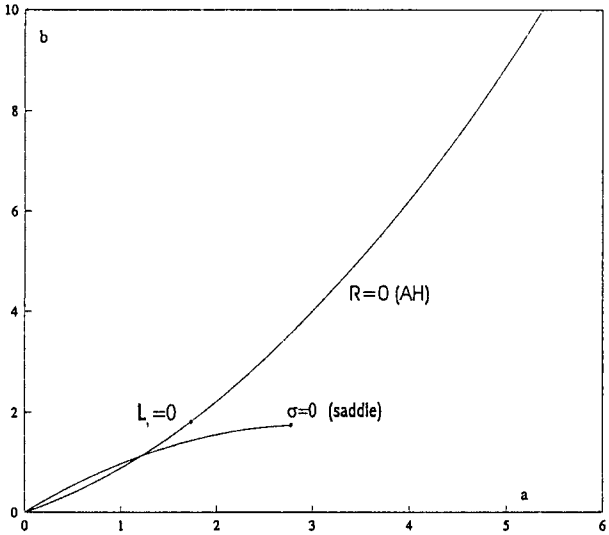

Fig. C.2.1. A part of the (a, b)-bifurcation diagram of the Chua's circuit; AH denotes the Andronov-Hopf bifurcation curve; $\sigma = 0$ corresponds to the vanishing of the saddle value when the origin is a saddle.

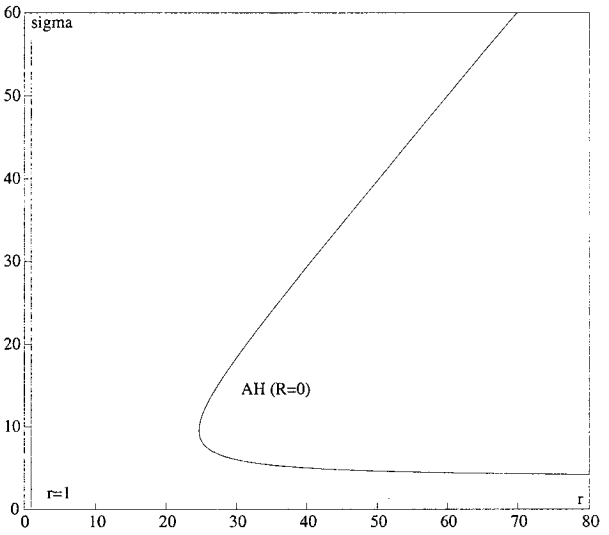

Fig. C.2.2. The Andronov-Hopf bifurcation curve AH and a pitch-fork curve $r = 1$ in the (r, σ)-plane of the Lorenz model at $b = 8/3$.

They become saddle-foci (1,2) when $R \leq 0$. This happens on, and to the right of the Andronov-Hopf bifurcation curve AH in the (r, σ)-parameter plane in Fig. C.2.2.

The stability of the bifurcating equilibria $O_{1,2}$ at the critical moment $R = 0$ is determined by the first Lyapunov value L_1. We will derive its analytical expression in Sec. C.5.

C.2.#9. Find a point in the (r, a)-parameter plane in Fig. C.2.3 where an equilibrium state of the asymmetric Lorenz model [189]

$$\begin{aligned} \dot{x} &= -10(x - y)\,, \\ \dot{y} &= rx - y - xz + a\,, \\ \dot{z} &= -\frac{8}{3}z + xy \end{aligned} \tag{C.2.18}$$

has a pair of zero eigenvalues. □

Consider next the following third-order system from atmospheric physics [128] and [183]

$$\begin{aligned} \dot{x} &= -y^2 - z^2 - ax + aF\,, \\ \dot{y} &= xy - bxz - y + G\,, \\ \dot{z} &= bxy + xz - z\,, \end{aligned} \tag{C.2.19}$$

where (a, b, F, G) are positive parameters. To find its equilibrium states (x_0, y_0, z_0), we equate the right-hand side of (C.2.19) to zero:

$$\begin{aligned} 0 &= -y_0^2 - z_0^2 - ax_0 + aF\,, \\ 0 &= x_0 y_0 - bx_0 z_0 - y_0 + G\,, \\ 0 &= bx_0 y_0 + x_0 z_0 - z_0\,. \end{aligned} \tag{C.2.20}$$

From the second and the third equations, we obtain

$$\begin{aligned} y_0 &= \frac{G(1 - x_0)}{1 - 2x_0 + (1 + b^2)x_0^2}\,, \\ z_0 &= \frac{bGx_0}{1 - 2x_0 + (1 + b^2)x_0^2}\,. \end{aligned} \tag{C.2.21}$$

Substituting (C.2.21) into the first equation in (C.2.20), we obtain

$$(1 + b^2)x_0^3 - [2 + (1 + b^2)F]x_0^2 + (1 + 2F)x_0 + \left(\frac{G^2}{a} - F\right) = 0\,. \tag{C.2.22}$$

Next, we introduce the new parameters

$$B = \frac{1}{1+b^2}, \quad G' = \frac{G^2}{a} - \frac{F}{1+b^2}\,,$$

and make a translation

$$x_0 = \bar{x} + \frac{2B+F}{3}\,.$$

Then (C.2.22) transforms into the cubic canonical equation

$$\bar{x}^3 + s\bar{x} + t = 0\,, \tag{C.2.23}$$

where

$$t = B(1+2F) - \frac{(2B+F)^2}{3}\,,$$
$$s = \frac{B(1+2F)(2B+F)}{3} + G' - \frac{2(2B+F)^3}{27}\,.$$

The discriminant of Eq. (C.2.23) is given by

$$\Delta = \frac{t^2}{4} + \frac{s^3}{27}\,.$$

The corresponding bifurcation curve determined by the condition $\Delta = 0$ is plotted in Fig. C.2.4. It breaks the parameter plane (F, G) into regions where system (C.2.19) possesses either one or three equilibrium states (inside the wedge in Fig. C.2.4). The precise location of the cusp, where all three equilibrium states coalesce, is determined by the simultaneous vanishing of s and t (the point labeled CP). This occurs when

$$G = \frac{2\sqrt{12}b\sqrt{ab}}{3(1+b^2)}, \quad F = \frac{1+\sqrt{3}b}{1+b^2}\,.$$

C.2.#10. Show that the system possesses an equilibrium state with characteristic exponents $(0, \pm i\omega)$ (Gavrilov-Guckenheimer bifurcation) at

$$F^* = \frac{3a^2 + 3a^2b^2 + 12ab^2 + 12b^2 + 4a}{4(a + ab^2 + 2b^2)}$$
$$G^* = \frac{\sqrt{a}(a^2 + a^2b^2 + 4ab^2 + 4b^2)}{4\sqrt{a + ab^2 + 2b^2}}\,.$$

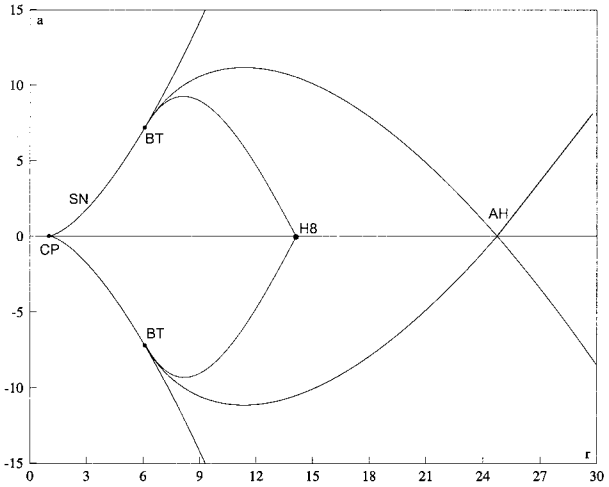

Fig. C.2.3. A partial bifurcation diagram for the asymmetric Lorenz model. The point CP is a cusp, at BT the system has a double-degenerate equilibrium state with two zero characteristic exponents (see Sec. 13.2).

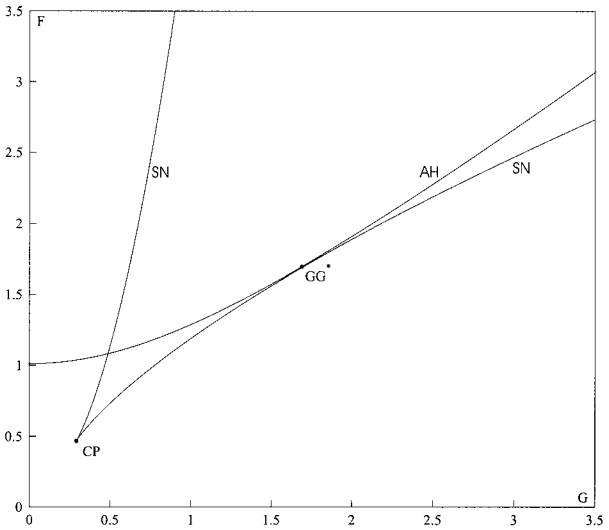

Fig. C.2.4. A fragment of the (F, G)-bifurcation portrait derived from a linear stability analysis for $a = 1/4$ and $b = 4$.

Hint: use the fact that at this bifurcation point the trace and the determinant of the Jacobian matrix must vanish simultaneously. □

C.2.#11. Carry out a linear stability analysis of the following system

$$\begin{aligned}\dot{r} &= r(\mu_1 + az + z^2)\,,\\ \dot{z} &= \mu_2 + z^2 + br^2\,,\\ \dot{\varphi} &= \omega + cz\,,\end{aligned}$$

where r, φ and z are cylindrical coordinates, $\mu_{1,2}$ are control parameters, and a, b, c assume the values ± 1. This is a truncated normal form for the Gavrilov-Guckenheimer bifurcation. □

C.2.#12. Find the transformation of coordinates and time which brings the Lorenz system (C.2.15) to the following form

$$\begin{aligned}\dot{x} &= y\,,\\ \dot{y} &= x - xz - ay + Bx^3\,,\\ \dot{z} &= -b'(z - x^2)\,.\end{aligned} \tag{C.2.24}$$

Hint: the corresponding relation between the parameters of both systems is

$$b' = \frac{b}{\sqrt{\sigma(r-1)}}, \quad a = \frac{1+\sigma}{\sqrt{\sigma(r-1)}}, \quad B = \frac{b}{2b-\sigma}\,. \qquad \square$$

The system (C.2.24) is the asymptotic normal form appearing in the study [129] of local codimension-three bifurcations of equilibria and periodic orbits of systems with a symmetry (see Sec. C.4). When $B = 0$, system (C.2.24) is the Shimizu-Morioka model [127], [191]

$$\begin{aligned}\dot{x} &= y\,,\\ \dot{y} &= x - xz - ay\,,\\ \dot{z} &= -bz + x^2\,,\end{aligned} \tag{C.2.25}$$

which can be viewed as the approximation of the Lorenz equation for large Raleigh numbers r. In a slightly different form, it can also be derived from PDEs describing a weekly nonlinear magneto-convection in the limit of tall, thin rolls [187].

The Shimizu-Morioka model has three equilibria when $b > 0$. The origin $O(0,0,0)$ is a saddle of type (2,1) with the characteristic exponents

$$\lambda_{1,2} = -a/2 \pm (a^2/4 + 1)^{1/2}, \quad \lambda_3 = -b\,.$$

The change of the leading direction in $\mathcal{E}^s$ occurs on the curve $a = (b^2 - 1)/b$ when $\lambda_2 = \lambda_3$. The saddle value $\sigma = \lambda_1 + \lambda_3$ vanishes on the curve $a = (1 - b^2)/b$.

C.2.#13. Write down the equations of the eigenspaces $\mathcal{E}^s$, $\mathcal{E}^u$, $\mathcal{E}^{sL}$ for the saddle at the origin. □

The characteristic equation at the non-trivial equilibria $O_{1,2}(\pm\sqrt{b},\, 0,\, 1)$ of the Shimizu-Morioka model is given by

$$\lambda^3 + (a+b)\lambda^2 + ab\lambda + 2b = 0\,.$$

The Andronov-Hopf bifurcation curve AH in Fig. C.2.5 is given by $(a + b)a - 2 = 0$. The characteristic exponents at $O_{1,2}$ on it are

$$\lambda_3 = -2/a, \qquad \lambda_{1,2} = \pm i\sqrt{2 - a^2}\,.$$

Above the curve AH the equilibria $O_{1,2}$ are stable foci; they are saddle-foci of type $(1, 2)$ below the curve.

The equilibrium states in the Rössler system [172, 188]

$$\begin{aligned} \dot{x} &= -y - z\,, \\ \dot{y} &= x + ay\,, \\ \dot{z} &= bx - cz + xz\,, \end{aligned}$$

are $O(0,0,0)$ and $O_1(c - ab,\, b - c/a,\, c/a - b)$. The characteristic equation at O is given by

$$\lambda^3 + (c-a)\lambda^2 + (1 + b - ac)\lambda + (c - ab) = 0\,.$$

It has the roots $(i\omega, -i\omega, \lambda)$ when

$$a = \frac{(1+c^2) + \sqrt{(1+c^2)^2 - 4bc^2}}{2c}, \quad \sqrt{c^2 + \frac{1}{4}} - \frac{1}{2} < b < \frac{(1+c^2)^2}{4c^2}$$

or

$$a = \frac{(1+c^2) - \sqrt{(1+c^2)^2 - 4bc^2}}{2c}, \quad b < \begin{cases} \sqrt{c^2 + \dfrac{1}{4}} - \dfrac{1}{2} & \text{for } c \geq \sqrt{2+\sqrt{5}}\,, \\ \dfrac{(1+c^2)^2}{4c^2} & \text{for } c \leq \sqrt{2+\sqrt{5}}\,. \end{cases}$$

This equilibrium state has one zero root when $a = c/b$.

The characteristic equation at O_1 assumes the form

$$\lambda^3 + a(b-1)\lambda^2 + \left(1 + \frac{c}{a} - a^2 b\right)\lambda + (ab - c) = 0\,.$$

It has a pair of purely imaginary roots on the curve

$$c = \frac{a}{b} + (b-1)a^3, \quad a^2 < 1 + \frac{1}{b}\,.$$

In addition, this equilibrium state may have a single zero root when $a = c/b$. Thus, the equilibrium states O_1 and O_2 coalesce when $ab = c$. The two other characteristic exponents of this degenerate point are given by

$$\lambda_{1,2} = \frac{a(1-b) \pm \sqrt{a^2(b+1)^2 - 4(b+1)}}{2}\,.$$

Hence, the exponents $\lambda_{1,2}$ become pure imaginary when

$$b = 1, \qquad 0 < a < \sqrt{2}\,.$$

The Rössler system and the new Lorenz system (C.2.19) are remarkable in that both have a doubly degenerate equilibrium state with characteristic exponents equal to $(0, \pm i\omega)$. The feature of this bifurcation is that the unfolding may contain a torus bifurcation curve along with curves corresponding to homoclinic loops to saddle-foci, and therefore non-trivial dynamics may emerge instantly in a neighborhood of the bifurcating equilibria. □

C.2.#14. Study the equilibria of the Hindmarsh-Rose model of neuronal activity [177]

$$\begin{aligned} \dot{x} &= y - z - x^3 + 3x^2 + I\,, \\ \dot{y} &= -y - 2 - 5x^2\,, \\ \dot{z} &= \varepsilon(2(x + 1.6) - z)\,, \end{aligned} \tag{C.2.26}$$

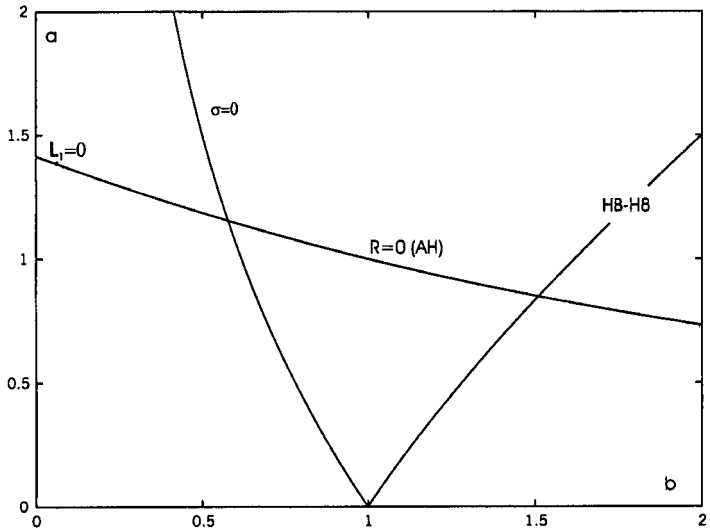

Fig. C.2.5. The (a, b)-bifurcation diagram in the Shimizu-Morioka system derived from a linear stability analysis. AH labels the Andronov-Hopf bifurcation curve; $\sigma = 0$ corresponds to zero saddle-value; $HB - H8$ corresponds to the change of the leading direction at the origin.

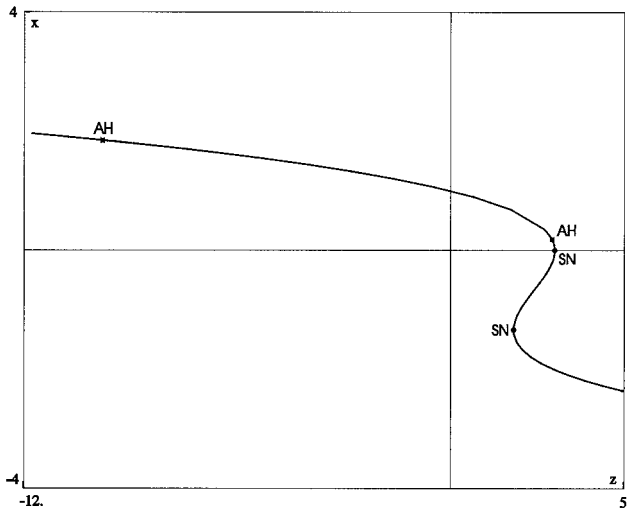

Fig. C.2.6. The x-coordinate of the equilibrium state versus z in the fast planar system at $I = 5$ and $\varepsilon = 0$. AH and SN denote, respectively, the Andronov-Hopf and the saddle-node bifurcations of the equilibria.

where I and ε are two control parameters. Start with the case $\varepsilon = 0$ (see Fig. C.2.6).

C.2.#15. Perform the linear stability analysis of the following systems describing bifurcations of an equilibrium state with three zero characteristic exponents in the case where the Jacobian matrix has a complete Jordan block [162, 163]:

$$\begin{aligned} &\dot{x} = y\,, && \dot{x} = y\,, \\ &\dot{y} = z\,, && \dot{y} = z\,, \\ &\dot{z} = ax - x^2 - by - z; && \dot{z} = ax - x^3 - by - z\,. \end{aligned} \tag{C.2.27}$$

How does the cubic term change the symmetry properties of the system? □

C.2.#16. The following "dimensional" perturbations of the Lorenz equation and the Shimizu-Morioka model are given by the following augmented systems

$$\begin{aligned} &\dot{x} = -\sigma(x - y)\,, && \dot{x} = y\,, && \dot{x} = y\,, \\ &\dot{y} = rx - y - xz\,, && \dot{y} = -ay + x - xz\,, && \dot{y} = -ay + x - xz\,, \\ &\dot{w} = z\,, && \dot{z} = -bz + \mu w + x^2\,, && \dot{z} = w\,, \\ &\dot{z} = -bw - az + xy\,, && \dot{w} = -bw - \mu z\,, && \dot{w} = -bw - \mu z + x^2 + cz^2\,. \end{aligned}$$

Find equilibrium states of these system and determine their types. □

C.2.#17. What are the minimum dimensions of W^s and W^u of the equilibrium state shown in Fig. C.2.7? □

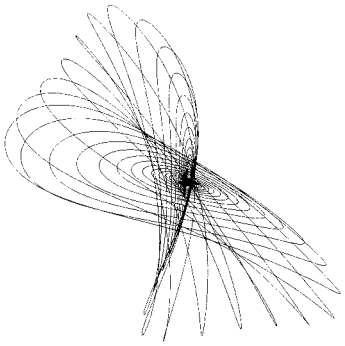

Fig. C.2.7. Trajectory homoclinic to a saddle-focus (2,2).

C.3 Periodically forced systems

Consider an n-dimensional system

$$\dot{x} = Ax + f(t)\,, \tag{C.3.1}$$

where $f(t)$ is a continuous periodic function of period 2π.

C.3.#18. Construct a Poincaré map of the plane $(x, y, t = 0)$ onto the plane $(x, y, t = \tau = 2\pi)$.

Solution. According to the Lagrange method of variations of parameters, the solution of (C.3.1) is given by

$$x(t) = e^{At}x_0 + \int_0^t e^{A(t-\tau)}f(\tau)d\tau\,.$$

Assuming $t = 2\pi$, we obtain the mapping

$$x_1 = e^{2\pi A}x_0 + \int_0^{2\pi} e^{A(2\pi-\tau)}f(\tau)d\tau\,. \tag{C.3.2}$$

□

C.3.#19. Determine the condition under which the above map has: (1) a unique fixed point and, (2) no fixed points.

Solution. The equation for the fixed points is given by

$$[I - e^{2\pi A}]x = C\,,$$

where C denotes the integral in (C.3.2). The two cases possible here are:

(1) $\det(I - e^{2\pi A}) \neq 0$. In this case there exists only one fixed point.
(2) $\det(I - e^{2\pi A}) = 0$. Then, it follows from the Kroneker-Capelli (consistency) theorem that if the rank of $(I - e^{2\pi A})$ is equal to that of the augmented matrix $(I - e^{2\pi A}|C)$, then there are infinitely many fixed points. Otherwise, there are no fixed points. □

C.3.#20. Show that the roots $z_1, \ldots, z_n$ of the characteristic equation $\det(zI - e^{2\pi A}) = 0$ are given by $e^{2\pi\lambda_1}, \ldots, e^{2\pi\lambda_n}$, where $\lambda_1, \ldots, \lambda_n$ are the eigenvalues of the linear system

$$\dot{x} = Ax\,. \tag{C.3.3}$$

□

C.3.#21. Prove that if the origin is a structurally stable equilibrium state of the system (C.3.3), then the corresponding fixed point of the map (C.3.2) is structurally stable as well. Furthermore, show that the topological types of the equilibrium state of (C.3.3) and the fixed point of (C.3.2) are the same. □

C.3.#22. Show that $\det(I - e^{2\pi A}) = 0$ if only one of the eigenvalues $\lambda_1, \ldots, \lambda_n$ is zero or is equal to $i\omega$ with integer ω. □

C.3.#23. Determine the condition under which the two-dimensional system

$$\begin{aligned} \dot{x} &= -\omega y + f(t)\,, \\ \dot{y} &= \omega x + g(t)\,, \end{aligned} \tag{C.3.4}$$

where f and g are continuous functions of period 2π, has an infinite number of periodic orbits of period $2\pi q$, where $q \geq 1$ is some integer.

Solution. The mapping T: $t = 0 \to t = 2\pi$ can be written in the form

$$\begin{aligned} x_1 &= x_0 \cos 2\pi\omega - y_0 \sin 2\pi\omega + C_1\,, \\ y_1 &= x_0 \sin 2\pi\omega + y_0 \cos 2\pi\omega + C_2\,, \end{aligned}$$

where

$$\begin{aligned} C_1 &= \int_0^{2\pi} (f(\tau)\cos\omega(2\pi - \tau) - g(\tau)\sin\omega(2\pi - \tau))d\tau\,, \\ C_2 &= \int_0^{2\pi} (f(\tau)\sin\omega(2\pi - \tau) + g(\tau)\cos\omega(2\pi - \tau))d\tau\,. \end{aligned}$$

When

$$\det \begin{pmatrix} \cos 2\pi\omega - 1 & -\sin(2\pi\omega) \\ \sin(2\pi\omega) & \cos(2\pi\omega) - 1 \end{pmatrix} = (\cos 2\pi\omega - 1)^2 + \sin^2 2\pi\omega \neq 0$$

this map has a unique fixed point. This condition is violated when ω is an integer. In the latter case, the map is recast as

$$x_1 = x_0 + C_1, \qquad y_1 = y_0 + C_2\,.$$

Therefore, if $C_1^2 + C_2^2 \neq 0$, it is clear that the map can have neither fixed nor periodic points; and if $C_1 = C_2 = 0$, all points are fixed ones.

Consider now the case where ω is not an integer. Let (x^*, y^*) be the coordinates of the fixed point. Applying the transformation $x = x^* + \xi$ and $y = y^* + \nu$ we translate the fixed point to the origin. Introducing polar coordinates, the map T assumes the form

$$\rho_1 = \rho_0\,,$$
$$\theta_1 = \theta_0 + 2\pi\omega \qquad \mod 2\pi\,.$$

One can see that every circle $r =$ constant is invariant here and that the map on every circle is the same:

$$\theta_1 = \theta_0 + 2\pi\omega \qquad \mod 2\pi\,.$$

The last one has no periodic points when ω is irrational. When $\omega = p/q$ with integer p and q, all the points are periodic with period q. □

Let us consider next a quasi-linear system

$$\begin{aligned} \dot{x} &= Ax + \mu f(x, y)\,, \\ \dot{y} &= By + \mu g(x, y)\,, \end{aligned} \tag{C.3.5}$$

where $x \in \mathbb{R}^n$ and $y \in \mathbb{R}^m$. The spectrum of A is supposed to lie on the imaginary axis, that of B lies in the left half-plane, and $f, g \in \mathbb{C}^k$.

C.3.#24. Prove the following theorem, which is analogous to the center manifold theorem:

Theorem C.1. *For any $R > 0$ there is a μ_0, such that for $|\mu| < \mu_0$ the sphere $\|(x, y)\| \le R$ contains an attracting invariant $\mathbb{C}^k$-smooth manifold $y = \mu\varphi(x, \mu)$.* □

It follows from the above theorem that the study of (C.3.5) is reduced to the study of the n-dimensional system

$$\dot{x} = Ax + \mu f(x, \mu\varphi(x, \mu)) = Ax + \mu\tilde{f}(x) + o(\mu)$$

where $\tilde{f}(x) = f(x, 0)$.

C.3.#25. Consider the analogous case of quasi-linear maps. □

C.3.#26. Prove the analog of Theorem C.1 for the following $(n + m)$-dimensional system

$$\begin{aligned} \dot{x} &= Ax + h_1(t) + \mu f(x, y, t)\,, \\ \dot{y} &= By + h_2(t) + \mu g(x, y, t)\,, \end{aligned} \tag{C.3.6}$$

where all functions are smooth and 2π-periodic. The spectra of A and B are supposed to lie on the imaginary axes and to the left of it, respectively.

Note that the truncated equation

$$\dot{y} = By + h_2(t)$$

has a unique 2π-periodic solution $y = \alpha(t)$. Thus, we can always make $h_2(t) \equiv 0$ (using the change $\tilde{y} \to y + \alpha(t)$). □

Let us consider the system

$$\dot{x} = \mu f(x,t)\,, \tag{C.3.7}$$

where $f(x,t) = f(x,t+2\pi)$ is a continuous function with respect to t and smooth with respect to x, $x \in \mathbb{R}^n$.

C.3.#27. Find the Poincaré map up to the terms of order μ^2.

Hint: the solution is found from the integral equation

$$x(t) = x_0 + \mu \int_0^t f(x(\tau),\tau)d\tau$$

using the method of successive approximations:

1st approximation is given by $\quad x(t) = x_0\,,$

2nd approximation is given by $\quad x(t) = x_0 + \mu \int_0^t f(x_0,\tau)d\tau\,,$

n-th approximation has the form $\quad x_{n+1}(t) = x_0 + \mu \int_0^t f(x_0,\tau)d\tau + O(\mu^2)\,.$

Solution:

$$x_1 = x_0 + \mu \int_0^{2\pi} f(x_0,\tau)d\tau + O(\mu^2)\,. \tag{C.3.8}$$

□

Denote $f_0(x) = \int_0^{2\pi} f(x_0,\tau)d\tau$.

C.3.#28. Show that the time 2π shift along the trajectories of the system

$$\dot{x} = \frac{\mu}{2\pi} f_0(x) \tag{C.3.9}$$

coincides with (C.3.8) up to the terms of order μ^2. The system (C.3.9) is called *an averaged system.* □

C.3.#29. Prove the following theorem

Theorem C.2. *Structurally stable equilibrium states of the averaged system correspond to structurally stable periodic orbits of the original system: if x^* is a structurally stable equilibrium state in* (C.3.9)*, then the Poincaré map* (C.3.8) *for the system* (C.3.7) *has a structurally stable fixed point close to x^* for all sufficiently small μ.* □

Proof. Let x^* be a structurally stable equilibrium state of the system (C.3.9); i.e.

$$f_0(x^*) = 0$$

and the roots $\lambda_1, \ldots, \lambda_n$ of the characteristic equation do not lie on the imaginary axis. Hence, we can seek them as $\lambda = \frac{\mu}{2\pi}\sigma$:

$$\det\left(\frac{\partial f_0}{\partial x}(x^*) - \sigma I\right) = 0\,. \tag{C.3.10}$$

The fixed points of (C.3.8) can be found from the equation

$$f_0(x) + O(\mu) = 0\,.$$

Since $f_0(x^*) = 0$ and $|\frac{\partial f_0}{\partial x}(x^*)| \neq 0$ because (C.3.10) has no zero roots, it follows that there exists a fixed point $x = x^* + O(\mu)$. The corresponding characteristic equation at this point is written in the form:

$$\det\left(I + \mu\frac{\partial f_0}{\partial x}(x^*) + O(\mu^2) - zI\right) = 0\,.$$

We seek the roots of this equation in the form $z = 1 + \mu\sigma$. Then we find that it recasts as

$$\det\left(\frac{\partial f_0}{\partial x}(x^*) + O(\mu) - \sigma I\right) = 0\,.$$

Therefore, for all small μ the roots σ will be close to those of (C.3.10). Thus, the fixed point will be structurally stable. Moreover, it has the same topological type as the equilibrium state of the averaged system. □

C.3.#30. Prove that in the general case

$$\dot{x} = Ax + \mu f(x,t)\,,$$

where $f(x,t)$ is a continuous function of time, smooth with respect to x, the associated Poincaré map is given by

$$x_1 = e^{2\pi A}x_0 + \mu\int_0^{2\pi} e^{A(2\pi-\tau)}f(e^{A\tau}x_0,\tau)d\tau + O(\mu^2)\,. \qquad \square$$

C.3.#31. Verify that if $\det(e^{2\pi A} - I) \neq 0$, it follows that for any given R, if μ is small enough, in the sphere of radius R there is a single fixed point $x^*(\mu)$ such that $x^*(\mu) \to 0$ as $\mu \to 0$. $\square$

Let us examine the system of two equations

$$\begin{aligned} \dot{x} &= -\omega y + \mu f(x,y,t), \\ \dot{y} &= \omega x + \mu g(x,y,t)\,. \end{aligned} \tag{C.3.11}$$

C.3.#32. Compute the map up to the terms of order μ^2.
Solution:

$$\begin{aligned} x_1 &= x_0\cos 2\pi\omega - y_0\sin 2\pi\omega + \mu\Phi_1(x_0,y_0) + \mu^2(\cdots)\,, \\ y_1 &= x_0\sin 2\pi\omega + y_0\cos 2\pi\omega + \mu\Phi_2(x_0,y_0) + \mu^2(\cdots)\,, \end{aligned} \tag{C.3.12}$$

where

$$\begin{aligned} \Phi_1 = \int_0^{2\pi} &[f(x_0\cos\omega\tau - y_0\sin\omega\tau, x_0\sin\omega\tau + y_0\cos\omega\tau,\tau)\cos\omega\tau \\ &+ g(x_0\cos\omega\tau - y_0\sin\omega\tau, x_0\sin\omega\tau + y_0\cos\omega\tau,\tau)\sin\omega\tau]d\tau \\ \Phi_2 = \int_0^{2\pi} &[-f(x_0\cos\omega\tau - y_0\sin\omega\tau, x_0\sin\omega\tau + y_0\cos\omega\tau,\tau)\sin\omega\tau \\ &+ g(x_0\cos\omega\tau - y_0\sin\omega\tau, x_0\sin\omega\tau + y_0\cos\omega\tau,\tau)\cos\omega\tau]d\tau\,. \end{aligned} \qquad \square$$

C.3.#33. Write the system (C.3.11) in polar coordinates $x = r\cos\theta$, $y = r\sin\theta$.
Solution:

$$\begin{aligned} \dot{r} &= \mu R(r,\theta,t), \\ \dot{\theta} &= \omega + \mu\Psi(r,\theta,t)\,, \end{aligned}$$

where

$$R = f(r\cos\theta, r\sin\theta, t)\cos\theta + g(r\cos\theta, r\sin\theta, t)\sin\theta$$

$$\Psi = \frac{1}{r}[-f(r\cos\theta, r\sin\theta, t)\sin\theta + g(r\cos\theta, r\sin\theta, t)\cos\theta]\,. \qquad \square$$

C.3.#34. Let

$$R(r,\theta,t) = \sum_{n=0}^{\infty}\sum_{m=0}^{\infty} a_{nm}(r)e^{i(m\theta+nt)}$$

$$\Psi(r,\theta,t) = \sum_{n=0}^{\infty}\sum_{m=0}^{\infty} b_{nm}(r)e^{i(m\theta+nt)}\,.$$

Construct the Poincaré map up to $O(\mu^2)$ for the case where ω is an integer.

Solution:

$$r_1 = r_0 + 2\pi\mu \sum_{m\omega+n=0} a_{nm}(r_0)e^{im\theta_0} + \mu^2(\cdots)$$

$$\theta_1 = \theta_0 + 2\pi\mu \sum_{m\omega+n=0} b_{nm}(r_0)e^{im\theta_0} + \mu^2(\cdots)\,. \qquad \square$$

If ω is an integer, the map (C.3.12) can be represented as follows

$$x_1 = x_0 + \mu\Phi_1(x_0, y_0) + \mu^2(\cdots)\,,$$

$$y_1 = y_0 + \mu\Phi_2(x_0, y_0) + \mu^2(\cdots)\,,$$

C.3.#35. Prove the following theorem:

Theorem C.3. (Averaging Theorem) *If ω is an integer, then for sufficiently small $\mu > 0$ structurally stable equilibrium states of the system*

$$\dot{x} = \frac{\mu}{2\pi}\Phi_1(x,y)\,,$$

$$\dot{y} = \frac{\mu}{2\pi}\Phi_2(x,y)$$

will correspond to structurally stable fixed points of the Poincaré map. Moreover, stable equilibria correspond to stable fixed points. $\square$

In polar coordinates the averaged system is given by

$$\dot{r} = \mu \sum_{mw+n=0} a_{nm}(r)e^{im\theta} = \mu R_0(r,\theta),$$

$$\dot{\theta} = \mu \sum_{mw+n=0} b_{nm}(r)e^{im\theta} = \mu \Psi_0(r,\theta)\,.$$

One should take into account that $r = 0$ is a singularity here.

C.3.#36. Find the associated averaged system for the van der Pol equation

$$\ddot{x} + \mu(1-x^2)\dot{x} + \omega^2 x = \mu A \sin t$$

provided that $\omega^2 = 1 + \mu\Delta$ (where Δ is called a detuning). Examine the types of equilibrium states as A and Δ vary. □

Consider now the case where ω is not an integer. According to C.3.#31, the map (C.3.12) has a unique fixed point close to zero in this case.

C.3.#37. Find the periodic motion $(x^*(t), y^*(t))$ corresponding to this fixed point and find the equations of the system after straightening this periodic solution (translate the origin into $(x^*(t), y^*(t))$).

Solution:

$$\dot{x} = -\omega y + \mu F(x,y,t) + \mu^2(\cdots)\,,$$

$$\dot{y} = \omega x + \mu G(x,y,t) + \mu^2(\cdots)\,,$$

where

$$F(x,y,t) = f(x,y,t) - f(0,0,t)\,,$$

$$G(x,y,t) = g(x,y,t) - g(0,0,t)\,.$$ □

Assume now $\omega = p/q$ where p and q are integers, $q > 1$. In this case, one is to find periodic motions of period $2\pi q$ that correspond to the fixed points of the map T^q. This map is written in the form

$$x_q = x_0 + \mu\Phi_1(x_0,y_0) + \mu^2(\cdots)\,,$$

$$y_q = y_0 + \mu\Phi_2(x_0,y_0) + \mu^2(\cdots)\,,$$

where

$$\Phi_1 = \int_0^{2\pi q} [f(\cdot)\cos\omega\tau + g(\cdot)\sin\omega\tau]d\tau\,,$$

$$\Phi_2 = \int_0^{2\pi q} [-f(\cdot)\sin\omega\tau + g(\cdot)\cos\omega\tau]d\tau\,,$$

where $(\cdot)$ stands for $(x_0\cos\omega\tau - y_0\sin\omega\tau, x_0\sin\omega\tau + y_0\cos\omega\tau)$ as above in (C.3.12), and $\omega = \frac{p}{q}$.

In the same manner as in the previous case, we can treat the averaged system

$$\dot{x} = \frac{\mu}{2\pi q}\Phi_1(x,y)\,,$$

$$\dot{y} = \frac{\mu}{2\pi q}\Phi_2(x,y)\,.$$

In polar coordinates, the map T^q can be recast as

$$r_q = r_0 + 2\pi q\mu \sum_{mp+nq=0} a_{nm}(r_0)e^{im\theta_0} + \mu^2(\cdots)\,,$$

$$\theta_q = \theta_0 + 2\pi q\mu \sum_{mp+nq=0} b_{nm}(r_0)e^{im\theta_0} + \mu^2(\cdots)\,.$$

Here, the averaged system is given by

$$\dot{r} = \mu R_0(r,\theta)\,,$$

$$\dot{\theta} = \mu\Psi_0(r,\theta)\,,$$

where $R_0 = \sum_{mp+nq=0} a_{nm}(r)e^{im\theta}$ and $\Psi_0 = \sum_{mp+nq=0} b_{nm}(r)e^{im\theta}$. It should be noted that $f(0,0,t) \equiv 0$ and $g(0,0,t) \equiv 0$ in this case, i.e. the averaged system in polar coordinates no longer has a singularity at $r = 0$. □

C.3.#38. Consider the case of irrational ω. As above, one may assume $f(0,0,t) \equiv 0$, $g(0,0,t) \equiv 0$ in (C.3.11). The system in polar coordinates takes the form

$$\dot{r} = \mu \sum_{n=0}^{\infty}\sum_{m=0}^{\infty} a_{nm}(r)e^{i(m\theta+nt)}, \qquad \dot{\theta} = \omega + \mu \sum_{n=0}^{\infty}\sum_{m=0}^{\infty} b_{nm}(r)e^{i(m\theta+nt)}$$

with non-singular (smooth) coefficients a_{nm}, b_{nm}. Prove that for any given N, M there exists a smooth coordinate transformation which brings the system to the form

$$\dot{r} = \mu a_{00}(r) + O(\mu^2) + \mu \sum_{n=N}^{\infty} \sum_{m=M}^{\infty} a_{nm}(r) e^{i(m\theta+nt)},$$

$$\dot{\theta} = \omega + \mu b_{00}(r) + O(\mu^2) + \mu \sum_{n=N}^{\infty} \sum_{m=M}^{\infty} b_{nm}(r) e^{i(m\theta+nt)}\,.$$

Note that since the series here tend to zero as $N, M \to +\infty$, it follows that for an arbitrarily small δ the map T in appropriate coordinates can be written as follows

$$r_1 = r_0 + 2\pi\mu a_{00}(r_0) + \delta O(\mu)\,,$$

$$\theta_1 = \theta_0 + 2\pi\omega + 2\pi\mu b_{00}(r_0) + \delta O(\mu)\,. \qquad \square$$

C.3.#39. Examine the shortened map

$$r_1 = r_0 + 2\pi\mu a_{00}(r_0)\,,$$

$$\theta_1 = \theta_0 + 2\pi\omega + 2\pi\mu b_{00}(r_0)\,.$$

Show that in addition to the trivial fixed point $(0, 0)$, the above map may have invariant closed curves determined by the zeros of the equation

$$a_{00}(r_0) = 0\,. \qquad \square$$

C.3.#40. Prove that for small $\mu > 0$, each root r^* of the equation

$$a_{00}(r_0) = 0\,,$$

for which

$$a'_{00}(r^*) < 0$$

corresponds to the stable invariant closed curve $r = r^*(\mu) = r^* + O(\mu)$.

Direction: take δ sufficiently small and apply the annulus principle. $\square$

In the case of irrational ω, the averaged system is given by

$$\dot{r} = \mu a_{00}(r)\,,$$

$$\dot{\theta} = \omega + \mu b_{00}(r)\,.$$

Here $r = 0$ is an equilibrium state, while the non-zero roots of $a_{00}(r) = 0$ correspond to the limit cycles.

C.3.#41. The next problem is almost equivalent to the previous one: show that for small $\mu > 0$ stable (unstable) limit cycles of the averaged system correspond to stable (unstable) invariant tori of the original system. □

Let us return to the resonant case ($\omega = p/q, q \geq 1$). The corresponding averaged system can then be recast as

$$\dot{r} = \mu R_0(r, \theta)\,,$$
$$\dot{\theta} = \mu \Psi_0(r, \theta)\,.$$

Assume that the system

$$\begin{aligned} \dot{r} &= R_0(r, \theta)\,, \\ \dot{\theta} &= \Psi_0(r, \theta) \end{aligned} \tag{C.3.13}$$

has a structurally stable periodic orbit $L : \{r = \alpha(t),\, \theta = \beta(t)\}$ of period τ, and let

$$\lambda = \int_0^\tau \left[\frac{\partial R_0}{\partial \tau}(\alpha(t), \beta(t)) + \frac{\partial \Psi_0}{\partial \tau}(\alpha(t), \beta(t)) \right] d\tau < 0.$$

This implies that the averaged system has a periodic solution $\{r = \alpha(\mu t),\, \theta = \beta(\mu t)\}$ of period τ/μ.

C.3.#42. Prove that the original system has a stable invariant torus for small $\mu > 0$.

Hint: modify (C.3.13) first. Introduce the normal coordinates (u, φ) near L (see Sec. 3.10). Then the system is written in the form

$$\dot{u} = A(\varphi)u + O(u^2)\,,$$
$$\dot{\varphi} = 1 + O(u)\,,$$

where the right-hand side is a periodic function of period τ_0. Note that

$$\lambda = \int_0^\tau A(\varphi) d\varphi\,,$$

and therefore

$$A(\varphi) = \lambda + A_0(\varphi)\,,$$

where $\int_0^\tau A_0(\varphi)d\varphi = 0$. Having introduced $v = ue^{-\int A_0(\varphi)d\varphi}$, the system assumes the form

$$\dot{v} = \lambda v + O(v^2)\,,$$
$$\dot{\varphi} = 1 + O(v)\,.$$

It follows from here that the averaged system in the new coordinates (v, φ) can be recast as

$$\dot{v} = \mu[\lambda v + O(v^2)]\,,$$
$$\dot{\varphi} = \mu[1 + O(v)]\,.$$

The corresponding *shift map* over $2\pi q$ is given by

$$v_1 = v_0 + \mu[2\pi q\lambda v_0 + O(v_0^2)] + O(\mu^2)\,,$$
$$\varphi_1 = \varphi_0 + 2\pi q\mu + O(\mu v_0) + O(\mu^2)\,.$$

The same form has the $2\pi q$-shift map of the original system (C.3.11). Introduce $v = \mu w$, after which the Poincaré map becomes

$$w_1 = w_0 + 2\pi q\mu\lambda w_0 + O(\mu^2)\,,$$
$$\varphi_1 = \varphi_0 + 2\pi q\mu + O(\mu^2)\,.$$

To complete the solution, apply the annulus principle. □

C.3.#43. Examine the Mathieu equation written in the following form

$$\dot{x} = y, \qquad \dot{y} = -\omega^2(1 + \varepsilon\cos\omega_0 t)x\,. \tag{C.3.14}$$

Show that the instability zones, which correspond to the parametric oscillations, are adjoined to the points $\omega/\omega_0 = k/2$ $(k = 1, 2, \ldots)$ in the plane $(\omega/\omega_0, \varepsilon)$ on the surface $\varepsilon = 0$ [20].

The solution of (C.3.14) starting from an initial point (x_0, y_0) has the following form at $\varepsilon = 0$:

$$\begin{aligned} x(t) &= \frac{y_0}{\omega_0}\sin\omega t + x_0\cos\omega t\,,\\ y(t) &= y_0\cos\omega t - \omega x_0\sin\omega t\,. \end{aligned} \tag{C.3.15}$$

Next we construct the map of the plane $(x, y, t = 0)$ onto the plane $(x, y, t = \tau = 2\pi/\omega_0)$. To do this, we substitute $t = 2\pi/\omega_0$ into (C.3.15) and replace $(x(t), y(t))$ by $(\bar{x}, \bar{y})$, and (x_0, y_0) by (x, y). The resulting operator $(x, y) \mapsto (\bar{x}, \bar{y})$ is given by

$$\begin{pmatrix} \bar{x} \\ \bar{y} \end{pmatrix} = \begin{pmatrix} \cos 2\pi \dfrac{\omega}{\omega_0} & \dfrac{1}{\omega} \sin 2\pi \dfrac{\omega}{\omega_0} \\ -\omega \sin 2\pi \dfrac{\omega}{\omega_0} & \cos 2\pi \dfrac{\omega}{\omega_0} \end{pmatrix} \begin{pmatrix} x \\ y \end{pmatrix}. \tag{C.3.16}$$

The characteristic equation of (C.3.16) is

$$\rho^2 + p\,\rho + q = 0\,,$$

where

$$p \equiv \text{tr T} = -2\cos 2\pi \frac{\omega}{\omega_0} \quad \text{and} \quad q \equiv \det T = 1\,.$$

This is an *area-preserving map*. The multipliers of the fixed point $O(x = y = 0)$ satisfy the relations

$$\rho_1 + \rho_2 = -p \quad \text{and} \quad \rho_1 \rho_2 = q = 1\,.$$

Therefore, when $|p| < 2$, the above map is a rotation through the angle $2\pi\omega/\omega_0$ such that all of its trajectories are stable.

Find a correction of the first order in ε to formula (C.3.15) (use C.3.#30). Note that the origin of the perturbed map becomes a saddle when $|p| > 2$. Furthermore, it is a saddle $(+,+)$ or a saddle $(-,-)$ if $p > 2$ and $p < -2$, respectively. □

C.3.#44. [166] Consider the system

$$\dot{\psi}_1 = \omega_1\,,$$
$$\dot{\psi}_2 = \omega_2\,,$$

where $\omega_{1,2} > 0$, which can be interpreted as a pair of two non-interacting harmonic oscillators.

The above system can be reduced to one equation

$$\frac{d\psi_1}{d\psi_2} = \frac{\omega_1}{\omega_2} \triangleq r\,.$$

We can always assume $r < 1$. The above system has the solution $\psi_1 = r\psi_2 + \psi_2^0$. Introducing the normalized coordinates $\theta = \psi_2^0/2\pi$ and $\bar{\theta} = (r2\pi + \psi_2^0)/2\pi$, one obtains the circle map

$$\bar{\theta} = \theta + r, \qquad \mod 1\,, \tag{C.3.17}$$

which can also be represented by the following map on the interval $[0, 1]$:

$$\bar{\theta} = \begin{cases} \theta + r & \text{for } 0 \le \theta \le 1 - r\,, \\ \theta - (1 - r) & \text{for } 1 - r \le \theta \le 1\,, \end{cases} \tag{C.3.18}$$

where the end points $\theta = 0$ and $\theta = 1$ are identified.

Let r be a rational number, i.e. $r = p/q$ where p and q are some mutually prime integers. Let us partition the segment $[0, 1]$ into p intervals of length $1/p$: $[0, 1/p]$, $[1/p, 2/p], \ldots, [(p-1)/p, 1]$. Choose an initial point $\theta_0 \in [0, 1/p]$. The positive semi-trajectory of (C.3.17) starting from θ_0 is the sequence of iterates

$$\left(\theta_0, \theta_1 = \theta_0 + \frac{p}{q} (\mod 1), \theta_2 = \theta_0 + \frac{2p}{q} (\mod 1), \ldots, \theta_i = \theta_0 + \frac{ip}{q} (\mod 1), \ldots\right).$$

The cycle of period n is given by

$$\left\{\theta_0 = \theta_0 + \frac{np}{q} \quad \mod 1, \quad \theta_i \neq \theta_0, \quad i = 1, 2, \ldots, n-1\right\}.$$

Under the above condition imposed on p and q it follows that the minimal period $n = p$. Therefore, there is only one point on the cycle on each interval $[(k-1)/p, k/p]$, $k = 1, \ldots, p$ because the number of points on the cycle and that of the intervals both equal p. Otherwise $n < p$, but this is impossible because two iterates of the cycle cannot belong to the same interval. Since θ_0 is an arbitrary point of $[0, 1/p]$, it follows that the segment $[0, 1]$ is filled in by p-period cycles entirely. Thus, when the rotation number is rational there is a continuum of coexisting cycles of period p in the system under consideration.

If the number r is irrational, it can be represented as

$$r = \lim_{l \to \infty} \frac{q_l}{p_l}$$

such that $p_l \to \infty$ as $l \to \infty$. In addition, the number of intervals $[(k-1)/p_l, k/p_l]$ on $[0, 1]$ also increases without bound. Therefore, the length of each interval decreases, and as $l \to \infty$ the whole segment [0, 1] is filled out by a quasi-periodic covering. □

C.3.#45. Examine the circle map:

$$\bar{\theta} = \theta + \omega + k \sin\theta \qquad \mod (2\pi)\,, \tag{C.3.19}$$

where ω is a frequency and k is some parameter.

Compute numerically the rotation number $R(\omega)$:

$$R = \frac{1}{2\pi} \lim_{N\to+\infty} \frac{1}{N} \sum_{n=0}^{N-1} (\theta_{n+1} - \theta_n)$$

for $\omega \in [0,\, 2\pi]$.

Hint: compute the iterates of the following two-dimensional mapping

$$\begin{aligned} \theta_{n+1} &= (\theta_n + \omega + k \sin x_n) \qquad \mod 2\pi\,, \\ R_{n+1} &= \frac{1}{n+1} \left(n R_n + \omega + \frac{\theta_{n+1} - \theta_n}{2\pi} \right), \end{aligned} \tag{C.3.20}$$

as ω varies from 0 to 2π.

As $n \to +\infty$, the iterates of R_n converge to the rotation number R at the given ω. Next plot the bifurcation diagram of R versus ω as in Fig. C.3.1. □

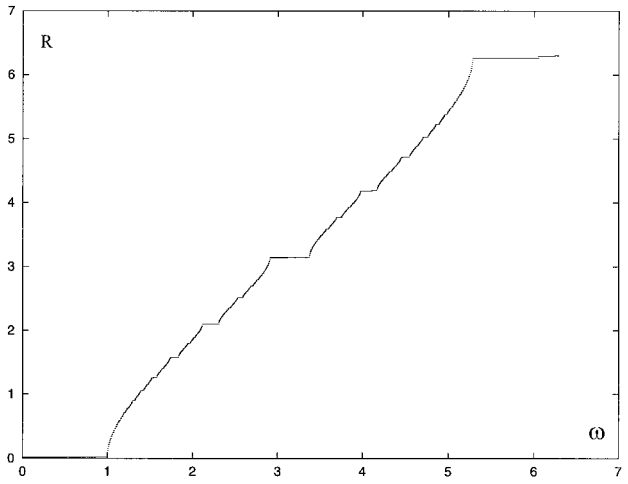

Fig. C.3.1. "Devil staircase" in (C.3.20).

C.4 Derivation of normal forms

In this section, we will discuss some algorithms for constructing normal forms. Due to the reduction principle, it is sufficient to construct the normal forms for the system on the center manifold only. Therefore, in order to consider bifurcations of an equilibrium state with a *single zero* characteristic root, we need a one-dimensional normal form. If it has a pair of zero characteristic exponents, one should examine the corresponding family of two-dimensional normal forms, and so on.

In certain situations the global properties of the original system must be taken into account. So, for instance, if the original system restricted to the center manifold is symmetric, the associated normal form will inherit this property as well. In essence, a normal form for a given bifurcation is a parameterized system of differential or difference equations, depending on what the problem under consideration is, whose right-hand sides are in the simplest form but sufficient to describe the main bifurcations in the given family.

In order to study bifurcations near a stability boundary one must introduce small governing parameters the number of which is at least equal to the order of degeneracy of the linear problem, or this number may even be greater provided that there are extra degeneracies due to the nonlinear terms. Since the unfolding parameters are small, the orbits on the center manifold may stay in a small neighborhood of the equilibrium state for a rather long time (there is no fast instability in the center manifold because all characteristic exponents of the reduced linearized system are nearly zero). Thus, it is reasonable to rescale the parameters and phase variables so that they assume finite values instead of asymptotically vanishing ones; the time variable must then be rescaled too.

This approach is a rather general one. Its advantage is that when the rescaling procedure has been carried out, many resonant monomials disappear. The most trivial example is a saddle-node bifurcation with a single zero eigenvalue. In this case the center manifold is one-dimensional. The Taylor expansion of the system near the equilibrium state may be written in the following form

$$\dot{x} = \mu + x^2 + l_3 x^3 + \cdots ,$$

where μ is a small governing parameter. The rescaling $x \to \sqrt{|\mu|}x$, $t \to t/\sqrt{|\mu|}$ brings the system to the form

$$\dot{x} = \pm 1 + x^2 + O(\sqrt{|\mu|}) ,$$

so that the second degree monomial only survives in the limit $\mu \to 0$.

An analogous algorithm can be applied to the multi-dimensional case. The limit of the rescaled system as governing parameters tend to zero gives a description "in the main order" of the behavior of the system near a bifurcation point. Such a limit system is called *an asymptotic normal form*.

The asymptotic normal forms that arise in the study of equilibria with single or double zero eigenvalues are one- or two-dimensional, respectively. The analysis of such forms is often very comprehensive so most effort is applied to establishing the rigorous correspondence between the dynamics in the asymptotic normal form and that in the original system [20, 64]. However, the analysis of bifurcations in two-dimensional normal forms may already require consideration of some other global bifurcations, sometimes of codimension two. Moreover, accounting for the dropped terms of higher order may also destroy the idealized picture occurring in truncated normal forms. The most vivid example is the bifurcations of an equilibrium state with exponents $(0, \pm i\omega)$ where the normal form possesses a rotational symmetry. If the original system does not support this symmetry, the simple dynamics in the shortened normal form may transform into chaos in the enlarged system.

The situation becomes different when one considers normal forms of higher dimensions. Three- (and higher) dimensional asymptotic normal forms may exhibit non-trivial dynamics by themselves. For example, a homoclinic loop to the saddle-focus was found in the asymptotic normal form

$$\begin{aligned} \dot{x} &= y\,, \\ \dot{y} &= z\,, \\ \dot{z} &= -z - by + ax - x^2\,, \end{aligned}$$

corresponding to the bifurcation of triple zero eigenvalues with a complete Jordan box [163]. Notably, the equations in some asymptotic normal forms coincide with some well-known models coming from different applications: the third-order Duffing equation, the Chua's circuit, the Shimizu-Morioka system and the Lorenz equation.

C.4.#46. Derive the normal form for the Shimizu-Morioka equation in the form [187]

$$\begin{aligned} \dot{x} &= y\,, \\ \dot{y} &= ax - ky - xz\,, \\ \dot{z} &= -z + x^2\,, \end{aligned} \tag{C.4.1}$$

near the codimension-two point $(k = a = 0)$.

First we should determine the characteristic exponents at the origin. It is easy to see that there is a pair of zero exponents and one equal to -1. The eigenspace corresponding to the zero pair is given by $\{z = 0\}$. The center invariant manifold, tangent to this plane at the origin, is written as

$$z = x^2 - 2xy + 2y^2 + \cdots$$

where the dots stand for the cubic and higher order terms in (x, y, z, a, k). The system on the center manifold thus takes the form

$$\begin{aligned} \dot{x} &= y\,, \\ \dot{y} &= ax - ky - x^3 + 2x^2y - 2xy^2 + \cdots\,, \end{aligned} \tag{C.4.2}$$

where the dots stand for the terms of the fourth order, at least.

Let us next rescale

$$(x, y, t, k, a) \to (\varepsilon x_{\rm new}, \varepsilon^2 y_{\rm new}, t_{\rm new}/\varepsilon, \varepsilon k_{\rm new}, \varepsilon^2 a_{\rm new})\,.$$

The system recasts as

$$\begin{aligned} \dot{x} &= y\,, \\ \dot{y} &= ax + ky - x^3 + 2\varepsilon x^2 y + O(\varepsilon^2)\,, \end{aligned} \tag{C.4.3}$$

where the new parameters $k_{\rm new}$ and $a_{\rm new}$ can now be arbitrary. Observe that the reflection symmetry $(x, y) \to (-x, -y)$ in (C.4.3) is inherited from the original system (C.4.1). Due to this fact the Taylor expansion of the functions in the right-hand side does not contain quadratic terms (and other terms of even order) in (x, y). In contrast to the generic Bogdanov-Takens bifurcation, which we analyze in Sec. 13.2, the bifurcations in the symmetric system are somewhat different: the equilibrium state at the origin always exists, and it undergoes a pitch-fork bifurcation instead of a saddle-node one. The bifurcation unfolding of the symmetric system also contains an additional curve which corresponds to the double semi-stable periodic orbit with multiplier equal to $+1$. The signs of the Lyapunov values on the Andronov-Hopf stability boundary for the origin and for the non-trivial equilibria are determined by the sign of ε. Note that when $\varepsilon = 0$ and $k = 0$, the system (C.4.3) becomes integrable with Hamiltonian

$$H(x, y) = \frac{y^2}{2} - \frac{x^2}{2} + \frac{x^4}{4}\,. \qquad \square$$

C.4.#47. Let us consider next the following version of Chua's circuit [168]

$$\dot{x} = \beta(g(y-x) - f(x))\,,$$
$$\dot{y} = g(x-y) + z\,,$$
$$\dot{z} = -y\,,$$

where α, β and g are some positive parameters. Here $f(x) = \alpha x(x^2-1)$ is the cubic approximation for the nonlinear element, and therefore this system possesses odd symmetry $(x, y, z) \to (-x, -y, -z)$. When $g > \alpha$, there is a single equilibrium state O at the origin. When $g < \alpha$, there also exists a pair of symmetric equilibrium states $O_{1,2}(\pm\sqrt{1-g/a}, 0, \mp g\sqrt{1-g/a})$. On the line $g = \alpha$, the characteristic equation at O has a single zero root when $\beta \neq 1/g^2$, and two zero roots at $\beta = 1/g^2$ (the third root is equal to $-g$ in this case). Like the case of the Shimizu-Morioka system, the structure of the bifurcation set in a plane transverse to this curve in the parameter space is determined by the Khorozov-Takens normal form with reflection symmetry. The outline of the reduction to this normal form on a two-dimensional center manifold is discussed below.

The Jacobian matrix corresponding to two null roots is given by

$$D = \begin{pmatrix} 0 & 1 & 0 \\ 0 & 0 & 0 \\ 0 & 0 & -\alpha \end{pmatrix}.$$

The linear part of the system reduces to the form

$$\begin{pmatrix} \dot{\xi} \\ \dot{\eta} \\ \dot{\zeta} \end{pmatrix} = D \begin{pmatrix} \xi \\ \eta \\ \zeta \end{pmatrix}$$

at $\alpha = g = 1/\sqrt{\beta}$ by means of the transformation

$$\begin{pmatrix} x \\ y \\ z \end{pmatrix} = \xi \begin{pmatrix} 1 \\ 0 \\ -g \end{pmatrix} + \eta \begin{pmatrix} 0 \\ g \\ g^2 \end{pmatrix} + \zeta \begin{pmatrix} 1 \\ -g^2 \\ -g \end{pmatrix}.$$

It is easy to compute and verify that in these coordinates the system assumes the form

$$\dot{\xi} = \eta + \left(1 - \frac{1}{g^2}\right) F\,,$$

$$\dot{\eta} = \frac{1}{g} F\,,$$

$$\dot{\zeta} = \frac{1}{g^2} F\,,$$

where

$$F = \gamma_1 \xi + \gamma_2 \eta + (\gamma_1 - g\gamma_2)\zeta - \beta\alpha(\xi + \zeta)^3\,,$$

and $\gamma_{1,2}$ are small parameters:

$$\gamma_1 = \beta(\alpha - g), \qquad \gamma_2 = \beta g^2 - 1\,.$$

The center manifold has the form

$$\zeta = \frac{\gamma_1}{g^3}\xi + \left(\frac{\gamma_2}{g^3} - \frac{\gamma_1}{g^4}\right)\eta + \cdots\,,$$

where the dots stand for the cubic and higher order terms with respect to $(\xi, \eta, \gamma_1, \gamma_2)$. The system on the center manifold is written as

$$\begin{aligned}
\dot{\xi} &= \eta\left(1 + \left(1 - \frac{1}{g^2}\right)\left(\gamma_2 + (\gamma_1 - g\gamma_2)\left(\frac{\gamma_2}{g^3} - \frac{\gamma_1}{g^4}\right)\right)\right) \\
&\quad + \xi\left(1 - \frac{1}{g^2}\right)\left(\gamma_1 + (\gamma_1 - g\gamma_2)\frac{\gamma_1}{g^3}\right) - \frac{1}{g}\left(1 - \frac{1}{g^2}\right)\xi^3 + \cdots\,, \\
\dot{\eta} &= \eta\frac{1}{g}\left(\gamma_2 + (\gamma_1 - g\gamma_2)\left(\frac{\gamma_2}{g^3} - \frac{\gamma_1}{g^4}\right)\right) + \xi\frac{1}{g}\left(\gamma_1 + (\gamma_1 - g\gamma_2)\frac{\gamma_1}{g^3}\right) \\
&\quad - \frac{1}{g^2}\xi^3 + \cdots\,,
\end{aligned}$$

where the dots denote terms of order higher than *three* with respect to $(\xi, \eta, \gamma_1, \gamma_2)$. Now the last step is to change the variable η so that the first equation would become $\dot{\xi} = \eta$. The final form of the system is given by

$$\dot{\xi} = \eta\,,$$

$$\dot{\eta} = \varepsilon_1\xi + \varepsilon_2\eta - \frac{1}{g^2}\xi^3 + 3\frac{1 - g^2}{g^3}\xi^2\eta + \cdots\,,$$

where

$$\varepsilon_1 = \frac{\gamma_1}{g}\left(1+\gamma_1\frac{1}{g^3}+\gamma_2\left(1-\frac{2}{g^2}\right)\right)$$

and

$$\varepsilon_2 = \gamma_1 - (\gamma_1 - g\gamma_2)\frac{g^3+1}{g^5} - (\gamma_1 - g\gamma_2)^2\frac{1}{g^5}\,. \qquad \square$$

C.4.#48. The equation of Chua's circuit can be re-parametrized in a way so that the system is written as

$$\begin{aligned}\dot{x} &= a(y + c_0 x - c_1 x^3)\,,\\ \dot{y} &= x - y + z\,,\\ \dot{z} &= -by\,.\end{aligned} \tag{C.4.4}$$

Then, y becomes a fast variable in the limit $(a,b)\to 0$, and all the dynamics of the original system (C.4.4) concentrates on the slow manifold $y = x + z$. The corresponding slow system is given by the following set of equations

$$\begin{aligned}\dot{x} &= \gamma(x + z + c_0 x - c_1 x^3)\,,\\ \dot{z} &= -x - z\,,\end{aligned} \tag{C.4.5}$$

where $\gamma = a/b$ is a parameter. Let us solve the first equation for z:

$$z = \dot{x}/\gamma - x - c_0 x + c_1 x^3\,,$$

and substitute this expression into the second equation in (C.4.5)

$$\dot{z} = -\dot{x}/\gamma + c_0 x - c_1 x^3\,.$$

Since

$$\dot{z} = \ddot{x}/\gamma - (1 + c_0 - 3c_1 x^2))\dot{x}\,,$$

we obtain

$$\ddot{x} - (\gamma(1 + c_0 - 3c_1 x^2) - 1)\dot{x} + \gamma(c_0 x - c_1 x^3) = 0\,.$$

Letting $\dot{x} = u$, we can rewrite this equation in the form

$$\begin{aligned}\dot{x} &= u\,,\\ \dot{u} &= c_0 x + (\gamma - 1 + \gamma c_0)y - 3\gamma c_1 x^2 y - \gamma c_1 x^3\,,\end{aligned}$$

which can be identified as the Khorozov-Takens normal form. $\square$

C.4.#49. Derivation of the normal form for an equilibrium state with three zero characteristic exponents in the model of a laser with saturable absorber [191]:

$$\begin{aligned}
\dot{E} &= -E + P_1 + P_2\,, \\
\dot{P}_1 &= -\delta_1 P_1 - E(m_1 + M_1)\,, \\
\dot{P}_2 &= -\delta_2 P_2 - E(m_2 + M_2)\,, \\
\dot{M}_1 &= -\rho_1 M_1 + E P_1\,, \\
\dot{M}_2 &= -\rho_2 M_2 + \beta E P_2\,.
\end{aligned} \tag{C.4.6}$$

Here E, P_1, and P_2 are the slow envelopes of electric field and atomic polarizations in the active and passive media. M_1 and M_2 are the deviations of the population differences in the active and passive medium from their values $m_1 < 0$ and $m_2 > 0$ in the absence of a laser field. δ_1 and δ_2 (ρ_1 and ρ_2) are transverse (longitudinal) relaxation rates in the active and passive media normalized by the cavity relaxation rate, β is the ratio of the saturation intensities of the intracavity media.

Linear stability of the trivial steady state

$$E = P_1 = P_2 = M_1 = M_2 = 0$$

is determined by the eigenvalues of the Jacobian matrix

$$\mathrm{J} = \begin{pmatrix}
-1 & 1 & 1 & 0 & 0 \\
-m_1 & -\delta_1 & 0 & 0 & 0 \\
-m_2 & 0 & -\delta_2 & 0 & 0 \\
0 & 0 & 0 & -\rho_1 & 0 \\
0 & 0 & 0 & 0 & -\rho_2
\end{pmatrix},$$

which are the roots of the characteristic equation

$$(\lambda^3 + a_2\lambda^2 + a_1\lambda + a_0)(\lambda + \rho_1)(\lambda + \rho_2)\,,$$

where

$$\begin{aligned}
a_2 &= 1 + \delta_1 + \delta_2\,, \\
a_1 &= m_1 + m_2 + \delta_1 + \delta_2 + \delta_1\,\delta_2\,, \\
a_0 &= m_2\delta_1 + m_1\delta_2 + \delta_1\delta_2\,.
\end{aligned}$$

Let $\delta_1 - \delta_2 > 0$, then at the codimension-three point given by

$$\begin{aligned} m_1 = m_{01} &= -\frac{\delta_1^2(1+\delta_2)}{\delta_1-\delta_2} < 0\,, \\ m_2 = m_{02} &= \frac{\delta_2^2(1+\delta_1)}{\delta_1-\delta_2} > 0, \qquad \rho_1 = 0\,, \end{aligned} \tag{C.4.7}$$

the Jacobian matrix J has a triply degenerate zero eigenvalue with geometric multiplicity two:

$$\lambda_{1,2,3} = 0, \quad \lambda_4 = \rho_2, \quad \lambda_5 = -\Lambda = -(1+\delta_1+\delta_2)\,.$$

By introducing the linear transformation of the coordinates

$$\begin{pmatrix} x_1 \\ x_2 \\ x_3 \\ x_4 \\ x_5 \end{pmatrix} = U \begin{pmatrix} E \\ P_1 \\ P_2 \\ M_1 \\ M_2 \end{pmatrix},$$

where

$$U = \begin{pmatrix} 1+\delta_2 & \dfrac{\delta_1(1+\delta_2)-\delta_2}{\delta_1^2} & 1 & 0 & 0 \\ \delta_2 & \dfrac{\delta_2}{\delta_1} & 1 & 0 & 0 \\ 0 & 0 & 0 & 1 & 0 \\ -(1+\delta_1) & \dfrac{1+\delta_1}{1+\delta_2} & 1 & 0 & 0 \\ 0 & 0 & 0 & 0 & 1 \end{pmatrix}$$

is such that

$$\mathrm{UJU}^{-1} = \begin{pmatrix} 0 & 1 & 0 & 0 & 0 \\ 0 & 0 & 0 & 0 & 0 \\ 0 & 0 & 0 & 0 & 0 \\ 0 & 0 & 0 & -\Lambda & 0 \\ 0 & 0 & 0 & 0 & -\rho_2 \end{pmatrix},$$

the system (C.4.6) assumes the form

$$\dot{x}_1 = x_2 - \frac{1}{\Lambda^2}\left[\frac{\delta_1 - \delta_2(1-\delta_1)}{{\delta_1}^2}(x_3+\xi_1) + (x_5+\xi_2)\right] S(x_1,x_2,x_4)\,,$$

$$\dot{x}_2 = -\frac{1}{\Lambda^2}\left(\frac{\delta_2}{\delta_1}(x_3+\xi_1) + (x_5+\xi_2)\right) S(x_1,x_2,x_4)\,,$$

$$\dot{x}_3 = -\rho_1 x_3 - \frac{m_{01}}{\Lambda^4}[\Lambda x_1 - (1+\Lambda)x_2 + x_4] S(x_1,x_2,x_4)\,,$$

$$\dot{x}_4 = -\Lambda x_4 - \frac{1}{\Lambda^2}\left(\frac{1+\delta_1}{1+\delta_2}(x_3+\xi_1) + (x_5+\xi_2)\right) S(x_1,x_2,x_4)\,,$$

$$\dot{x}_5 = -\rho_2 x_5 - \frac{\beta}{\Lambda^4}\left[\frac{m_{02}}{\delta_2^2}(\Lambda\delta_1\delta_2 x_1 - (\Lambda\delta_1 - \delta_2)(1+\delta_2)x_2) - \frac{\delta_2^2 m_{01}}{\delta_1^2}x_4\right]$$
$$\times\, S(x_1,x_2,x_4)\,.$$

Here m_{01} and m_{02} are defined in (C.4.7), $\xi_1 = m_1 - m_{01}$, $\xi_2 = m_2 - m_{20}$ and ρ_1 are small parameters, and

$$S(x_1,x_2,x_4) = \delta_1\Lambda(x_1 - x_2) + (1+\delta_2)(x_2 - x_4)\,.$$

After reduction to center manifold (we simply substitute $x_4 = x_5 = 0$ into the first three equations) we obtain (the dots stand for the terms of order 3 and higher):

$$\dot{x}_1 = x_2 + ax_1(x_3+\xi_1) + bx_2(x_3+\xi_1) + \xi_2 s(x_1,x_2) + \cdots\,,$$

$$\dot{x}_2 = -cx_1(x_3+\xi_1) + dx_2(x_3+\xi_1) + \xi_2 s(x_1,x_2) + \cdots\,,$$

$$\dot{x}_3 = -\rho_1 x_3 + ex_1^2 + fx_1x_2 + gx_2^2 + \cdots\,,$$

where

$$s(x_1,x_2) = -\frac{\delta_1}{\Lambda}x_1 - \frac{1+\delta_2-\delta_1\Lambda}{\Lambda^2}x_2, \qquad a = -\frac{\delta_1 - (1-\delta_1)\delta_2}{\Lambda\delta_1}\,,$$

$$b = \frac{(\delta_1 - (1-\delta_1)\delta_2)(\Lambda\delta_1 - (1+\delta_2))}{\Lambda^2\delta_1^2}, \qquad c = \frac{\delta_2}{\Lambda}\,,$$

$$d = \frac{\delta_2(\Lambda\delta_1 - 1 - \delta_2)}{\Lambda^2\delta_1}, \qquad e = -\frac{\delta_1 m_{01}}{\Lambda^2}$$

and

$$f = \frac{m_{01}(\delta_1(1+2\Lambda)-1-\delta_2)}{\Lambda^3}, \qquad g = -\frac{m_{01}(1+\Lambda)(\Lambda\delta_1-1-\delta_2)}{\Lambda^4}\,.$$

Finally, applying the coordinate transformation

$$\begin{aligned} x_1 &= z_1\,,\\ x_2 &= z_2 - az_1(z_3+\xi_1) - bz_2(z_3+\xi_1) - \xi_2 s(z_1,z_2)\,,\\ x_3 &= z_3 + \frac{f}{2}z_1^2 + gz_2z_1\,, \end{aligned}$$

we obtain

$$\begin{aligned} \dot z_1 &= z_2 + \cdots\,,\\ \dot z_2 &= \epsilon_1 z_1 + \epsilon_2 z_2 - cz_1z_3 + d'z_2z_3 + \cdots\,,\\ \dot z_3 &= -\rho_1 z_3 + ez_1^2 + \cdots\,, \end{aligned} \tag{C.4.8}$$

where

$$c = \frac{\delta_2}{\Lambda}, \qquad e = -\frac{\delta_1 m_{01}}{\Lambda^2}, \qquad d' = -\frac{1+\delta_1}{\Lambda^2}\,,$$

and the small parameters $\varepsilon_{1,2}$ are given by

$$\varepsilon_1 = -\frac{\xi_1\delta_2+\delta_1\xi_2}{\Lambda}, \qquad \varepsilon_2 = -\frac{(1+\delta_1)\xi_1+(1+\delta_2)\xi_2}{\Lambda^2}\,.$$

We can rescale the small parameters as follows:

$$\epsilon_1 = \varepsilon^2 \qquad \epsilon_2 = \mu\varepsilon, \qquad \rho_1 = \rho\varepsilon\,.$$

By neglecting the third order terms and rescaling the variables $z_1 = x\varepsilon^{3/2}/\sqrt{ce}$, $z_2 = y\varepsilon^{5/2}/\sqrt{ce}$, $z_3 = z\varepsilon^2/c$, we arrive at the following asymptotic normal form

$$\frac{dx}{d\tau} = y, \qquad \frac{dy}{d\tau} = x + \mu y - xz, \qquad \frac{dz}{d\tau} = -\rho z + x^2 \tag{C.4.9}$$

which coincides with the Shimizu-Morioka model. □

C.4.#50. Let a Jacobian of the system linearized at the equilibrium state have three zero eigenvalues. In addition, let the system on the center manifold

possess the symmetry $(x, y, z) \to (-x, -y, z)$, where y, z are the coordinate projections on the eigenvectors and x is the projection onto the adjoined vector. Then, generically, the system may be reduced to the following form

$$\begin{aligned}
&\dot{x} = y\,,\\
&\dot{y} = x[\bar{\mu} - az(1 + g(x, y, z)) - a_1(x^2 + y^2)(1 + \cdots)]\\
&\qquad - y[\bar{\alpha} + a_2 z(1 + \cdots) + a_3(x^2 + y^2)(1 + \cdots)]\,,\\
&\dot{z} = -\bar{\beta} + z^2(1 + \cdots) + b(x^2 + y^2)(a + \cdots)\,,
\end{aligned} \tag{C.4.10}$$

where $a_i \neq 0$, $i = 1, 2, 3$ and $b \neq 0$. Here, $\bar{\mu}$, $\bar{\alpha}$ and $\bar{\beta}$ are small parameters, and g and the dots denote the terms which vanish at the origin. Suppose $ab > 0$. Let $\tau^2 = \mu + a\sqrt{\bar{\beta}}(1 + g(0, 0, -\sqrt{\bar{\beta}})) > 0$, $\bar{\beta} > 0$. By scaling the time $t \to s/\tau$, changing the variables

$$x \to x\sqrt{\frac{\tau^3}{ab}}, \qquad y \to \tau y\sqrt{\frac{\tau^3}{ab}}, \qquad z \to -\sqrt{\bar{\beta}} + \frac{\tau^2}{a} z$$

and defining the new parameters as $\bar{\alpha} = \alpha\tau$ and $\bar{\beta} = (\beta\tau/2)^2$, we obtain the following system

$$\begin{aligned}
&\dot{x} = y\\
&\dot{y} = x(1 - z) - \alpha y + O(\tau)\,,\\
&\dot{z} = -\beta z + x^2 + O(\tau)\,,
\end{aligned} \tag{C.4.11}$$

where α and β are parameters which are no longer small. Dropping the terms of order τ, we obtain the Shimizu-Morioka model. □

C.4.#51. In addition to the conditions of the above case, let the system be invariant with respect to the involution $(x, y, z) \to (x, y, -z)$, i.e. it possesses two symmetries. The normalized system can then be recast as

$$\begin{aligned}
&\dot{x} = y\,,\\
&\dot{y} = x[\bar{\mu} - az^2(1 + g(x, y, z^2)) - b(x^2 + y^2)(1 + \cdots)]\\
&\qquad - y[\bar{\alpha} + a_1 z^2(1 + \cdots) + b_1(x^2 + y^2)(1 + \cdots)]\,,\\
&\dot{z} = z(\bar{\beta} - cz^2(1 + \cdots) + d(x^2 + y^2)(a + \cdots)\,.
\end{aligned} \tag{C.4.12}$$

Suppose $c > 0$ and $ad > 0$. In the parameter region $\tau^2 = \bar{\mu} - a\bar{\beta}c(1 + g(0, 0, \bar{\beta}/c)) > 0$ and $\beta > 0$, let us introduce the renormalization:

$$t \to s/\tau, \quad x \to x\tau\sqrt{\frac{c}{ad}}, \quad y \to \tau^2 y\sqrt{\frac{c}{ad}}, \quad z \to \sqrt{\frac{\bar{\beta}}{c} + \frac{\tau^2}{a}}z$$

and $\bar{\alpha} = \tau\alpha$, $\bar{\beta} = \tau\beta/2$. Denoting $B = \frac{bc}{ad}$ and omitting the terms of order τ we arrive at the following system

$$\begin{aligned} \dot{x} &= y\,, \\ \dot{y} &= x(1 - z) - \alpha y + Bx^3\,, \\ \dot{z} &= -\beta(z - x^2)\,. \end{aligned} \tag{C.4.13}$$

The above system is remarkable because the Lorenz equation can be reduced to it when $r > 1$. The relations between the parameters of two systems are given by

$$\beta = \frac{b}{\sigma(r-1)}, \quad \alpha = \frac{1+\sigma}{\sigma(r-1)}, \quad B = \frac{b}{2\sigma - b}\,.$$

It follows from the above relations that the region of the positive parameters (r, b, σ) in the Lorenz equation is bounded by the plane $\beta = 0$ and the surface $\frac{\alpha}{\beta} = \frac{1}{2}(\frac{1}{B} + 1)$, which tends to $\beta = 0$ as $B \to 0$.

We should also note that the Shimizu-Morioka system is a particular case (i.e. $B = 0$) of the Lorenz system in the form (C.4.13). □

C.4.#52. *The bifurcation of a periodic orbit with three multipliers* $+1$. On the center manifold we introduce the coordinates (x, y, z, ψ), where ψ is the angular coordinate and (x, y, z) are the normal coordinates (see Sec. 3.10). Assuming that the system is invariant under the transformation $(x, y) \to (-x, -y)$, the normal form truncated up to second order terms is given by

$$\begin{aligned} \dot{x} &= y\,, \\ \dot{y} &= x(\bar{\mu} - az) - y(\bar{\alpha} + a_2 z)\,, \\ \dot{z} &= -\bar{\beta} + z^2 + b(x^2 + y^2)\,, \\ \dot{\psi} &= 1\,, \end{aligned} \tag{C.4.14}$$

where the periodic orbit is supposed to be of period 1. Because the first three equations in the above system are independent of the fourth one, the resulting normal form is analogous to the Shimizu-Morioka system. □

C.4.#53. Below we present (following [185]) a *list* of asymptotic normal forms which describe the trajectory behavior of a triply-degenerate equilibrium state near a stability boundary in systems with discrete symmetry. We say there is a *triple instability* when a dynamical system has an equilibrium state such that the associated linearized problem has a triplet of zero eigenvalues. In such a case, the analysis is reduced to a three-dimensional system on the center manifold. Assuming that (x, y, z) are the coordinates in the three-dimensional center manifold and a bifurcating equilibrium state resides at the origin, we suppose also that our system is equivariant with respect to the transformation $(x, y, z) \leftrightarrow (-x, -y, z)$.

We note that the listed systems have a natural "physical" meaning and do appear in some realistic applications, see for example the above laser equations. Thus, this method may be viewed as a recipe for exclusion of irrelevant terms in the nonlinearity as well as for selection of those nonlinear terms which are responsible for specific details of such behavior.

In addition to the symmetry assumption, we will also suppose that the linear part of the system near the origin O restricted to the invariant plane $z = 0$ has a complete Jordan block. Then, the system in the restriction to the center manifold may locally be written in the form

$$\begin{cases} \dot{x} = y\,, \\ \dot{y} = x(az + F(x^2, xy, y^2, z)) + yG(y^2, z)\,, \\ \dot{z} = H(x^2, xy, y^2, z)\,, \end{cases} \tag{C.4.15}$$

where neither $H(0, 0, 0, z)$ nor $F(0, 0, 0, z)$ contain linear terms.

Let us consider a three-parameter perturbation of the system in the form

$$\begin{cases} \dot{x} = y\,, \\ \dot{y} = x(\mu_1 + az + F(x^2, xy, y^2, z)) + y(-\mu_2 + G(y^2, z))\,, \\ \dot{z} = -\mu_3 z + H(x^2, xy, y^2, z)\,, \end{cases} \tag{C.4.16}$$

where $\mu = (\mu_1, \mu_2, \mu_3)$ are small parameters, and the functions F, G and H may also depend on μ.

Let us also suppose that

$$a \neq 0\,. \tag{C.4.17}$$

It is then obvious that a change of the z-coordinate reduces (C.4.16) to the following form (with some new functions G and H)

$$\begin{cases} \dot{x} = y\,, \\ \dot{y} = x(\mu_1 - z) + y(-\mu_2 + G(y^2, z))\,, \\ \dot{z} = -\mu_3 z + H(x^2, xy, y^2, z)\,. \end{cases} \tag{C.4.18}$$

Let us rescale the variables and time:

$$x \to \delta_x x, \quad y \to \delta_y y, \quad z \to \delta_z z, \quad t \to t/\tau\,,$$

where δ_x, δ_y, δ_z and τ are some small quantities. We assume $\mu_1 \neq 0$ and let

$$\delta_y = \tau\delta_x, \quad \delta_z = \tau^2 = |\mu_1|\,.$$

Then (C.4.18) assumes the form

$$\begin{cases} \dot{x} = y\,, \\ \dot{y} = x(\pm 1 - z) - \lambda y + O(\tau)\,, \\ \dot{z} = -\alpha z + H(\delta_x^2\, x^2, \tau\delta_x^2\, xy, \tau^2\delta_x^2\, y^2, \tau^2 z)/\tau^3\,, \end{cases} \tag{C.4.19}$$

where α and λ are new rescaled parameters, which are no longer small:

$$\alpha = \mu_3/\sqrt{|\mu_1|}, \quad \lambda = \mu_2/\sqrt{|\mu_1|}\,.$$

The asymptotic normal form is a finite limit of the system (C.4.19) as $\mu \to 0$. Note that different choices of proportion between the scaling factors δ_x and τ yield different normal forms.

In the last equation of (C.4.19), the terms which contain z^2, y^3 and yz, tend to zero as $\tau \to 0$. Thus, by cutting out small terms, we transform (C.4.19) to

$$\begin{cases} \dot{x} = y\,, \\ \dot{y} = x(\pm 1 - z) - \lambda y\,, \\ \dot{z} = -\alpha z + \delta_x^2 x^2 H_1(\delta_x^2 x^2)/\tau^3 + \delta_x^2 xy H_2(\delta_x^2 x^2)/\tau^2 \\ \qquad + \delta_x^2 y^2 H_3(\delta_x^2 x^2)/\tau + \delta_x^2 z x^2 H_4(\delta_x^2 x^2)/\tau\,. \end{cases} \tag{C.4.20}$$

The right-hand side in (C.4.20) is to be finite, i.e. if the Taylor expansions of the functions H_i begin with x^{2m_i} for zero values of the perturbation parameters

μ_1, μ_2, and μ_3, then the following inequalities must hold

$$\delta_x^{2(m_1+1)}/\tau^3 < \infty\,,$$
$$\delta_x^{2(m_2+1)}/\tau^2 < \infty\,,$$
$$\delta_x^{2(m_3+1)}/\tau < \infty\,,$$
$$\delta_x^{2(m_4+1)}/\tau < \infty\,.$$

Therefore, we can choose τ so that

$$\tau \sim \delta_x^{\beta}\,, \tag{C.4.21}$$

where

$$\beta = \min\left\{\frac{2}{3}(m_1+1),\ m_2+1,\ 2(m_3+1),\ 2(m_4+1)\right\}. \tag{C.4.22}$$

For example, in the most generic case where $H_i(0) \neq 0$ $(i = 1, \ldots, 4)$, the exponent $\beta = 2/3$ in (C.4.21) and (C.4.22). Then, system (C.4.20) reduces to the form

$$\begin{cases} \dot{x} = y\,, \\ \dot{y} = x(\pm 1 - z) - \lambda y\,, \\ \dot{z} = -\alpha z + x^2 H_1(0) + O(\tau)\,. \end{cases} \tag{C.4.23}$$

In the limit $\tau \to 0$, this system becomes the Shimizu-Marioka model, where the parameters α and λ may take arbitrary finite values.

Let us now consider an extra degeneracy: $H_1(0) = 0$ and $H_1'(0) \neq 0$. In order to study bifurcations in this case one should introduce a new independent governing parameter which is the constant term of the Taylor expansion of H_1. If we set $\beta = 1$ according to relation (C.4.22), then system (C.4.20) reduces to the following asymptotic form:

$$\begin{cases} \dot{x} = y\,, \\ \dot{y} = x(\pm 1 - z) - \lambda y\,, \\ \dot{z} = -\alpha z + x^2 \tilde{h}_{10} + H_2(0) xy\,. \end{cases} \tag{C.4.24}$$

This is equivalent to the Lorenz equations. Here, $\tilde{h}_{10} = H_1(0)/\tau$ is the third rescaled governing parameter which may take arbitrary finite values.

The next degeneracy $H_2(0) = 0$, $H_2'(0) \neq 0$ modifies the third equation in (C.4.24) in the following way:

$$\dot{z} = -\alpha z + x^2\tilde{h}_{10} + \tilde{h}_{20}xy + H_1'(0)x^4\,, \tag{C.4.25}$$

where $\tilde{h}_{10} = H_1(0)/\tau^{3/2}$ and $\tilde{h}_{20} = H_2(0)/\tau^{1/2}$. Here, $\beta = 4/3$.

By repeating this procedure we can get a hierarchy of the asymptotic normal forms. Let us denote

$$H_i(x^2) = \sum_j^{\infty} H_{ij}x^{2j}\,.$$

We assume that at the moment of bifurcation the values of H_{ij} for $j = 0, \ldots, m_i - 1$ vanish. As before, we can treat these non-zero H_{ij} as additional independent small parameters.

It is obvious that in the rescaled system (C.4.20) there are non-zero coefficients in front of those terms which correspond to such m_i for which the minimum in (C.4.22) is achieved; all terms of higher order vanish in the limit $\tau \to 0$. The terms of degree less then $2m_i$, which appear in H_i for non-zero parameter values, also survive after the rescaling; their normalized coefficients appear as the independent parameters that may assume arbitrary finite values.

Thus, if we get rid of all asymptotically vanishing terms, system (C.4.20) takes the form

$$\begin{cases} \dot{x} = y\,, \\ \dot{y} = x(\pm 1 - z) - \lambda y\,, \\ \dot{z} = -\alpha z + x^2\tilde{H}_1(x^2) + xy\tilde{H}_2(x^2) + y^2\tilde{H}_3(x^2) + zx^2\tilde{H}_4(x^2)\,, \end{cases} \tag{C.4.26}$$

where $\tilde{H}_i$'s are polynomials of degree n_i such that

$$\begin{aligned} &\max\left\{\frac{2}{3}(n_1+1),\ n_2+1,\ 2(n_3+1),\ 2(n_4+1)\right\} \\ &\qquad = \frac{1}{\beta} < \min\left\{\frac{2}{3}(n_1+2),\ n_2+2,\ 2(n_3+2),\ 2(n_4+2)\right\} \end{aligned} \tag{C.4.27}$$

(if some $\tilde{H}_i$ vanish identically, then we let $n_i = -1$). The coefficients of $\tilde{H}_{ij}$ are defined as follows:

$$\tilde{h}_{ij} = H_{ij}/\tau^{s_i - \frac{2(j+1)}{\beta}}\,,$$

where $s_1 = 3, s_2 = 2, s_3 = s_4 = 1$.

It follows immediately from (C.4.27) that $n_3 = n_4$, i.e. the degrees of $\tilde{H}_3$ and $\tilde{H}_4$ are always equal. Hence, the list of asymptotic normal forms which are given by (C.4.26) and (C.4.27) can be ordered as the common degree $n(= n_3 = n_4)$ increases.

The first in the list are the systems given by (C.4.23), (C.4.24) and (C.4.25), which correspond to $n = -1$. For each of the greater values of n there are four sub-cases below. Each consecutive case corresponds to additional degeneracies. This is a cyclic list: after the fourth case, we return to the beginning with $n = n + 1$ and so forth.

(1) $n_1 = 3n + 2$, $n_2 = 2n + 1$; at the moment of bifurcation the first $(n-1)$ coefficients vanish in both H_3 and H_4, the first $2n$ and $(3n+1)$ coefficients vanish in H_2 and H_1, respectively.
(2) $n_1 = 3n + 3$, $n_2 = 2n + 1$; at the moment of bifurcation the first n coefficients vanish in both H_3 and H_4, the first $(2n + 1)$ and $(3n + 2)$ coefficients vanish in H_2 and H_1, respectively.
(3) $n_1 = 3n + 3$, $n_2 = 2n + 2$; at the moment of bifurcation the first n coefficients vanish in both H_3 and H_4, the first $(2n + 1)$ and $(3n + 3)$ coefficients vanish in H_2 and H_1, respectively.
(4) $n_1 = 3n + 4$, $n_2 = 2n + 2$; at the moment of bifurcation the first n coefficients vanish in both H_3 and H_4, the first $(2n + 2)$ and $(3n + 3)$ coefficients vanish in H_2 and H_1, respectively. □

C.5 Behavior on stability boundaries

C.5.#54. A stable limit cycle bifurcates from infinity in the system

$$\begin{aligned} \dot{x} &= x - y - a(x^2 + y^2)x\,, \\ \dot{y} &= x + y - a(x^2 + y^2)y\,, \end{aligned} \tag{C.5.1}$$

at $a = 0$. At this value, the system becomes linear

$$\begin{aligned} \dot{x} &= x - y\,, \\ \dot{y} &= x + y\,, \end{aligned} \tag{C.5.2}$$

and it has an unstable focus at the origin. One can compose the Lyapunov function $V(x, y) = x^2 + y^2$ and verify that all the orbits diverge to infinity (i.e. the infinity is stable) since the time derivative of the Lyapunov function

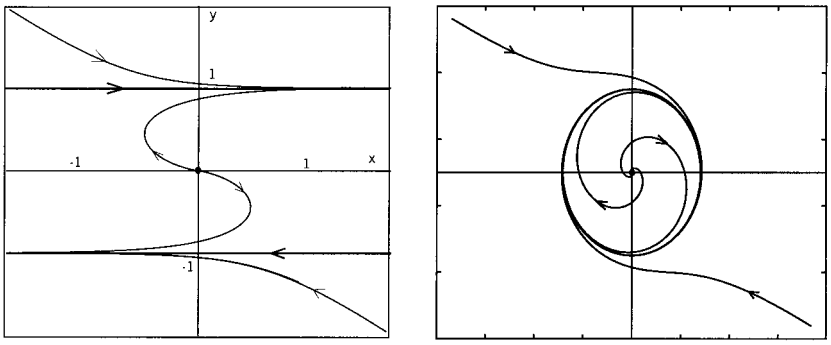

(a) (b)

Fig. C.5.1. Limit cycle in (C.5.3) for $a > 0$ (b) and at $a = 0$ (a).

$\dot{V}(x, y) = 2(x^2 + y^2)$ is positive, and hence each level $(x^2 + y^2) = C$ is a curve without contact and every trajectory must flow outside of every such curve C as time increases.

When $a \neq 0$, we have

$$\frac{d\,(x^2 + y^2)}{dt} = 2(x^2 + y^2)(1 - a(x^2 + y^2))\,.$$

It is apparent that $\dot{V}(x, y) < 0$ if $x^2 + y^2 > 1/a$, and $\dot{V}(x, y) > 0$ when $V < 1/a$. Thus, $x^2 + y^2 = 1/a$ is a stable invariant curve (a limit cycle), and all trajectories (except for the equilibrium state at the origin) tend to it as $t \to +\infty$.

C.5.#55. [25] Explain how the stable limit cycle in Fig. C.5.1 of the system

$$\begin{aligned} \dot{x} &= y - x(ax^2 + y^2 - 1)\,, \\ \dot{y} &= -ay - y(ax^2 + y^2 - 1) \end{aligned} \tag{C.5.3}$$

evolves as $a \to +0$. □

C.5.#56. Find a Lyapunov function for Khorozov-Takens normal form

$$\begin{aligned} \dot{x} &= y\,, \\ \dot{y} &= -x^3 - x^2 y\,. \end{aligned}$$

□

C.5.#57. Reveal the role of the cubed y in making the following system asymptotically stable: find a proper Lyapunov function.

$$\dot{x} = y\,,$$
$$\dot{y} = ay + x - x^3 - by^3\,.$$

Here a and b are some control parameters. □

C.5.#58. Prove the global asymptotic stability of solutions of the Lorenz equation

$$\begin{aligned} \dot{x} &= -\sigma(x-y)\,, \\ \dot{y} &= rx - y - xz\,, \\ \dot{z} &= -bz + xy\,, \end{aligned} \tag{C.5.4}$$

when $r < 1$, $\sigma > 0$ and $b > 0$.

The following function

$$V_0(x,y,z) = \frac{1}{2}(x^2 + \sigma y^2 + \sigma z^2)$$

is a Lyapunov function, since its time derivative

$$\dot{V}_0 = -\sigma(x^2 - (1-r)xy + y^2 + bz^2)$$

is a negatively defined quadratic form. □

C.5.#59. Prove that the infinity is unstable in the Lorenz system.

Solution. The time derivative of the function

$$V(x,y,z) = \frac{x^2}{2} + \frac{y^2}{2} + (z - r - \sigma)^2$$

is given by

$$\dot{V}(x,y,z) = x\dot{x} + y\dot{y} + (z-\sigma-r)\dot{z} = -\sigma x^2 - y^2 - b\left(z - \frac{r+\sigma}{2}\right)^2 + \frac{b}{4}(r+\sigma)^2\,.$$

The condition $\dot{V} = 0$ determines an ellipsoid outside of which the derivative is negative. Therefore, all "outer" positive semi-trajectories of the Lorenz system flow inside the surface

$$\sigma x^2 + y^2 + b\left(z - \frac{r+\sigma}{2}\right)^2 = \frac{b}{4}(r+\sigma)^2\,.$$ □

C.5.#60. Prove that infinity is unstable in a Chua's circuit modeled by

$$\begin{aligned} \dot{x} &= a(y + x/6 - x^3/6)\,, \\ \dot{y} &= x - y + z\,, \\ \dot{z} &= -by\,. \end{aligned} \tag{C.5.5}$$

Use the Lyapunov function

$$V_0(x, y, z) = \frac{x^2}{2a} + \frac{y^2}{2} + \frac{z^2}{2b}\,,$$

and analyze its time-derivative

$$\dot{V}_0 = \frac{x\dot{x}}{a} + y\dot{y} + \frac{z\dot{z}}{b} = \frac{1}{6}(x^2 - x^4) + 2xy - y^2$$

for large x and y. □

C.5.#61. Consider the following perturbation of the Bogdanov-Takens normal form:

$$\begin{aligned} \dot{x} &= y\,, \\ \dot{y} &= \mu y - \varepsilon^2 x + a_{20}x^2 + a_{11}xy + a_{02}y^2 + Q(x, y)\,, \end{aligned} \tag{C.5.6}$$

where μ and ε are small, and $Q(x, y)$ starts with cubic terms. One can see that the origin $O(0, 0)$ is a weak focus for the above system at $\mu = 0$ and small $\varepsilon \neq 0$: the characteristic roots are $\pm i\varepsilon$. To determine the stability of the weak focus, let us rescale first the variables $x \mapsto \varepsilon^2 x$, $y \mapsto \varepsilon^3 y$, and the time $t \mapsto \varepsilon^{-1}t$. The system will take the form

$$\begin{aligned} \dot{x} &= y\,, \\ \dot{y} &= -x + a_{20}x^2 + \varepsilon a_{11}xy + O(\varepsilon^2)\,. \end{aligned} \tag{C.5.7}$$

The following normalizing coordinate transformation

$$x_{\text{new}} = x - \frac{a_{20}}{3}(x^2 + 2y^2) + \frac{\varepsilon}{3}a_{11}xy, \qquad y_{\text{new}} = \dot{x}_{\text{new}}$$

brings the system to the form

$$\begin{aligned} &\dot{x} = y\,, \\ &\dot{y} = -x + 2a_{20}^2\left(x^3 - \frac{4}{3}xy^2\right) + \varepsilon a_{20}a_{11}\left(5x^2y - \frac{4}{3}y^3\right) + O(\varepsilon^2) + \cdots\,, \end{aligned}$$

where the dots stand for the terms of order higher than three. So, we eliminate all quadratic terms (up to $O(\varepsilon^2)$-terms) and now the first Lyapunov value can be immediately computed. Thus, let us introduce the complex variable $z = x + iy$ so that the system will recast as

$$\dot{z} = -iz + \left(\frac{\varepsilon}{8}a_{20}a_{11} + i\frac{5}{12}a_{20}^2 + O(\varepsilon^2)\right) z^2 z^* + \cdots ,$$

where the dots stand for negligible cubic and higher order terms. The first Lyapunov value is the real part of the coefficient of $z^2 z^*$, i.e. it is equal to

$$L_1 = \frac{\varepsilon}{8}[a_{20}a_{11} + O(\varepsilon)] .$$

It follows that the weak focus is stable when $a_{20}a_{11} < 0$, and unstable for $a_{20}a_{11} > 0$ for small ε. At $\varepsilon \neq 0$, only one limit cycle is born from the weak focus, provided $a_{20}a_{11} \neq 0$. □

C.5.#62. Let us give a general formula for the first Lyapunov value at a weak focus of the three-dimensional system

$$\dddot{\xi} + P\ddot{\xi} + Q\dot{\xi} + R\xi = f(\xi, \dot{\xi}, \ddot{\xi})$$

where f is a nonlinearity, i.e. its Taylor expansion at the origin begins with quadratic terms, and the coefficients P, Q, R satisfy the relation

$$PQ = R, \qquad Q > 0 .$$

Denoting $y \equiv (y_1, y_2, y_3) = (\xi, \dot{\xi}, \ddot{\xi})$ we can rewrite the above equation as

$$\dot{y} = Ay + f(y) \cdot \begin{pmatrix} 0 \\ 0 \\ 1 \end{pmatrix} ,$$

where

$$A = \begin{pmatrix} 0 & 1 & 0 \\ 0 & 0 & 1 \\ -R & -Q & -P \end{pmatrix} .$$

The eigenvalues of the matrix A are $-P$ and $\pm i\omega$, with $\omega^2 = Q$. The corresponding eigenvectors are

$$\begin{pmatrix} 1 \\ -P \\ P^2 \end{pmatrix} , \quad \begin{pmatrix} 1 \\ i\omega \\ -Q \end{pmatrix} , \quad \text{and} \quad \begin{pmatrix} 1 \\ -i\omega \\ -Q \end{pmatrix} ,$$

and the eigenvectors of the adjoint matrix are respectively given by

$$\begin{pmatrix} Q \\ 0 \\ 1 \end{pmatrix}, \quad \begin{pmatrix} P\omega \\ \omega - iP \\ -i \end{pmatrix}, \quad \text{and} \quad \begin{pmatrix} P\omega \\ \omega + iP \\ i \end{pmatrix}.$$

Thus, we can introduce the new variables $u \in R^1$ and $z \in C^1$ as follows:

$$y = u \begin{pmatrix} 1 \\ -P \\ P^2 \end{pmatrix} + z \begin{pmatrix} 1 \\ i\omega \\ -Q \end{pmatrix} + z^* \begin{pmatrix} 1 \\ -i\omega \\ -Q \end{pmatrix}.$$

The derivatives $\dot{u}$ and $\dot{z}$ are computed by the following rule

$$\dot{u} = \frac{1}{Q + P^2}(Q\dot{y}_1 + \dot{y}_3), \qquad \dot{z} = \frac{1}{2P\omega}(P\omega\dot{y}_1 + (\omega - iP)\dot{y}_2 - i\dot{y}_3)\,,$$

so that we arrive at the system whose linear part is already diagonal

$$\begin{aligned} \dot{u} &= -Pu + \alpha_1 z^2 + \alpha_2 z z^* + \cdots\,, \\ \dot{z} &= i\omega z + \beta_1 z^2 + \beta_2 z z^* - \beta_1^* z^{*2} + \gamma u z - \gamma^* u z^* + \delta z^2 z^* + \cdots\,, \end{aligned} \tag{C.5.8}$$

where the dots stand for the nonlinear terms which are negligible for the computation of the first Lyapunov value. If we expand the nonlinearity up to the third order in y:

$$f(y) = \sum c_{kj} y_j y_k + \sum d_{kjl} y_k y_j y_l + \cdots\,, \tag{C.5.9}$$

then the coefficients $\alpha, \beta, \gamma, \delta$ in (C.5.8) are found as follows:

$$\begin{aligned} &(Q + P^2)\alpha_1 = 2iP\omega\beta_1 = \textstyle\sum c_{kj}(i\omega)^{k+j-2}\,, \\ &(Q + P^2)\alpha_2 = 2iP\omega\beta_2 = -\textstyle\sum((-1)^k + (-1)^j)c_{kj}(i\omega)^{k+j-2}\,, \\ &\gamma = \frac{1}{2}\textstyle\sum c_{kj}((-P)^{k-2}(i\omega)^{j-2} + (-P)^{j-2}(i\omega)^{k-2})\,, \\ &\delta = -\frac{1}{2PQ^2}\textstyle\sum d_{kjl}(i\omega)^{k+j+l}((-1)^k + (-1)^j + (-1)^l)\,. \end{aligned} \tag{C.5.10}$$

System (C.5.8) has a center manifold given by

$$u = \frac{\alpha_1}{P + i\omega} z^2 + \frac{\alpha_2}{P} z z^* + \cdots\,.$$

On the center manifold the system assumes the form

$$\dot{z} = i\omega z + \beta_1 z^2 + \beta_2 z z^* - \beta_1^* z^{*2} + \left(\gamma \frac{\alpha_2}{P} - \gamma^* \frac{\alpha_1}{P + i\omega} + \delta\right) z^2 z^* + \cdots . \quad \text{(C.5.11)}$$

The normalizing transformation

$$z_{\rm new} = z + i\frac{\beta_1}{\omega} z^2 - i\frac{\beta_2}{\omega} z z^* + i\frac{\beta_1^*}{3\omega} z^{*2}$$

kills all quadratic terms, so that the system on the center manifold takes the form

$$\dot{z} = i\omega z + (L_1 + i\Omega_1) z^2 z^* + \cdots ,$$

where

$$L_1 + i\Omega_1 = \frac{i}{\omega}\left(\beta_1\beta_2 - |\beta_1|^2 - \frac{2}{3}|\beta_2|^2\right) + \gamma\frac{\alpha_2}{P} - \gamma^*\frac{\alpha_1}{P + i\omega} + \delta\,. \quad \text{(C.5.12)}$$

By definition, L_1 is the *first* Lyapunov value. □

C.5.#63. Let us apply the above algorithm to determine the stability of the structurally unstable equilibria $O_{1,2}$ in the Lorenz model, see Sec. C.2. To find whether the corresponding Andronov-Hopf bifurcation is sub- or supercritical on the stability boundary of these equilibria we will compute the analytical expression for the first Lyapunov value L_1.

Following [165, 186], let us first bring the original system

$$\dot{x} = -\sigma(x - y)\,,$$
$$\dot{y} = rx - y - xz\,,$$
$$\dot{z} = -bz + xy$$

to a single third-order differential equation

$$\dddot{x} + (\sigma + b + 1)\ddot{x} + b(1 + \sigma)\dot{x} + b\sigma(1 - r)x = \frac{(1 + \sigma)\dot{x}^2}{x} + \frac{\dot{x}\ddot{x}}{x} - x^2\dot{x} - \sigma x^3\,. \quad \text{(C.5.13)}$$

Then, we introduce the new variable $\xi = x - x_0$, where $x_0 = \pm\sqrt{b(r-1)}$ for $O_{1,2}$, respectively. We stress that only quadratic and cubic terms in the nonlinearity are needed and hence the first order terms of the expansion of

$(x_0+\xi)^{-1}$ are sufficient in order to find the first Lyapunov value. Taking into account the needed terms, the equation (C.5.13) can be rewritten as follows

$$\dddot{\xi} + (\sigma+b+1)\ddot{\xi} + [b(1+\sigma)+x_0^2]\dot{\xi} + [b\sigma(1-r)+3\sigma x_0^2]\xi$$
$$= -3\sigma x_0\xi^2 - 2x_0\xi\dot{\xi} + \frac{1+\sigma}{x_0}\dot{\xi}^2 + \frac{1}{x_0}\dot{\xi}\ddot{\xi} - \sigma\xi^3 - \xi^2\dot{\xi}$$
$$- \frac{1+\sigma}{x_0^2}\xi\dot{\xi}^2 - \frac{1}{x_0^2}\xi\dot{\xi}\ddot{\xi} + \cdots . \qquad \text{(C.5.14)}$$

The stability boundary for both O_1 and O_2 is given by

$$r = \sigma(\sigma+b+3)(\sigma-b-1)^{-1} .$$

The first Lyapunov value computed by the above algorithm is

$$L_1 = b[p^3q(p^2+q)(p^2+4q)(\sigma-b-1)]^{-1}B , \qquad \text{(C.5.15)}$$

where

$$B = [9\sigma^4 + (20-18b)\sigma^3 + (20b^2+2b+10)\sigma^2$$
$$- (2b^3-12b^2-10b+4)\sigma - b^4 - 6b^3 - 12b^2 - 10b - 3] .$$

On the stability boundary, the inequality $\sigma > b+1$ is fulfilled. Upon substituting $\sigma = \sigma_* + b + 1$, the expression for B becomes a polynomial of σ_* and b with positive coefficients. Hence, if $\sigma_* > 0$ and $b > 0$, then $L_1 > 0$. Thus, both equilibria $O_{1,2}$ are unstable (saddle-foci) on the stability boundary. The boundary itself is dangerous in the sense of the definition suggested in Chap. 14. Therefore, the corresponding Andronov-Hopf bifurcation of $O_{1,2}$ is sub-critical. □

C.5.#64. Compute the first Lyapunov value in the Chua's circuit (C.5.5). Verify that for $c_1 = c_3 = 1/6$ it vanishes at the point ($a \simeq 1.72886$, $b \simeq 1.816786$), labeled by $L_1 = 0$ on the Andronov-Hopf curve in Fig. C.2.1. This is the point of codimension two from which a curve of saddle-node periodic orbit originates. □

C.5.#65. Find the expression for the first Lyapunov value in the Shimizu-Marioka system (C.2.25) reduced to the following third order differential equation

$$\dddot{x} + (a+b)\ddot{x} + ab\dot{x} - bx + x^3 - \frac{a}{x}\dot{x}^2 - \frac{\dot{x}\ddot{x}}{x} = 0 . \qquad \text{(C.5.16)}$$

Show that it is negative (positive) to the right (left) of the point ($a \simeq 1.359, b \simeq 0.1123$) on the Andronov-Hopf bifurcation curve given by $(a+b)a - 2 = 0$. □

C.6 Bifurcations of fixed points and periodic orbits

C.6.#66. Consider the *logistic* map

$$\bar{x} = ax(1-x) \equiv f(x)\,,$$

with $0 < a < 4$ and $x \in I = [0,1]$. When $0 < a < 1$, the origin is a unique stable fixed point. It is semi-stable at $a = 1$ since $f'(0) = 1$. It becomes unstable as a increases, and another fixed point $O_1(x_1 = (a-1)/a)$ bifurcates from the origin (hence we have a transcritical bifurcation here). The point O_1 is stable when $1 < a \le a_1 = 3$ [see Fig. C.6.1(a)]. It flip-bifurcates when $f'(O_1) = a - 2ax_1 = -1$ at $a = 3$. The first Lyapunov value at this point is equal to $-\frac{1}{6}(f'''(O_1) + \frac{3}{2}f''(O_1)^2) = -\frac{2}{3}a_1 = -2$. Since it is negative, the point is asymptotically stable at $a = 3$. Thus, a stable cycle C_2 of period 2 bifurcates from O_1 as a exceeds 3, as shown in Fig. C.6.1(b).

The cycle of period two consists of a pair of period-two points

$$x_2^{(1,2)} = \frac{a+1 \pm \sqrt{a^2-2a-3}}{2a}\,,$$

which are the roots of the equation $x = f^2(x)$ other than those corresponding to O and O_1. The direct computation of the multiplier of the cycle, which is given by $f'(x_2^{(1)}) \cdot f'(x_2^{(2)})$, reveals that it is stable when $3 < a < 1 + \sqrt{6}$. Moreover, the multiplier is positive when $3 < a < 1 + \sqrt{5}$, and negative when $1 + \sqrt{5} < a$, but still less than 1 in absolute value. This cycle becomes repelling when $a > 1 + \sqrt{6}$, and its stability switches to the cycle C_4 of period 4, shown in Fig. C.6.1(c). When this cycle goes through the flip bifurcation at $a = a_3 \simeq 3.54$, then a stable period-8 cycle is born, and so forth [see Fig. C.6.2(d)–(f)].

Note that the first Lyapunov value is always negative for a flip-bifurcation of any periodic orbit in the logistic map. Indeed, the Schwarzian derivative:

$$S(f)(x) = \frac{f'''}{f'} - \frac{3}{2}\left(\frac{f''}{f'}\right)^2$$

is negative everywhere within the interval $[0,1]$ where the map is defined. It is easy to check that if for some map $S(f) < 0$ everywhere, then $S(f \circ f \circ \cdots \circ f) < 0$ everywhere too, i.e. it is negative for every power of the map. It remains to note that $\frac{1}{6}S(f)$ coincides with the first Lyapunov value at the fixed point at the moment of flip-bifurcation (when $f'(x) = -1$).

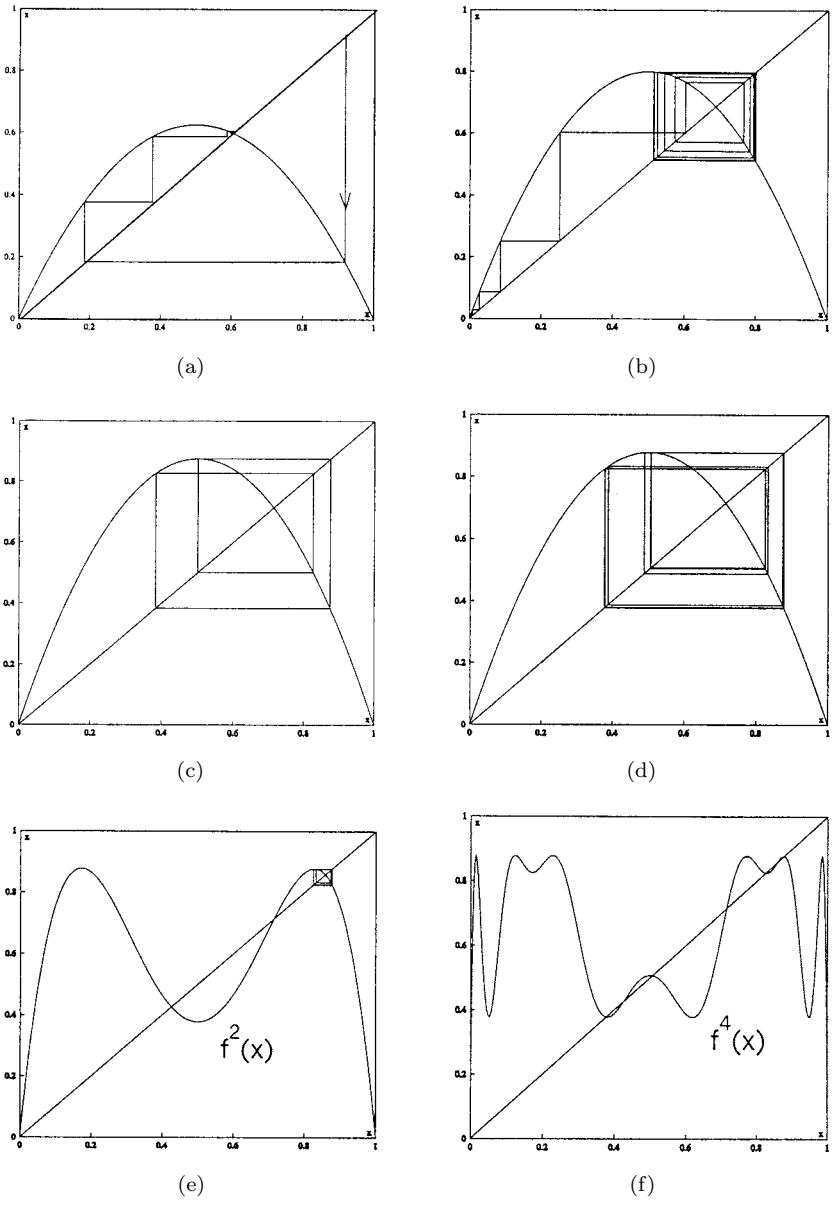

Fig. C.6.1. Period doubling in the logistic map.

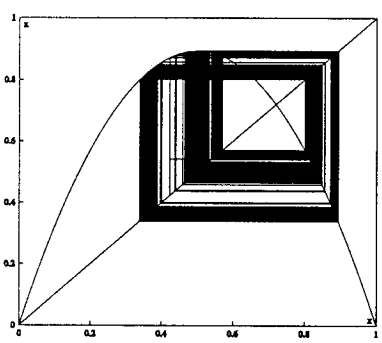

(g)

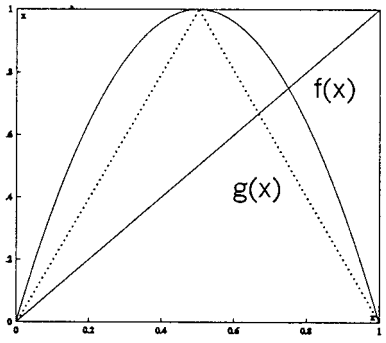

(h)

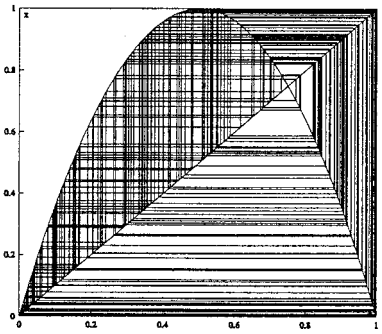

(i)

Fig. C.6.1. (*Continued*)

This sequence of period-doubling bifurcations ends up at approximately $a \simeq 3.569$, after which the logistic map exhibits chaotic behavior, see Fig. C.6.1(g) and (i).

Feigenbaum [170] noticed that the bifurcation values of a_n, $n = 1, 2, \ldots$ increase asymptotically in geometrical progression with the multiplier

$$\delta = \lim_{n\to\infty} \frac{a_n - a_{n-1}}{a_{n+1} - a_n} \simeq 4.66920\,. \qquad \square$$

C.6.#67. Find the critical value of a that corresponds to the situation depicted in Fig. C.6.1(h). Can this map have stable orbits at this moment? To answer this question reduce it first to a piece-wise linear map.

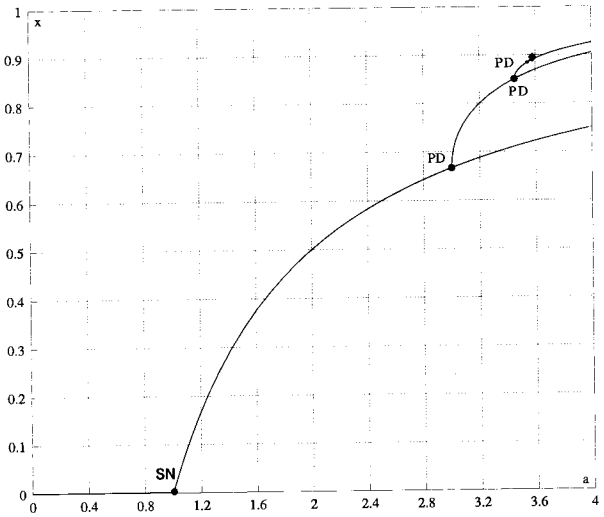

Fig. C.6.2. (x versus a) bifurcation diagram of the logistic map in the period-doubling process.

Evaluate the values of a_n that correspond to the flip bifurcations of the orbits of period 16, 32, respectively. Find the corresponding maximal x-coordinates of these cycles and plot them on Fig. C.6.2. □

C.6.#68. Examine the map

$$\bar{x} = x + x(a(1-x) - b(1-x)^2) = f(x)\,,$$

where a and b are some positive parameters. Find its fixed points, and detect the corresponding stability boundaries. Determine the asymptotic stability of the fixed points and period-2 cycle at critical cases. □

C.6.#69. Examine the maps $\bar{x} = \mu_1 + Ax^{1+\mu_2}$ and $\bar{x} = \mu_1 - \mu_2 x^\nu + x^{2\nu}$, where $0 < \nu < 1$, and $|\mu_1| \ll 1$. Consider the subcases $0 < \nu < 1/2$ and $1/2 < \nu$ separately. What happens at $\nu = 1/2$? Analyze bifurcations of symmetric periodic points in the two maps $\bar{x} = (\mu_1 + A|x|^{1+\mu_2})\,\mathrm{sign}(x)$ and $\bar{x} = (\mu_1 - \mu_2|x|^\nu + |x|^{2\nu})\,\mathrm{sign}(x)$, $|\mu_{1,2}| \ll 1$. Such maps appear in the study of homoclinic bifurcations of codimension two (see Sec. 13). □

C.6.#70. Consider the Hénon map:

$$\bar{x} = y\,, \qquad \bar{y} = a - bx - y^2\,.$$

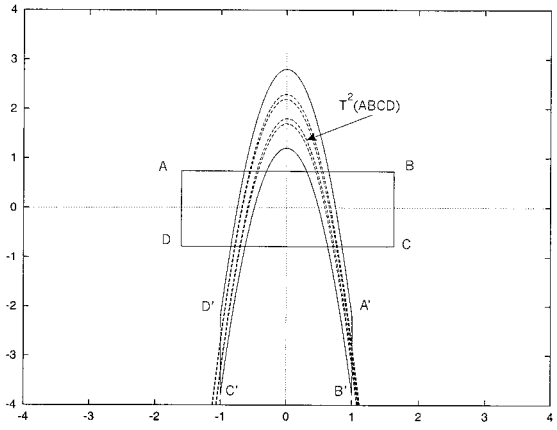

(a)

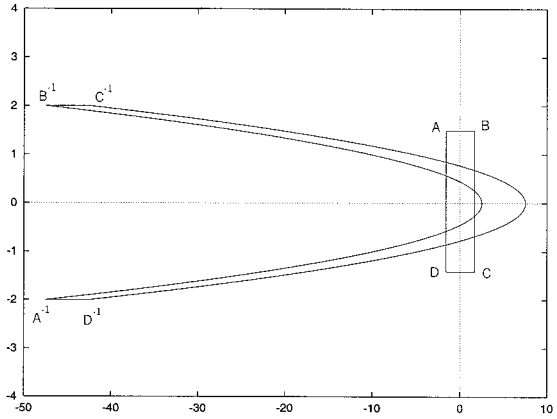

(b)

Fig. C.6.3. Horseshoe in the Hénon map for $a = 2$ and $b = 0.4$ and in its inverse.

This map is a canonical example illustrating the chaotic behavior. For certain parameter values the Hénon map models the mechanism of the creation of the Smale horseshoe as illustrated in Fig. C.6.3, for the map and for its inverse:

$$y = \bar{x}\,,$$
$$x = (a - \bar{y} - \bar{x}^2)/b\,,$$

defined for $b \neq 0$.

The Jacobian of the Hénon map is constant and equal to b. Therefore, when $b > 0$, the Hénon map preserves orientation in the plane, whereas orientation is reversed when $b < 0$. Note also that if $|b| < 1$, the map contracts areas, so the product of the multipliers of any of its fixed or periodic points is less than 1 in absolute value. Hence, in this case the map cannot have completely unstable periodic orbit (only stable and saddle ones). On the contrary, when $|b| > 1$, no stable orbits can exist. When $|b| = 1$, the map becomes conservative. At $b = 0$, the Hénon map degenerates into the above logistic map, and therefore one should expect some similar bifurcations of the fixed points when b is sufficiently small.

Next, let us find the fixed points in the Hénon map and analyze how they bifurcate as the parameters a and b vary. The bifurcation portrait is shown in Fig. C.6.4. It contains three bifurcation curves: SN: $a = -\frac{1}{4}(1+b)^2$, PD: $a = \frac{3}{4}(1+b)^2$, and AH: $b = 1, -1 < a < 3$. For $(a,b) \in SN$ the map has a fixed point with one multiplier $+1$; when $|b| < 1$, this point is a saddle-node with an attracting sector, while when $|b| > 1$, this is a saddle-node with a repelling zone. For $(a,b) \in PD$ the map has a fixed point with multiplier -1; when $|b| < 1$, the other multiplier is less than 1 in absolute value and the first Lyapunov value is negative, so the bifurcating point is stable. For $|b| > 1$,

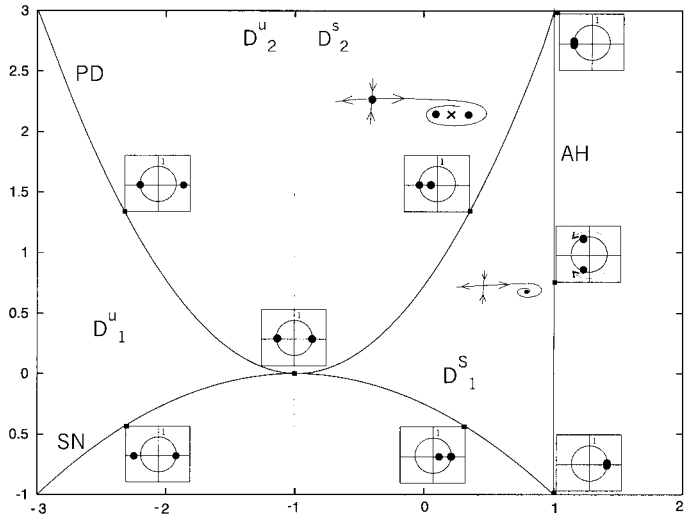

Fig. C.6.4. Bifurcation portrait of the fixed points in the Hénon map.

the other multiplier is greater than 1 in absolute value and the first Lyapunov value is positive, so the bifurcating point is completely unstable. (Check the equations for the bifurcation curves and compute the Lyapunov values.)

In the region D_1 there are two fixed points, one of which is a saddle, and the other one is stable for $(a,b) \in D_1^s$, and repelling when $(a,b) \in D_1^u$. Transition from D_1 to D_2 is accompanied with the period-doubling bifurcations of the fixed point, correspondingly, stable on the route $D_1^s \to D_2^s$, and repelling on the route $D_1^u \to D_2^u$. Meanwhile the point becomes a saddle $(-)$, and in its neighborhood a stable cycle of period two bifurcates from it when $(a,b) \in D_2^s$; in the region D_2^u, this period-two cycle is repelling.

When $b = 1$, the Hénon map becomes conservative, as its Jacobian equals $+1$. At $b = 1$ and $a = -1$, it has an unstable parabolic fixed point with two multipliers $+1$; at $b = 1$ and $a = 3$, it is a stable parabolic fixed point with two multipliers -1. In between these points, for $-1 < a < 3$ (i.e. $(a,b) \in T$), the map has a fixed point with multipliers $e^{\pm i\psi}$ where $\cos\psi = 1 - \sqrt{a+1}$. This is a generic elliptic point for $\psi \notin \{\pi/2, 2\pi/3, \arccos(-1/4)\}$ [167]. Since the Hénon map is conservative when $b = 1$, the Lyapunov values are all zero. When we cross the curve AH, the Jacobian becomes different from 1, hence the map either attracts or expands areas which, obviously, prohibits the existence of invariant closed curves. Thus, no invariant curve is born upon crossing the curve AH. □

C.6.#71. Let us consider the following map

$$\begin{aligned} \bar{x} &= y + \alpha y^2\,, \\ \bar{y} &= a - bx - y^2 + \beta xy \end{aligned} \tag{C.6.1}$$

with small α and β. This map can therefore be treated as a slight perturbation of the Hénon map. We may wonder what bifurcations occur in some bounded subregion in the (x,y)-plane which remains of finite size as both α and β tend to zero. This question is typical in the study of bifurcations of a quadratic homoclinic tangency between the stable and unstable manifolds of a neutral saddle fixed point (with the multipliers $|\nu| < 1 < |\gamma|$ such that $|\nu\gamma| = 1$) [175].

Let us derive the equations of the bifurcation curves $\widetilde{SN}$, $\widetilde{PD}$ and $\widetilde{AH}$ for (C.6.1) for small α and β; these curves correspond to the saddle-node, period-doubling and torus creation, respectively.

Consider the characteristic equation for (C.6.1)

$$\det \begin{pmatrix} -\lambda & 1+2\alpha y \\ -b+\beta y & -2y+\beta x-\lambda \end{pmatrix} = 0\,.$$

Since $x = y + \alpha y^2$ at a fixed point, this equation recasts as

$$\lambda^2 + \lambda(2y - \beta y - \alpha\beta y^2) + b + y(2b\alpha - \beta) - 2\alpha\beta y^2 = 0\,. \tag{C.6.2}$$

The equation for the coordinate y of a fixed point of (C.6.1) is given by

$$a - y(1+b) - y^2(1 + b\alpha - \beta) + \alpha\beta y^3 = 0\,. \tag{C.6.3}$$

Let us derive the equation of the curve $\widetilde{SN}$ of saddle-node fixed points. Since one of the eigenvalues of such points equals 1, plugging $\lambda = 1$ into (C.6.2) yields

$$1 + b + 2y(1 + b\alpha - \beta) - 3\alpha\beta y^2 = 0\,. \tag{C.6.4}$$

This equation has only one solution in any fixed finite region, provided that α and β are sufficiently small:

$$y = -\frac{1+b}{2(1+b\alpha-\beta)} + O(\alpha\beta)\,.$$

Substituting this in (C.6.3) gives the following equation for $\widetilde{SN}$

$$a = -\frac{(1+b)^2}{4}(1 - b\alpha + \beta) + O(\alpha^2 + \beta^2)\,. \tag{C.6.5}$$

Analogously, the equation of the curve $\widetilde{PD}$ corresponding to a period-doubling bifurcation is given by

$$a = \frac{3}{4}(1+b)^2\left(1 + \frac{4}{3}b\alpha - \frac{\beta}{3}\right) + O(\alpha^2 + \beta^2)\,. \tag{C.6.6}$$

Note that the curves $\widetilde{SN}$ and $\widetilde{PD}$ are close to the curves SN and PD of the original Hénon map.

Let us derive next the equation for the curve $\widetilde{AH}$ which corresponds to the creation of an invariant curve (the Andronov-Hopf bifurcation for maps). Since eigenvalues of such a point are $\lambda_{1,2} = e^{\pm i\varphi}$, it follows that the Jacobian

of the map at the fixed point equals 1 and the trace of the Jacobian matrix equals $2\cos\varphi$. This yields the following system for solving y and b:

$$\begin{aligned} &2y - \beta y - \alpha\beta y^2 = -2\cos\varphi \\ &b + y(2b\alpha - \beta) - 2\alpha\beta y^2 = 1\,. \end{aligned} \tag{C.6.7}$$

We obtain from the first equation that

$$y = -\frac{\cos\varphi}{1-\beta/2} + O(\alpha\beta)\,, \tag{C.6.8}$$

and from the second one that

$$b = 1 - (\beta - 2\alpha)\cos\varphi + O(\alpha^2 + \beta^2)\,. \tag{C.6.9}$$

Finally, we find from (C.6.3) that

$$a = \cos^2\varphi[1 + \beta - \alpha] - 2\cos\varphi[1 + \beta/2] + O(\alpha^2 + \beta^2)\,. \tag{C.6.10}$$

The curve $\widetilde{AH}$ is given by (C.6.9)–(C.6.10). Since the Jacobian of the map (C.6.1) is no longer constant, one should expect that the corresponding bifurcation of the birth of the invariant curve will be non-degenerate at the fixed point. To make sure, let us compute the first Lyapunov value L_1.

Let $(a, b) \in \widetilde{AH}$. Then $b = -1+O(\alpha,\beta)$ and $-1+O(\alpha,\beta) < a < 3+O(\alpha,\beta)$. The bifurcating fixed point with multipliers $e^{\pm i\varphi}$ has coordinates

$$\begin{aligned} x &= -\cos\varphi(1 + \beta/2) + \alpha\cos^2\varphi + O(\alpha^2 + \beta^2)\,, \\ y &= -\cos\varphi(1 + \beta/2) + O(\alpha^2 + \beta^2)\,. \end{aligned} \tag{C.6.11}$$

Let us translate the origin to the fixed point. The map (C.6.1) then assumes the form

$$\begin{aligned} \bar{x} &= y(1 + \rho) + \alpha y^2 + \cdots\,, \\ \bar{y} &= -x/(1 + \rho) + 2y\cos\varphi - y^2 + \beta xy + \cdots\,. \end{aligned}$$

where $\rho = 2\alpha\cos\varphi + O(\alpha^2 + \beta^2)$ and the dots stand for nonlinear terms of order $O(\alpha^2 + \beta^2)$. By rescaling the x-variable to $(1 + \rho)$, the map is brought to the form

$$\begin{aligned} \bar{x} &= y + \alpha y^2 + \cdots\,, \\ \bar{y} &= -x + 2y\cos\varphi - y^2 + \beta xy + \cdots\,. \end{aligned} \tag{C.6.12}$$

Now, make a linear transformation $x = \xi$ and $y = (\cos\varphi)\xi - (\sin\varphi)\eta$ after which the linear part of the map becomes a rotation through an angle φ:

$$\begin{aligned}
\bar{\xi} &= \xi\cos\varphi - \eta\sin\varphi + \alpha(\xi\cos\varphi - \eta\sin\varphi)^2 + \cdots\,,\\
\bar{\eta} &= \xi\sin\varphi + \eta\cos\varphi + \frac{1}{\sin\varphi}(\xi\cos\varphi - \eta\sin\varphi)^2(1+\alpha\cos\varphi)\\
&\quad - \frac{\beta}{\sin\varphi}\xi(\xi\cos\varphi - \eta\sin\varphi) + \cdots\,.
\end{aligned} \tag{C.6.13}$$

Denoting $z = \xi + i\eta$, we obtain

$$\bar{z} = ze^{i\varphi} + c_{20}z^2 + c_{11}zz^* + c_{02}(z^*)^2 + \cdots\,, \tag{C.6.14}$$

where z^* is complex-conjugate to z and the coefficients c_{ij} are given by

$$\begin{aligned}
c_{20} &= \frac{1}{4}[-2\cos\varphi - \alpha + \beta] + \frac{i}{4}\left[\frac{\cos 2\varphi}{\sin\varphi} + \frac{\cos\varphi}{\sin\varphi}(\alpha-\beta)\right],\\
c_{11} &= \frac{\alpha}{2} + \frac{i}{2}\left[\frac{1}{\sin\varphi} + \frac{\cos\varphi}{\sin\varphi}(\alpha-\beta)\right],\\
c_{02} &= \frac{1}{4}[2\cos\varphi + \alpha(3\cos^2\varphi - \sin^2\varphi) - \beta]\\
&\quad + \frac{i}{4}\left[\frac{\cos 2\varphi}{\sin\varphi} + \alpha\frac{\cos\varphi}{\sin\varphi}(\cos^2\varphi - 3\sin^2\varphi) - \beta\frac{\cos\varphi}{\sin\varphi}\right].
\end{aligned} \tag{C.6.15}$$

According to Sec. 3.13, the quadratic terms are eliminated by the following normalizing transformation (when $\varphi \neq 2\pi/3$):

$$z_{\text{new}} = z - \frac{c_{20}}{e^{2i\varphi} - e^{i\varphi}}z^2 - \frac{c_{11}}{1 - e^{i\varphi}}zz^* - \frac{c_{02}}{e^{-2i\varphi} - e^{i\varphi}}(z^*)^2 + \cdots\,. \tag{C.6.16}$$

This transformation does not change the linear part and it is known to eliminate all quadratic terms. Thus, we need only to collect the coefficients in front of the cubic term z^2z^*. This gives

$$\bar{z}_{\text{new}} = e^{i\varphi}z_{\text{new}} + e^{i\varphi}z_{\text{new}}^2 z_{\text{new}}^*(L + i\Omega) + O_3(z)\,, \tag{C.6.17}$$

where $O_3(z)$ stands for the remaining cubic and higher order terms, and

$$L + i\Omega = -c_{20}c_{11}e^{-2i\varphi}\frac{1 - 2e^{i\varphi}}{1 - e^{i\varphi}} - |c_{11}|^2\frac{1}{1 - e^{i\varphi}} - |c_{02}|^2\frac{2}{1 - e^{3i\varphi}}\,. \tag{C.6.18}$$

Taking the real part of the right-hand side we arrive at the following formula for the first *Lyapunov value* L_1 [184]

$$L_1 = \mathrm{Re}(c_{20}c_{11})\frac{\cos 3\varphi - 3\cos 2\varphi + 2\cos\varphi}{2(1-\cos\varphi)} + \mathrm{Im}(c_{20}c_{11})\frac{\sin 3\varphi - 3\sin 2\varphi + 2\sin\varphi}{2(1-\cos\varphi)} - |c_{02}|^2 - \frac{1}{2}|c_{11}|^2 . \quad \text{(C.6.19)}$$

When we plug (C.6.15) into the above formula, we finally obtain the following expression:

$$L_1 = \frac{1}{16(1-\cos\varphi)}[\beta - 2\alpha] + O(\alpha^2 + \beta^2) . \quad \text{(C.6.20)}$$

Observe that L_1 vanishes at $\alpha = \beta = 0$ as it is to be identically zero in the Hénon map.

Thus, when α and β are small, the sign of the first Lyapunov value equals the sign of the difference $(\beta - 2\alpha)$. If it is negative, the stable invariant curve is born through the super-critical Andronov-Hopf bifurcation when crossing the curve $\widetilde{AH}$ towards larger β. □

C.6.#72. Using a computer, trace the evolution of the invariant curve as b grows (choose $\alpha = \beta = 0.001$).

Let us first discuss the case $L_1 < 0$. In the region to the left of $\widetilde{AH}$ the point O is stable, see Fig. C.6.5. The point O becomes unstable to the right of the Andronov-Hopf bifurcation curve $\widetilde{AH}$, and a stable invariant curve bifurcates from it. The stable curve evolves in the following way: as the parameter increases further, it "glues" to a homoclinic loop to the saddle fixed point O_1. By the term "gluing" we mean that the stable invariant curve becomes a part of the non-wandering set of the complex homoclinic structure existing due to intersections of the stable and unstable manifolds of the saddle fixed point O_1. As the parameters vary further, this non-wandering set vanishes as the result of the homoclinic tangency.

Such a scenario of stability loss is often referred to in the literature as "soft" (see Chap. 14). In the case $L_1 > 0$, the loss of stability develops in a *dangerous* way: the point O is stable initially; meanwhile an unstable invariant curve "materializes" from the homoclinic tangles of O_1, and shrinks to the origin as the curve $\widetilde{AH}$ is reached. The fixed point at the origin becomes unstable upon crossing $\widetilde{AH}$, and all nearby trajectories escape from its neighborhood. □

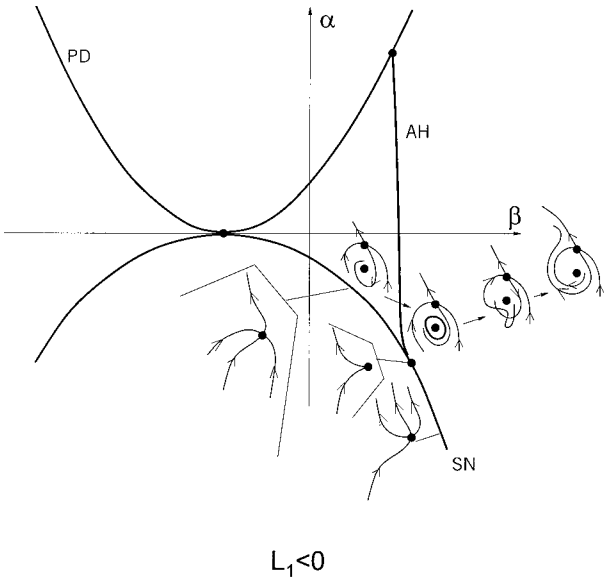

Fig. C.6.5. Bifurcation portrait of the perturbed Hénon map.

C.6.#73. Examine the following map

$$\bar{x} = y\,,$$
$$\bar{y} = \mu_1 + \mu_2 y + dy^3 - bx\,,$$

where μ_1, μ_2, b are control parameters, and $d = \pm 1$. Such maps appear in the study of the Lorenz attractor, as well as in modeling the behavior of the periodic forced equations with cubic nonlinearity, like the Duffing system [176, 184].

The Jacobian of the map is equal to b, and therefore, when $b \neq 0$, it is a diffeomorphism. The inverse is given by

$$\bar{y} = x\,,$$
$$\bar{x} = \frac{1}{b}(\mu_1 + \mu_2 x + dx^3 - y)\,.$$

One can easily see from the above formula that the cases $|b| > 1$ and $|b| < 1$ are symmetric. When $b = 0$, the original map becomes "one-dimensional" in the

sense that it has an invariant curve $y = dx^3+\mu_2 x+\mu_1$ to which any point of the plane is mapped onto after one iteration. It should be noticed that the map is invariant with respect to the transformation $(x, y, \mu_1, \mu_2) \to (-x, -y, -\mu_1, \mu_2)$, and hence bifurcations curves in the (μ_1, μ_2)-parameter plane are symmetric with respect to the μ_2-axis. □

C.6.#74. Find analytically the equations of the basic bifurcation curves of the fixed points and period-2 cycles of these maps.

Partial solution: the curve SN corresponding to a fixed point with multiplier $+1$ is given by

$$\mu_1 = \pm\frac{2}{3}\left(\frac{-1+b-\mu_2}{3d}\right)^{\frac{1}{2}} ;$$

that with multiplier -1 is given by

$$\mu_1 = \pm\frac{2}{3}\left(\frac{-1+b-\mu_2}{3d}\right)^{\frac{1}{2}} (2+2b-\mu_2)\,.$$

The bifurcation curves of the period-2 cycle with multiplier $+1$ are given by

$$\mu_1 = \pm\frac{2}{3\sqrt{3}}(-\mu_2-2(b+1))^{\frac{3}{2}}, \qquad \text{at } d=+1\,,$$

$$\mu_1 = \pm\frac{2}{3\sqrt{3}}(\mu_2+2b-1)^{\frac{3}{2}}, \quad \mu_2 > -\frac{2}{3}(b+1), \qquad \text{at } d=-1\,,$$

Those corresponding to period-4 doubling are given by

$$\mu_1^2 = \frac{1}{216d}(b(b+1)+\mu_2 \pm q)^2(-5\mu_2-6(b+1)\pm q)\,,$$

where $q = \sqrt{(3\mu_2+2b+2)^2-8(b^2+1)}$. □

C.6.#75. The following system is an asymptotic normal form for the bifurcation of an equilibrium state with triple zero characteristic exponent [162, 163]

$$\dot{x} = y\,,$$

$$\dot{y} = z\,,$$

$$\dot{z} = ax - x^2 - by - z\,,$$

in the case of complete Jordan block (continued from Sec. C.2). Here a and b are control parameters. A fragment of the bifurcation diagram of this system

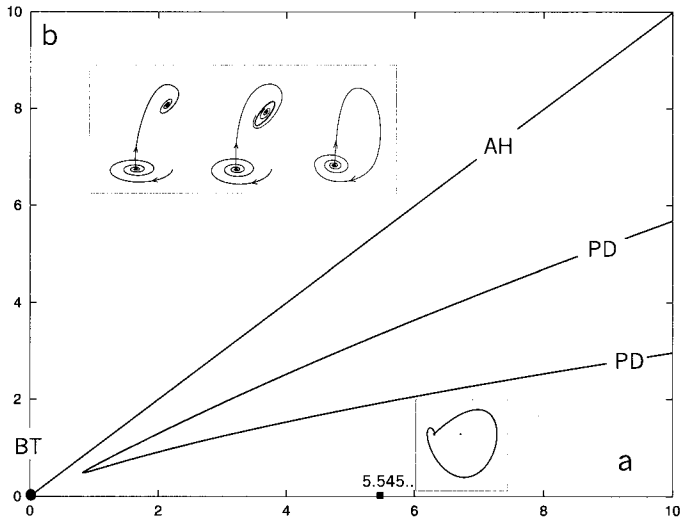

Fig. C.6.6. A part of the bifurcation diagram. AH labels the Andronov-Hopf bifurcation of the non-trivial equilibrium state O_1; PD labels a flip-bifurcation of the stable periodic orbits that generates from O_1.

is shown in Fig. C.6.6. For $a, b \geq 0$, this system has two equilibrium states: $O(0,0,0)$ and $O_1(a,0,0)$. The origin $a = b = 0$ corresponds to the Bogdanov-Takens bifurcation of codimension two (see Sec. 13.4).

Let us describe the essential bifurcations in this system on the path $b = 2$ as μ increases. On the left of the curve AH, the equilibrium state O_1 is stable. It undergoes the super-critical Andronov-Hopf bifurcation on the curve AH. The stable periodic orbit becomes a saddle through the period-doubling bifurcation that occurs on the curve PD. Figure C.6.7 shows the unstable manifold of the saddle periodic orbit homeomorphic to a Möbius band. As a increases further, the saddle periodic orbit becomes the homoclinic loop to the saddle point $O(0,0,0,)$ at $a \simeq 5.545$. What can one say about the multipliers of the periodic orbit as it gets closer do the loop? Can the saddle periodic orbit shown in this figure get "pulled apart" from the double stable orbit after the flip bifurcation? In other words, in what ways are such paired orbits linked in $\mathbb{R}^3$, in $\mathbb{R}^4$? □

C.6.#76. Using a computer detect the bifurcation curve in the (a, b)-parameter plane that corresponds to the pitch-fork bifurcation of a symmetric

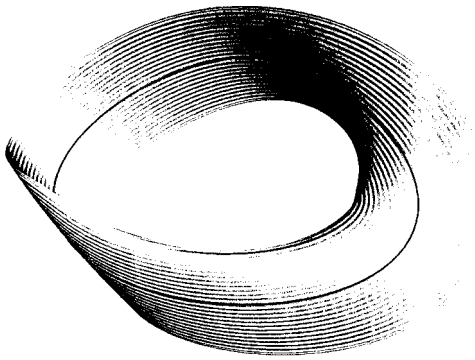

Fig. C.6.7. Shown is a piece of the stable manifold of the saddle periodic orbit (dark circle) at $a = 3.2$; courtesy of H. Osinga and B. Krauskopf [181].

periodic orbit in the Shimizu-Morioka model [191]:

$$\begin{aligned} \dot{x} &= y\,, \\ \dot{y} &= x - xz - ay\,, \\ \dot{z} &= -bz + x^2\,, \end{aligned} \tag{C.6.21}$$

at $a \simeq 0.4$ and $b \simeq 0.45$. Can a symmetric limit cycle go through a period-doubling bifurcation in this system? In the Lorenz equation? In a Chua circuit? What makes the difference? □

C.6.#77. Let us consider an example of a system with torus bifurcation. Our example here is the following model coming from meteorology [128, 183]

$$\begin{aligned} \dot{x} &= -y^2 - z^2 - ax + aF\,, \\ \dot{y} &= xy - bxz - y + G\,, \\ \dot{z} &= bxy + xz - z\,. \end{aligned} \tag{C.6.22}$$

It follows from the linear stability analysis (see Sec. C.2) that the (a, b)-parameter plane has a codimension-two point corresponding to an equilibrium state with characteristic exponents $(0, \pm i\omega)$. Therefore, the dimension of the center manifold in such a case must be equal to 3 at least. For the complete account on this bifurcation the reader is referred to [51, 64]. Below, we will give its brief outline.

Observe that at such a codimension-two point the Andronov-Hopf and saddle-node bifurcations occur simultaneously. Let μ_1 and μ_2 be the same

parameters that govern these bifurcations in each versal family, respectively:

$$\begin{cases} \dot{r} = r(\mu_1 + L_1 r^2) + \cdots , \\ \dot{\varphi} = \omega(\mu_1) + \Omega(\mu_1) r^2 + \cdots , \\ \dot{z} = \mu_2 - z^2 + \cdots , \end{cases}$$

where $\omega(0) \neq 0$, $\Omega(0) \neq 0$, and L_1 denotes a Lyapunov value. Taking the interaction into account, the resulting normal form can be written as

$$\begin{aligned} \dot{r} &= r(\tilde{\mu}_1 + L_1 r^2 + az + z^2) + O(|(r,z)|^4) , \\ \dot{z} &= \tilde{\mu}_2 + z^2 + br^2 + O(|(r,z)|^4) , \\ \dot{\varphi} &= \omega + cz + O(|(r,z)|^2)) , \end{aligned}$$

where a, b may be set ± 1. Note that if we drop the $O(|(r,z)|^4)$-terms, the system becomes invariant with respect to rotation around the z-axis, so its trajectories lie on integral surfaces determined by trajectories of the planar system consisting of the first two equations, which are decoupled from the third one. In this planar system, equilibrium states with $r = 0$ correspond to equilibrium states of the three-dimensional normal form, those with $r \neq 0$ correspond to periodic orbits, and a structurally stable limit cycle will correspond to an invariant torus. Depending on the signs of a and b, there may be four essentially different cases. We will focus on the case $a = -1$ and $b = 1$ only where the torus-bifurcation takes place, and leave the other ones for exercises on linear stability analysis. The corresponding bifurcation diagram is shown in Fig. C.6.8. Let us describe next the corresponding bifurcations in terms relevant to the original three-dimensional system (C.6.22).

The point O_1 is repelling in the region to the right of AH. On the left of AH it becomes a saddle-focus (2,1) and a repelling periodic orbits generates from it. This periodic orbit is the edge of the stable manifold of O_1 (Fig. C.6.9(a)). This periodic orbit becomes stable upon crossing TB, and a repelling two-dimensional invariant torus bifurcates from it (see Fig. C.6.9(b)). This torus becomes the heteroclinic connection between both saddle-foci (Fig. C.6.9(c)) on the curve H in Fig. C.6.8.

The bifurcations described above are subject to the condition of invariance with respect to rotation around the z-axis. The straight-line $r = 0$ is then an integral curve, and in the case where O_1 and O_2 are both saddles, this is

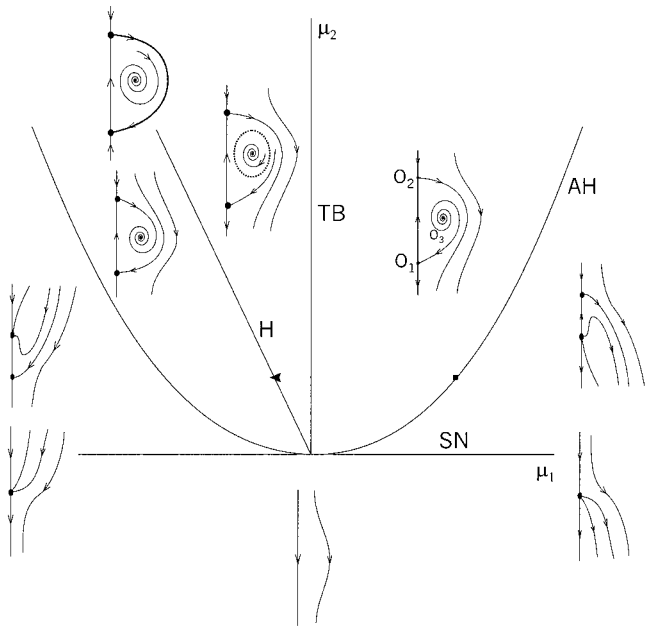

Fig. C.6.8. Unfolding of the planar system with $a = -1$ and $b = 1$.

their common one-dimensional separatrix. Moreover, in such symmetrical systems, both two-dimensional stable and unstable invariant manifolds of these saddles may either coalesce or have no common points. In generic systems which are not rotationally invariant, one-dimensional separatrices of the saddles may coincide at particular (codimension-two) parameter values, whereas two-dimensional manifolds of the saddles may cross transversely each other along some trajectories for an open set of parameters. Taking into account the terms destroying the rotational symmetry may significantly change the structure of the heteroclinic connection, namely it may split. If this is the case, the situation is likely where a one-dimensional separatrix becomes bi-asymptotic to either saddle-focus shown in Fig. C.6.9(d). Moreover, if the saddle value is positive at either saddle-focus, the separatrix loop will give rise to a homoclinic explosion when the neighborhood is filled by infinitely many saddle periodic orbits (see Sec. 13). □

C.6.#78. The Medvedev's construction of the blue-sky catastrophe on the torus [95] is illustrated by Fig. C.6.11. It is supposed that there exists a pair

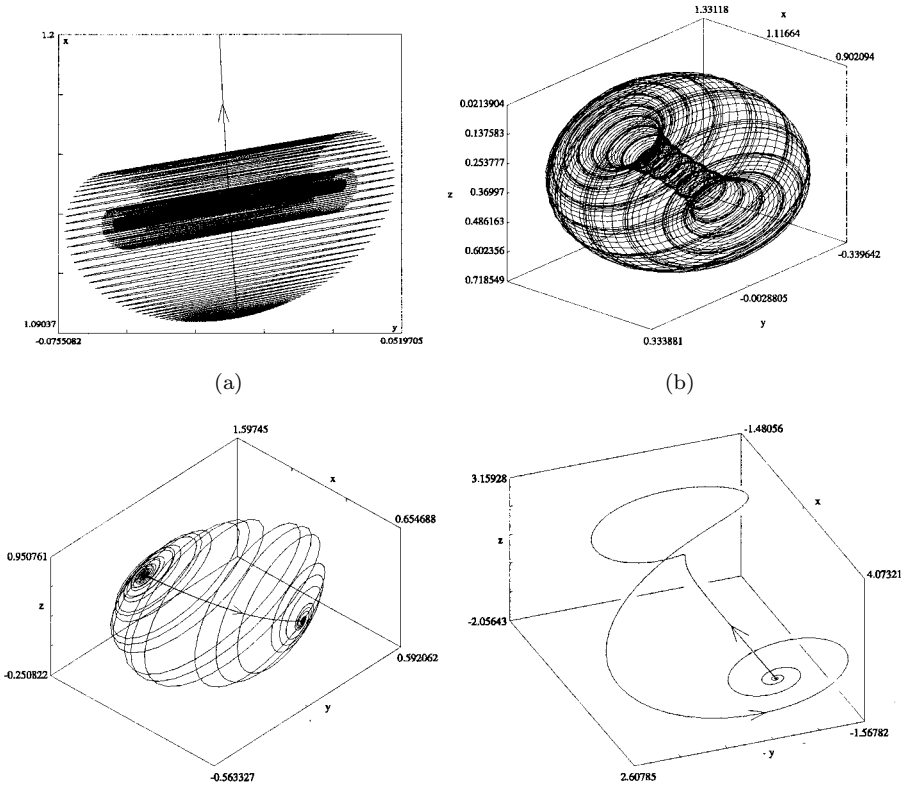

(a) (b)

(c) (d)

Fig. C.6.9. Phase portraits of system (C.6.22): (a) $(F = 1.77, G = 1.8)$; (b) $(F = 1.8, G = 1.65)$; (c) $(F = 1.8, G = 1.5)$; (d) $(F \simeq 1.416, G \simeq 2.195)$.

of saddle-node cycles C_1 and C_2 on the torus at some $\mu = 0$. By introducing the direction of the motion of the torus, one can assign that one cycle rotates in the clockwise direction whereas the other one spins in the opposite direction. Discuss the way on how the blue-sky catastrophe may flow in. How many cycles of what stability can appear through this bifurcation? Let $n_1(\mu)$ and $n_2(\mu)$, $\mu > 0$ be the number of gyrations which a closed trajectory on the torus makes near the ghosts of $C_{1,2}$. What is $\lim_{\mu \to +0} n_{1,2}(\mu)$? □

C.6.#79. Challenge: following the underlying idea on the development of the blue-sky catastrophe in a two time scales system which is discussed in

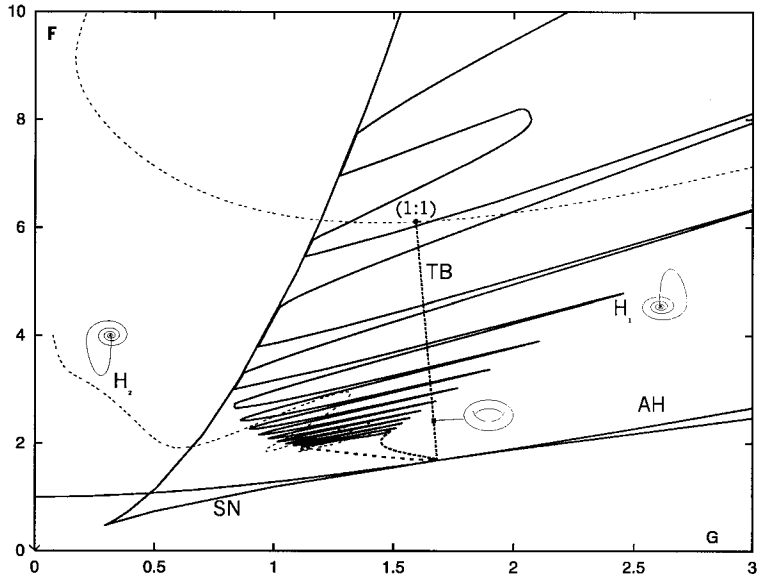

Fig. C.6.10. Part of the bifurcation diagram of the system (C.6.22).

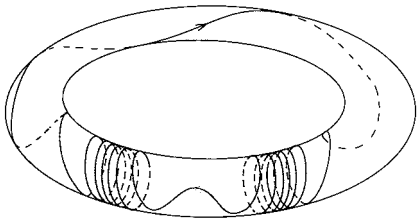

Fig. C.6.11. Blue-sky catastrophe on a torus.

Sec. 12.4, find the blue-sky catastrophe in the modified Hindmarsh-Rose model of neuronal activity

$$\begin{aligned} \dot{x} &= y - z - x^3 + 3x^2 + 5\,, \\ \dot{y} &= -y - 2 - 5x^2\,, \\ \dot{z} &= \varepsilon(2(x + 2.1) - z) - \frac{A}{(z - 1.93)^2 + 0.003}\,, \end{aligned} \tag{C.6.23}$$

where A and ε are two control parameters. Figure C.6.12 represents the bifurcation diagram of the slow system. Prove the stability of the resulting periodic

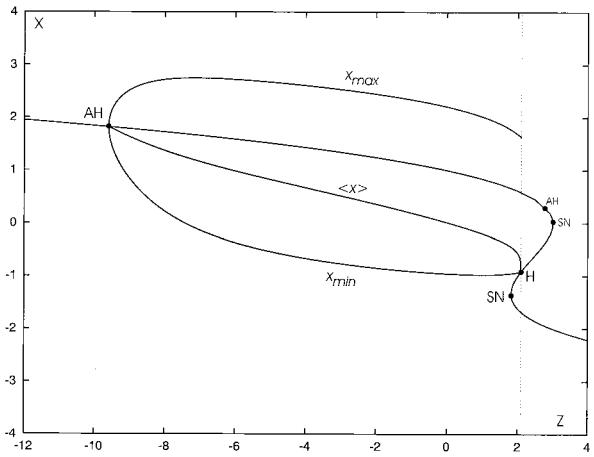

Fig. C.6.12. Plot of the x-coordinate of the equilibrium state versus z at $\varepsilon = 0$. The symbols $x_{\min}$, $x_{\max}$ and $\langle x \rangle$ denote, respectively, the maximal, minimal and averaged values of the x-coordinates of the stable limit cycle which bifurcates from a stable focus at AH and terminates in the separatrix loop to the saddle O (see the next figure) at the point H: $z \simeq 2.086$.

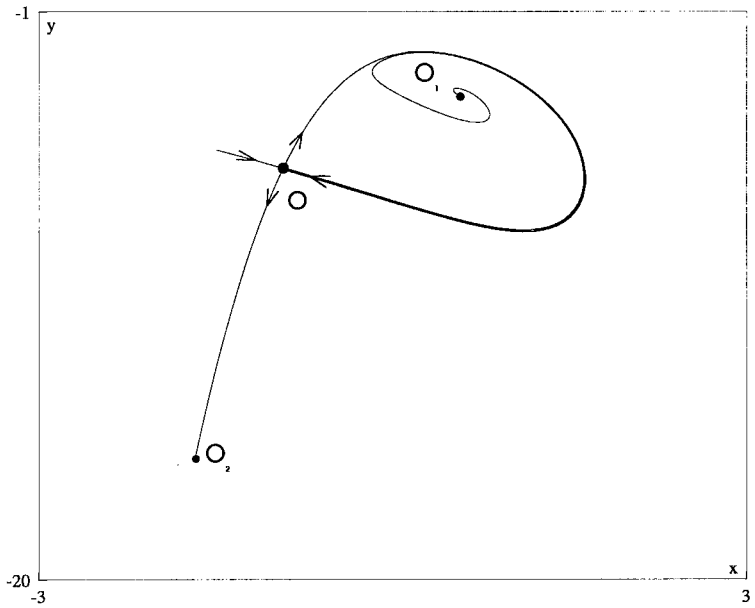

Fig. C.6.13. A separatrix loop to the saddle O at $z \simeq 2.086$ and $\varepsilon = 0$.

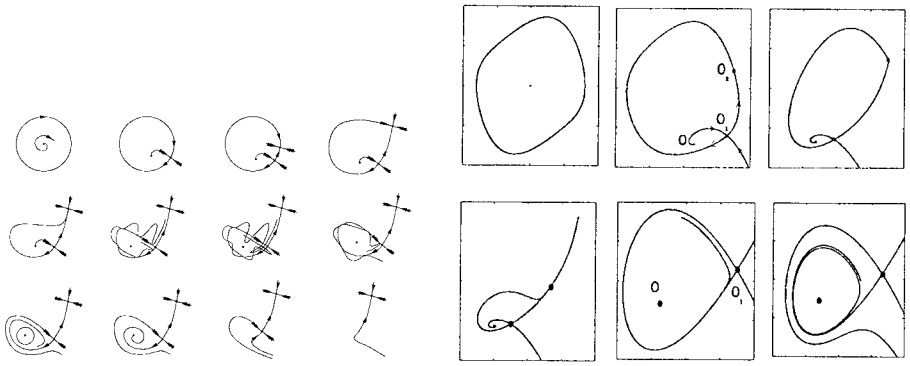

(a) (b)

Fig. C.6.14. Shift map over $2\pi/\omega$: ideal bifurcation puzzle (a) and numeric result (b) for $a = 0.4$, $\omega = 0.893$, and at $\beta = 0.0, 0.37, 0.37409, 0.375, 0.376, 0.3761$. Both figures are courtesy of B. Krauskopf and H. Osinga [180].

orbit. How can you explain the delayed loss of stability of the equilibrium state O_1: contrast the corresponding diagram at zero and small nonzero ε. The curious reader is advised to consult [21] for more details concerning this phenomenon. □

C.6.#80. Study a mechanism of the appearance and breakdown of an invariant torus in the periodically forced Van der Pol equation

$$\begin{aligned} \dot{x} &= y\,, \\ \dot{y} &= -x - a(x^2-1)y + \beta\cos\omega t\,, \\ \dot{t} &= \omega\,, \end{aligned} \tag{C.6.24}$$

as β increases from zero; Start with the Andronov-Hopf bifurcation of the origin in the unperturbed equation. What occurs with the limit cycle at $a = 2$? The phenomenological scenario of the evolution of the torus is shown in Fig. C.6.14. What bifurcations precede its breakdown, and when does it lose its smoothness? Attention should be drawn to the behavior of the separatrices of the saddle near the stable resonant cycle. □

C.7 Homoclinic bifurcations

Homoclinic bifurcations are *a priori* not a local problem. The detection of a homoclinic bifurcation in a specific set of ODE's is an art in itself. Besides,

it often requires performing rather sophisticated numerical computations. However, as we have seen in our study of the Bogdanov-Takens normal form, in some specific cases one can prove analytically the existence of a homoclinic loop. This concerns systems close to integrable ones. Another instance is that of systems with piece-wise linear right hand sides, as well as by two time scales systems with slow and fast variables. Nevertheless, these examples are exceptions. As for generic nonlinear dissipative systems are concerned, the situation is quite non-trivial, especially if the saddle in question has unstable and stable manifolds of dimensions equal or exceeding two (so far, the known regular numerical methods are applied well to saddles with one-dimensional stable or unstable separatrices). What really simplifies the problem is that there are not so many bifurcation scenarios that usually precede the appearance of the homoclinic loop. We will illustrate some of them below. However, this list is undoubtedly incomplete, and we hope that the lucky reader will run into novel bifurcations in further research.

A homoclinic bifurcation is a composite construction. Its first stage is based on the local stability analysis for determining whether the equilibrium state is a saddle or a saddle-focus, as well as what the first and second saddle values are, and so on. On top of that, one deals with the evolution of ω-limit sets of separatrices as parameters of the system change. A special consideration should also be given to the dimension of the invariant manifolds of saddle periodic trajectories bifurcating from a homoclinic loop. It directly correlates with the ratio of the local expansion versus contraction near the saddle point, i.e. it depends on the signs of the saddle values.

C.7.#81. Following the same steps as in the study of the generic Bogdanov-Takens normal form, analyze the structure of the bifurcation set near the origin $\mu_1 = \mu_2 = 0$ in the Khorozov-Takens normal form with reflection symmetry:

$$\dot{x} = y\,,$$

$$\dot{y} = \mu_1 x + \mu_2 y \pm x^3 - x^2 y\,.$$

The rescaling

$$x \to \varepsilon u, \quad y \to \varepsilon^2 v, \quad |\mu_1| \to \varepsilon^2, \quad \mu_2 \to \varepsilon^2 \nu, \quad t \to t/\varepsilon$$

gives

$$\dot{u} = v\,,$$
$$\dot{v} = \gamma u + \nu v \pm u^3 - \varepsilon u^2 v\,,$$

where $\gamma = \text{sign}\ \mu_1 = \pm 1$. Then, at $\varepsilon = 0$, the system becomes a Hamiltonian one

$$\dot{u} = -\frac{\partial H}{\partial v}\,,$$
$$\dot{v} = \frac{\partial H}{\partial u}\,,$$

with the first integral

$$H = \frac{v^2}{2} + \gamma\frac{u^2}{2} \pm \frac{u^4}{4}\,.$$

The most interesting case is when the sign of γ is opposite to the sign of the coefficient of the fourth-order term in H, so let us assume further

$$H = \frac{v^2}{2} + \gamma\frac{u^2}{2} - \gamma\frac{u^4}{4}\,.$$

This integrable system has three equilibrium states $O(0,0)$ and $O_{1,2}(\pm 1, 0)$. When $\gamma = 1$, the origin is a center while $O_{1,2}$ are the saddles [see Fig. C.7.1(a)].

The saddles have a closed symmetric heteroclinic connection at the level $H = 1/4$. The equations of the trajectories connecting the saddles can be found explicitly, and for the upper one it is given (verify this) by

$$u = \frac{e^{\sqrt{2}t} - 1}{e^{\sqrt{2}t} + 1}, \qquad v = \frac{2\sqrt{2}e^{\sqrt{2}t}}{(e^{\sqrt{2}t} + 1)^2}\,.$$

In the case $\gamma = -1$, the origin becomes a saddle and $O_{1,2}$ are centers [see Fig. C.7.1(b)]. The distinguishable figure-of-eight lies at the zero level of the associated Hamiltonian. The equation of its right lobe is given by

$$u(t) = \frac{2\sqrt{2}e^{t}}{1 + e^{2t}}, \qquad v(t) = \frac{2\sqrt{2}e^{t}(1 - e^{2t})}{(1 + e^{2t})^2}\,.$$

The heteroclinic connection or the homoclinic-8 in a perturbed system persists on the curve $\mu_2 = \nu\mu_1 + O(\mu_1^2)$, where ν is found from the condition

$$\int_{-\infty}^{+\infty} \frac{\partial}{\partial\varepsilon}\,\frac{d}{dt} H(u(t), v(t))dt\Big|_{\varepsilon=0} = 0\,.$$

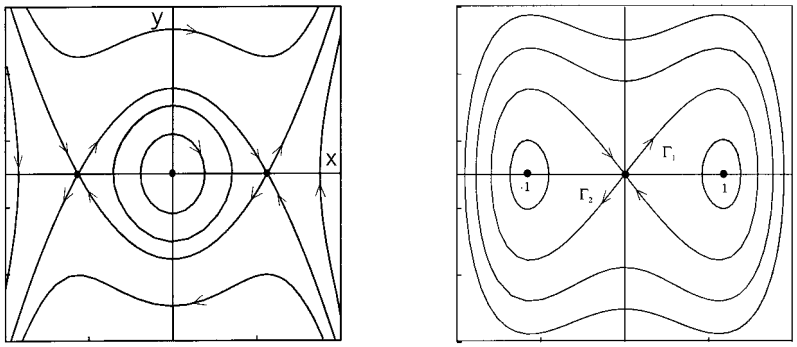

(a) (b)

Fig. C.7.1. Integral curves of the Hamiltonian systems: cases $\gamma = 1$(a) and $\gamma = -1$(b).

The latter can be rewritten as

$$\nu = \frac{\int_{-\infty}^{+\infty} u^2(t)v(t)dt}{\int_{-\infty}^{+\infty} v(t)dt}\,,$$

which gives

$$\nu = \frac{1}{5}, \quad \text{and} \quad \frac{4}{5}\,,$$

respectively, for each case. Compute the saddle value on the curve $H8$ in the case $\gamma = -1$. Show that the stable symmetric limit cycle cannot terminate in the homoclinic-8 on this curve. See the complete bifurcation diagrams in Fig. C.7.2.

C.7.#82. Apply the Shilnikov theorem and explain what kind of behavior one should anticipate in the Rössler system [172, 188]

$$\dot{x} = -y - z\,,$$

$$\dot{y} = x + ay\,,$$

$$\dot{z} = 0.3x - cz + xz\,,$$

near the homoclinic loops of the saddle-foci O shown in Fig. C.7.3. Determine the corresponding characteristic exponents, and evaluate the saddle values.

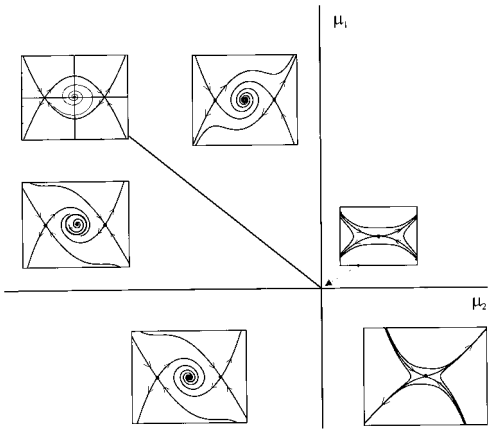

(a)

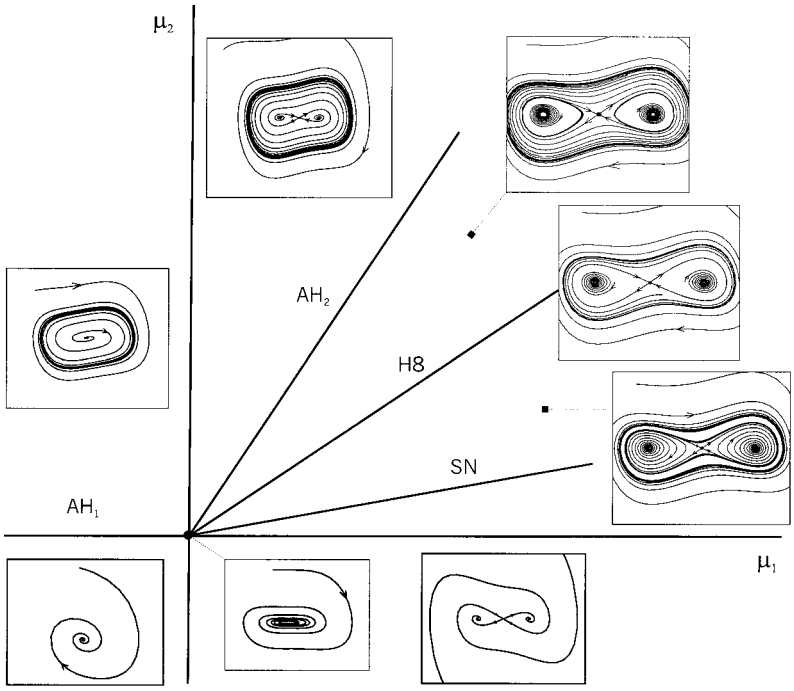

(b)

Fig. C.7.2. Bifurcation diagrams of the Khorozov-Takens normal form.

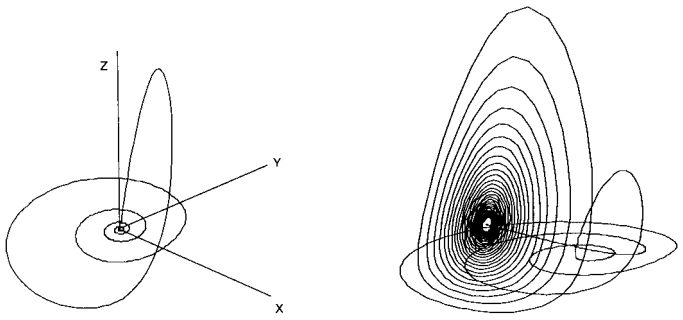

(a) (b)

Fig. C.7.3. Homoclinic loops to the saddle-foci O and O_1 in the Rössler model for $(a = 0.380, c = 4.820)$ and $(a = 0.4853, c = 4.50)$, respectively. Initial conditions are chosen on the unstable manifolds at a distance of about 0.47 from O on the plane $y = 0$, and about 0.14 from O_1, respectively.

Direct computation reveals that for the given parameters the saddle-focus O has the exponents $\lambda_{1,2} \simeq 0.1597 \pm i0.9815$ and $\lambda_3 \simeq -4.7594$. Since the complex exponents $\lambda_{1,2}$ are nearest to the imaginany axis, the homoclinic loop implies the emergence of infinitely many saddle periodic orbits. Moreover, since the second saddle value $\sigma_2 = \lambda_3 + 2\mathrm{Re}\lambda_{1,2}$ is negative (here it is equal to the divergence of the vector field at O), it follows that near the homoclinic loop there may also exist stable periodic orbits along with saddle ones. These stable orbits have long periods and weak attraction basins, and therefore they are practically invisible in numerical experiments.

In the second case, the equilibrium state O_2 has the characteristic exponents $(-0.0428 \pm 3.1994, 0.4253)$. In contrast to the first case, there are no stable periodic ordits in a small neighborhood of the loop, because the divergence of the vector field at O_2 is positive. □

C.7.#83. Consider the following $\mathbb{Z}_2$-symmetric Chua's circuit with cubic nonlinearity [179]:

$$\begin{aligned} \dot{x} &= a\left(y - \frac{x}{6} + \frac{x^3}{6}\right), \\ \dot{y} &= x - y + z, \\ \dot{z} &= -by, \end{aligned} \tag{C.7.1}$$

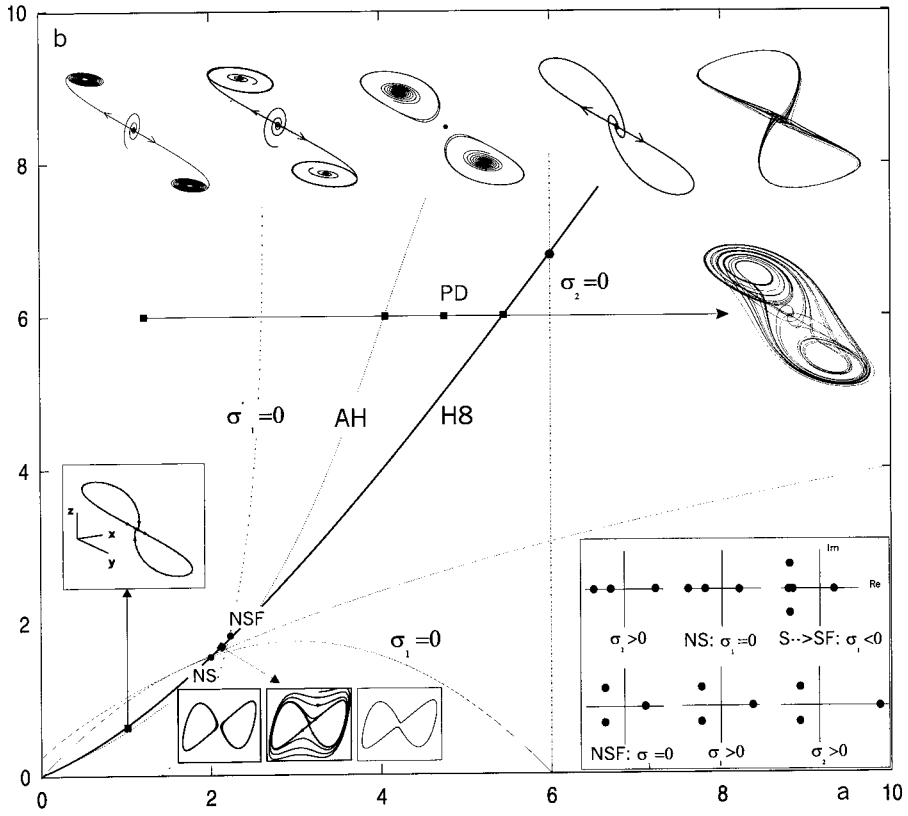

Fig. C.7.4. Bifurcation diagram for the Chua's circuit.

where $a \geq 0$ and $b \geq 0$ are control parameters. When $a = b = 0$, the bifurcation unfolding of (C.7.1) is the same as that of the Khorozov-Takens normal form. In particular, it includes the bifurcation of a homoclinic-8. Thus, the corresponding bifurcation curve, labeled $H8$, starts from the origin in the (a, b)-parameter plane in Fig. C.7.4. Of special consideration here are the four codimension-two points on this curve at which the following resonant conditions hold (after Sec. C.2):

(1) NS ($a \simeq 1.13515, b \simeq 1.07379$) corresponds to the saddle (at the origin) with zero saddle value σ. Below this point, σ is positive.

(2) The point $S \to SF$ ($a \simeq 1.20245, b \simeq 1.14678$) corresponds to the transition from a saddle to a saddle-focus (2,1). It is important that $\sigma < 0$ at this point.
(3) The abbreviation NSF stands for the neutral saddle-focus at which the saddle value σ vanishes.
(4) Introduce the second saddle value σ_2 as the sum of the three leading characteristic exponents at the saddle-focus. In the three-dimensional case, it is the divergence of the vector field at the origin. Here, the curve $\sigma_2 = 0$, given by the equation $a = 6$, intersects $H8$ at ($a = 6, b = 7.19137$). Above this point, $\sigma_2 > 0$.

These points break the bifurcation curve $H8$ into the four segments the trajectory behaviour on which is described next.

Segment $(0, NS)$:

On this interval, the homoclinic-8 bifurcates in the same way as in the Khorozov-Takens normal form. Both loops, which form the homoclinic-8 are orientable. The dimension of the center homoclinic manifold is equal to 2. The third dimension does not yet play a significant role. Therefore, it follows from the results in Sec. 13.7 that on the right of $H8$, there are two unstable cycles (*cycles* 1 *and* 2 in Fig. 13.7.9). To the left of $H8$, a symmetric saddle periodic orbit (cycle 12) bifurcates from the homoclinic-8 (see also Fig. C.7.5).

The point NS. This point is of codimension two as $\sigma = 0$ here. The behavior of trajectories near the homoclinic-8, as well as the structure of the bifurcation set near such a point depends on the separatrix value A (see formula (13.3.8)). Moreover, they do not depend only on whether A is positive (the loops are orientable) or negative (the loops are twisted), but it counts also whether $|A|$ is smaller or larger than 1. If $|A| < 1$, the homoclinic-8 is "stable", and unstable otherwise. To find out which case is ours, one can choose an initial point close sufficiently to the homoclinic-8 and follow numerically the trajectory that originates from it. If the figure-eight repels it (and this is the case in Chua's circuit), then $|A| > 1$. Observe that a curve of double cycles with multiplier $+1$ must originate from the point NS by virtue of Theorem 13.5.

On the segment between NS and NSF, the saddle value is negative, i.e., $\sigma < 0$. Moving up along $H8$, we go through the point above which the origin becomes a saddle-focus. By virtue of Theorem 13.11, in either case (i.e., when the origin is a saddle, or a saddle focus with $\sigma < 0$), only two stable cycles, or a single symmetric stable cycle bifurcate from the homoclinic-8 on

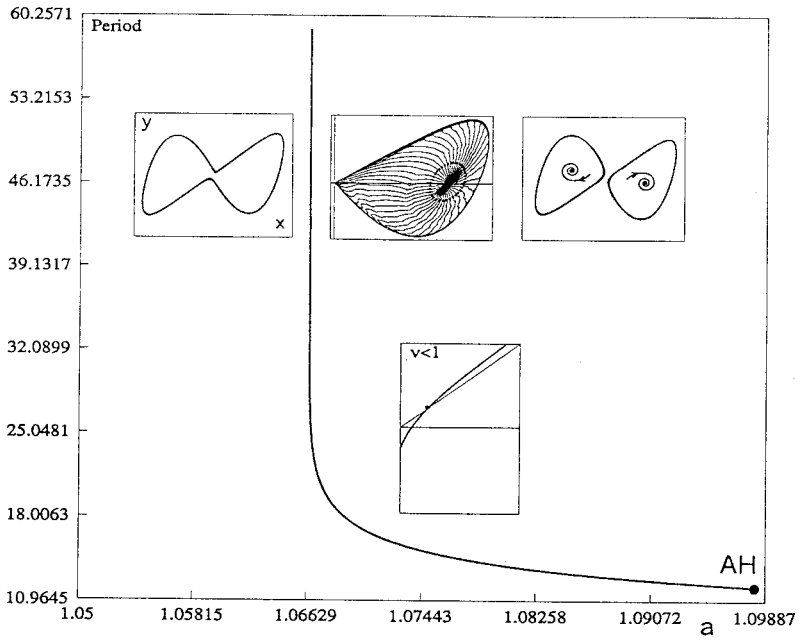

Fig. C.7.5. Period T of the periodic orbit born through a sub-critical Andronov-Hopf bifurcation versus the parameter a ($b = 1$), as the cycle approaches the homoclinic loop. The origin is a saddle with $\sigma > 0$.

the opposite sides from $H8$. Therefore, the point $S \to SF$ is not a bifurcation point. However, by introducing a small perturbation, that breaks down the symmetry of Chua's circuit, one can make the resulting bifurcation unfolding essentially different (see the contrast in Figs. 13.7.5 and 13.7.9). It should be merely noted that the transition from saddle to saddle-focus would cause dramatical changes in the dynamics of the system if σ were positive at such a point. Taking into consideration one homoclinic loop only, this would cause a homoclinic explosion from a single saddle periodic orbit in the case of a saddle to infinitely many ones in the case of a saddle-focus (see Theorems 13.7–10 and [29]).

The point NSF: $\sigma = 0$ corresponds to a neutral saddle-focus. At this codimension-two point the dynamics of the trajectories near the homoclinic loops to the saddle-focus becomes chaotic. This bifurcation indeed preceeds the origin of the chaotic double scroll attractor in Chua's circuit. In the general case, this bifurcation was first considered in [29]. The complete unfolding of

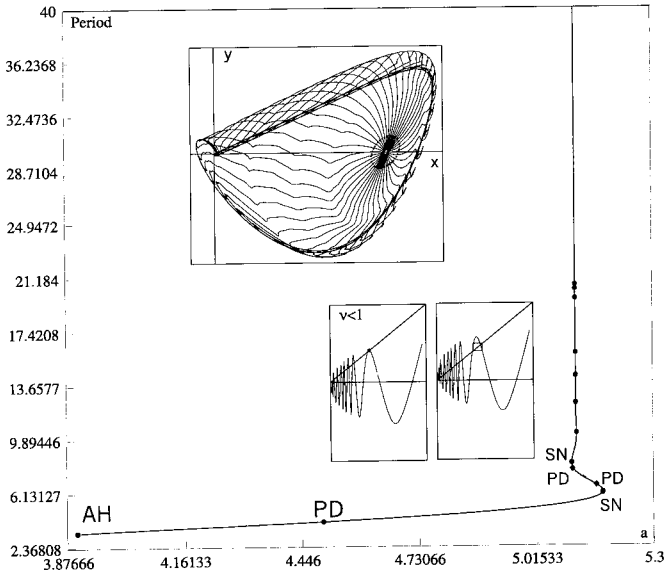

Fig. C.7.6. Dependence of period T of the periodic orbit generating via a super-critical Andronov-Hopf bifurcation on the parameter a ($b = 6$) as the cycle approaches the homoclinic loop to a saddle-focus with $\sigma > 0$.

such bifurcation is unknown. The brief outline of [29] is as follows: there is an infinite series of codimension-1 bifurcation curves that accumulate to the curve $H8$ above the point NSF. These curves correspond to subsequent homoclinic bifurcations, saddle-node and period doubling bifurcations of periodic orbits close to the primary homoclinic one. To understand this phenomena (homoclinic explosion) one may examine a simplified picture of the evolution of the one-dimensional map with the saddle index $\nu > 1$ (corresponding to $\sigma < 0$), and $\nu < 1$ ($\sigma > 0$) shown in Fig. C.7.6. Recall that in the case under consideration, $\nu = |\mathrm{Re}\lambda^*|/\lambda_1$, where $\lambda_1 > 0$ and λ^* is the real part of the complex-conjugate pair of the exponents at the saddle-focus. One can see from this figure that the period of the periodic orbit tends to infinity as the parameter converges to the critical value. In the saddle-focus case with $\nu < 1$, it has a distinctive oscillatory component. Every turning point, corresponds to the saddle-node bifurcation which is followed by a period-doubling bifurcation. Therefore, there takes place an infinite sequence of such bifurcations accumulating to the homoclinic one [173].

Thus, in a neighborhood of the homoclinic loop to the saddle-focus with $\nu < 1$, there may exist structurally unstable periodic orbits, in particular saddle-nodes. This gives rise to the question: does the saddle-node bifurcations of periodic orbits result in the appearance of stable ones?

To answer it, one must examine the two-dimensional Poincaré map instead of the one-dimensional one, and evaluate the Jacobian of the former map. If its absolute value is larger than one, the map has no stable periodic points, and hence there are no stable orbits in a neighborhood of the homoclinic trajectory because the product of the multipliers of the fixed point is equal to the determinant of the Jacobian matrix of the map. One can see from formula (13.4.2) that the value of the Jacobian is directly related to whether $2\nu - 1 > 0$ or $2\nu - 1 < 0$, or, equivalently, $\nu > 1/2$ or $\nu < 1/2$. Rephrasing in terms of the characteristic exponents of the saddle-focus, the above condition translates into whether the second saddle value $\sigma_2 = \lambda_1 + 2\mathrm{Re}\lambda^*$ is positive or negative. It can be shown [100] that if $\sigma > 0$ but $\sigma_2 < 0$ ($a < 6$ in Fig. C.7.4), there may be stable periodic orbits near the loop, along with saddle ones. However, when $\sigma_2 > 0$ ($\sigma > 0$, automatically), totally unstable periodic orbits emerge from the saddle-node bifurcations.

The last comment on the Chua circuit concerns the bifurcations along the path $b = 6$ (see Fig. C.7.4). Notice that this sequence is very typical for many symmetric systems with saddle equilibrium states. We follow the stable periodic orbit starting from the super-critical Andronov-Hopf bifurcation of the non-trivial equilibrium states at $a \simeq 3.908$. As a increases, both separatrices tend to the stable periodic orbits. The last ones go through the pitch-fork bifurcations at $a \simeq 4.496$ and change into saddle type. Their size increases and at $a \simeq 5.111$, they merge with the homoclinic-8. This, as well as subsequent bifurcations, lead to the appearance of the strange attractor known as the double-scroll Chua's attractor in the Chua circuit. □

C.7.#84. Homoclinic bifurcations in the Shimizu-Morioka model [127]:

$$\begin{aligned} \dot{x} &= y\,, \\ \dot{y} &= x - ay - xz\,, \\ \dot{z} &= -bz + x^2\,. \end{aligned} \tag{C.7.2}$$

We will be seeking homoclinic bifurcations by starting from the Andronov-Hopf bifurcation at the non-trivial equilibria $O_{1,2}$ that takes place on the curve AH: $b = \frac{(2-a^2)}{a}$ (see Sec. C.2). This bifurcation can be super-critical — the first

Lyapunov value is negative to the right of the point GH, and it is subcritical to the right of the point GH. Let us consider next the evolution of the behavior of the separatrices of the saddle O at the origin as the parameter a decreases while keeping $b = 0.9$ fixed. Above AH the separatrices tend to the stable equilibria $O_{1,2}$ which looses stability via an Andronov-Hopf bifurcation at $a \simeq 1.0341$. In the region between AH and HB the separatrices are attracted to the newborn stable periodic orbits. As a decreases further, the amplitude of the stable orbits increases, and they both merge with the origin at $a \simeq 0.8865$, thereby forming a homoclinic butterfly. Such a symmetric homoclinic bifurcation with $\sigma < 0$ is often called a *gluing* bifurcation regardless of the geometry the homoclinic configuration which can be a butterfly or a figure-eight. One can see that the leading direction at the saddle in the given parameter values is the z-axis corresponding to the eigenvalue $\lambda_2 = -b$. Therefore, in our classification we are dealing with a homoclinic butterfly: both separatrices enter the saddle touching each other. The homoclinic butterfly transforms into a figure-8 when the separatrices enter the saddle from the opposite direction given by the eigenvector of the other negative eigenvalue which becomes leading when $\lambda_2 < \lambda_3 = -a/2 - \sqrt{a^2/4 + 1}$ on HB. In both cases, upon exiting from the homoclinic bifurcation a stable symmetric periodic orbit appears. Thus, the results of the homoclinic metamorphosis is always the same if $\sigma < 0$. This is not the case when $\sigma > 0$ where the geometry of the homoclinics is a key factor.

The more important resonant condition on HB takes place at ($a \simeq 1.044$, $b \simeq 0.608$) where the saddle value σ vanishes (see Sec. 13.6). Near such a point the local consideration reduces to the corresponding truncated"normal form" — a one-dimensional Poincaré map

$$\bar{x} = (-\mu + A|x|^{1+\sigma})\,\mathrm{sign}(x)\,, \tag{C.7.3}$$

where $\|\mu, \sigma\| \ll 1$, A is a separatrix value. In our interpretation, the fixed point at the origin at $\mu = 0$ corresponds to the homoclinic butterfly. It follows from Sec. 13.6 that the structure of the bifurcation unfolding near such a codimension-two point counts strongly on the magnitude and the sign of A. We have earlier emphasized the role of A, but it is worth repeating that the sign of A determines the orientation of homoclinic loops. Moreover, in the "linear case" (i.e. at $\sigma = 0$), the value of A also determines the stability of the homoclinic butterfly. There is almost no way to find the value of A in the specific set of ODE's without computer simulations. The simplest way to do that is to carry out a numerical experiment analogous to that we have already used in the

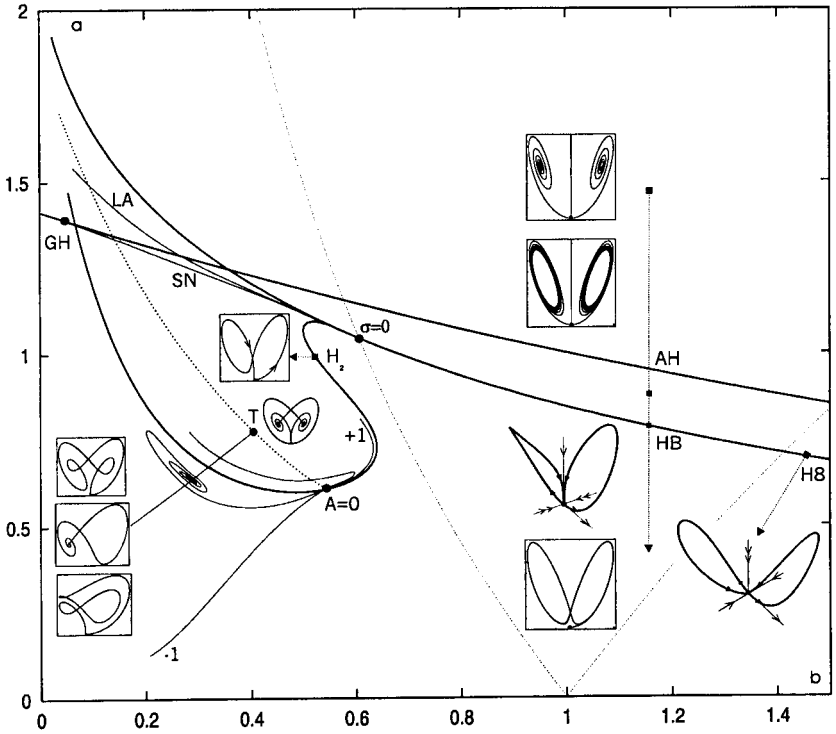

Fig. C.7.7. Fragment of bifurcation diagram of the Shimizu-Morioka model.

analysis of the Chua's circuit. The separatrix value will satisfy $|A| < 1$ if the separatrices of the saddle remain in a small neighborhood of the homoclinic butterfly after it splits. The other issue is how to determine the "orientation" condition, i.e., to find whether A is positive or negative; and we will return to this question later.

It is not hard to conclude from numerical experiments, which reveal the manner in which the separatrices converge to the homoclinic butterfly that A must be within the range (0,1). In this case, when $\sigma < 0$, everything is simple: the homoclinic butterfly splits into either two stable periodic orbits (Fig. C.7.8(g)), or just one stable symmetric periodic orbit (Fig. C.7.8(i)). It follows from Sec. 13.6 that when $\sigma > 0$, two bifurcation curves originate from this codimension-two point. They correspond to the saddle-node bifurcation (Fig. C.7.8(d)) and to the double homoclinic loop (Fig. C.7.8(f)). The

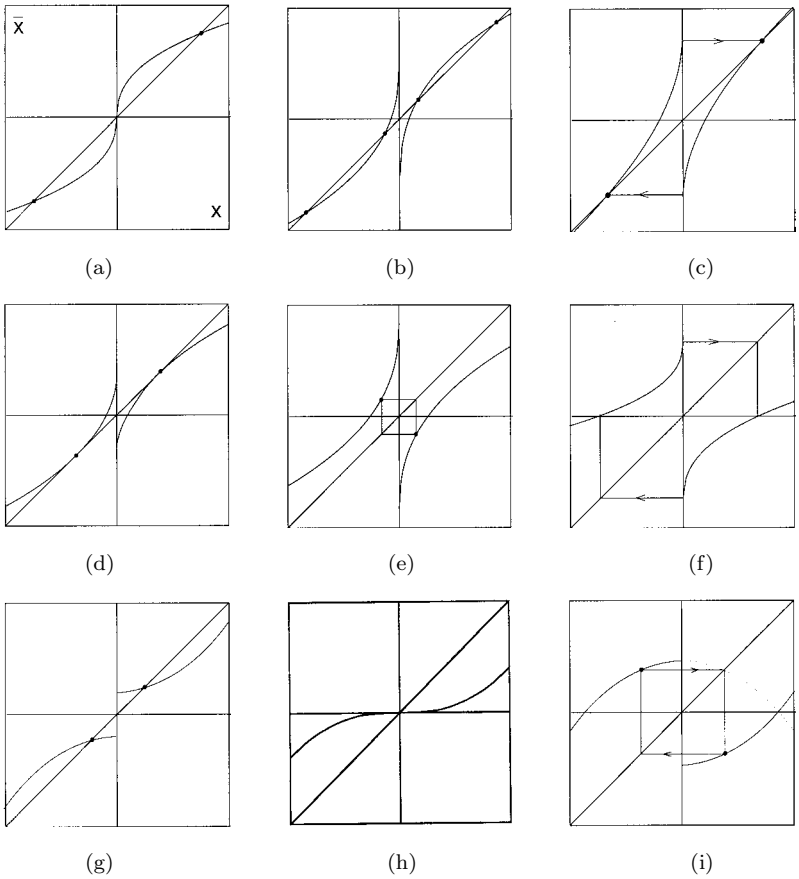

Fig. C.7.8. Bifurcations in one-dimensional map near the codimension-two point $\sigma = 0$; (a)–(f) corresponds to the case $\sigma > 0$, whereas (g)–(i) correspond to $\sigma < 0$.

symmetry adds to the problem a plethora of other bifurcation phenomena. Of very special interest is the bifurcation shown in Fig. C.7.8(c). It leads to the formation of the closed interval which is mapped onto itself. Furthermore, since the derivative of the map is larger than 1 on this integral, it contains no stable periodic points but infinitely many unstable ones. This is the moment of the appearance of the invariant attractive set without stable trajectories — a Lorenz-like attractor. In terms of the flow, this bifurcation occurs when the one-dimensional separatrices of the saddle at the origin lie on two-dimensional

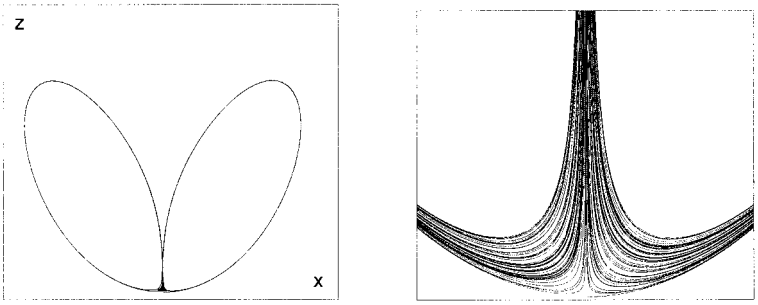

Fig. C.7.9. The Lorenz-like attractor in the Shimizu-Morioka model near the point $\sigma = 0$.

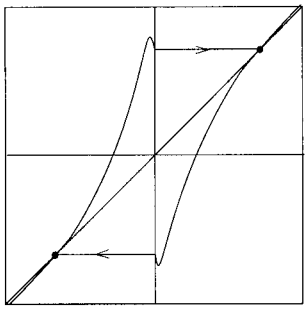

Fig. C.7.10. The Lorenz attractor does not appear if $A < 0$ on the curve LA.

stable manifolds of the saddle periodic orbits that have earlier bifurcated from each loop (see an analogous bifurcation for the Lorenz equation shown in Fig. C.7.14). Since $A > 0$, these manifolds are homeomorphic to a cylinder. This bifurcation occurs on the curve LA in Fig. C.7.7. Near the codimension-two point $\sigma = 0$, the Lorenz attractor is very thin, and looks like a stable periodic orbit (see Fig. C.7.9). Note that one should verify that the separatrix value A does not vanish anywhere on the curve LA. If so, there may arise the situation sketched in Fig. C.7.10 which shows schematically how the primary bifurcation of the Lorenz attractor can be ruined when the separatrix value A becomes negative. We will discuss this possibility below.

So far an important conclusion: since there is a homoclinic butterfly with $|A| < 1$, the region of the existence of the Lorenz attractor adjoins to the codimension-two point in the parameter space. The interested reader is advised to consult [127, 129, 187] on the bifurcations of Lorenz attractor in the

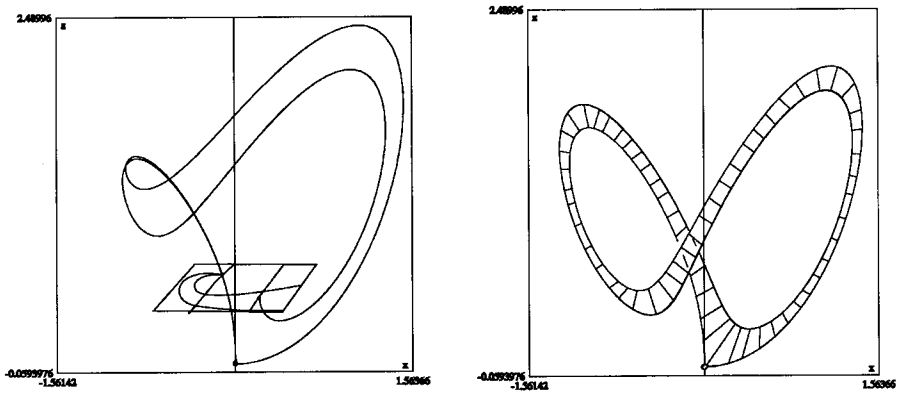

Fig. C.7.11. Twisted ($A < 0$) and orientable ($A > 0$) double homoclinic loops. The two-dimensional Poincaré map has a distinctive hook-like shape after the separatrix value A becomes negative.

Shimizu-Morioka model, and [114, 115, 117, 161] for the original Lorenz and some other Lorenz-like equations. □

C.7.#85. Consider the bifurcations of the symmetric cycle as σ evolves from positive to negative values. Can it undergo a period-doubling bifurcation? saddle-node one? Exploit the symmetry of the problem. For the map (C.7.3), find the analytical expression for the principal bifurcation curves. Does the saddle-node bifurcation here precede the appearance of the Lorenz attractor (i.e. can chaos "emerge through the intermittence")? Vary A from positive to negative values. Examine the piece-wise linear map with $A > 1$, and determine the critical value of A, after which the Lorenz attractor emerges. □

Another codimension-two homoclinic bifurcation in the Shimizu-Morioka model occurs at ($a \simeq 0.605, b \simeq 0.549$) on the curve H_2 corresponding to the double homoclinic loops. At this point, the separatrix value A vanishes and the loops become twisted, i.e. we run into inclination-flip bifurcation [see Figs. 13.4.8 and C.7.11]. The geometry of the local two-dimensional Poincaré map is shown in Fig. 13.4.5 and 13.4.6. To find out what our case corresponds to in terms of the classification in Sec. 13.6, we need also to determine the saddle index ν at this point. Again, as in the case of a homoclinic loop to the saddle-focus, it is very crucial to determine whether $\nu < 1/2$ or $\nu > 1/2$. Simple calculation shows that $\nu > 1/2$ for the given parameter values. Therefore,

the bifurcation unfolding for each of the homoclinic loops in the butterfly is the same as in Sec. 13.6. The following four bifurcation curves originate from such a point. They correspond to a saddle-node bifurcation (labeled "+1" in Fig. C.7.7), the period doubling ("−1"), and to two curves of the doubled separatrix loops (these curves end up spiraling to T-points in the (a, b)-plane). The dashed curve in the (a, b)-plane corresponds to the $A = 0$-axis in the bifurcation diagram in Fig. 13.6.4. Above this curve all homoclinic loops of the origin are orientable, and they are twisted below it. At each point of intersection of the curve $A = 0$ and a homoclinic bifurcation curve the structures of the bifurcation sets are similar, unless $\nu < 1/2$. The importance of this ratio becomes evident upon studying the one-dimensional Poincaré map

$$\bar{x} = (\mu + A|x|^{\nu} + |x|^{\gamma}) \operatorname{sign}(x)\,, \tag{C.7.4}$$

where $|\mu, A| \ll 1$, $\nu = |\lambda_2|/\lambda_1$, and $\gamma = |\max\{2\lambda_2, \lambda_3\}|/\lambda_1$; here $\lambda_{1,2}$ are, respectively, the leading unstable and stable characteristic exponents at the saddle, and λ_3 is a non-leading stable characteristic exponent.

When $A = 0$, the stability of the trajectories of the above map is determined by the third term. It is clear that depending on γ, the map for the parameter values on the curve $A = 0$ may be either a contraction if $\gamma > 1$, or an expansion if $\gamma < 1$. Assuming $2\lambda_2 > \lambda_3$, the condition on γ reduces to either $\nu < 1/2$ or $\nu > 1/2$. Thus, it is not hard to see that the map may have the form shown in Fig. C.7.8(a) at $\nu < 1/2$ and in Fig. C.7.8(h) at $\nu > 1/2$. If $\nu < 1/2$, there can be no stable points for zero values of A.

The structure of the bifurcation set of the truncated map (without the term $|x|^{\gamma}$) with $1/2 < \nu < 1$ and $A > 0$ is the same as in the above resonant case $\nu = 1$. The case $A < 0$ is presented in Fig. C.7.12(a)–(c). The reader is challenged to examine the bifurcations in this map. The feature of the case $A < 0$ is that the map may have an invariant attracting interval, which is mapped onto itself (Fig. C.7.12(c)). We can identify the chaotic behavior on this interval with a "non-orientable Lorenz attractor" [127, 129].

In terms of the flow, this means that for the parameter values from an exponentially narrow region in the parameter space, which adjoins to the point $A = 0$ on $H8$ from the side of $A < 0$, there exists a Lorenz-like attractor containing infinitely many saddle periodic orbits whose stable and unstable manifolds are homeomorphic to a Möbius band.

The one-dimensional map (C.7.4) has, when $A < 0$, a parabola-like graph shown in Fig. C.7.12(d)–(f). Obviously, one should foresee the period-doubling

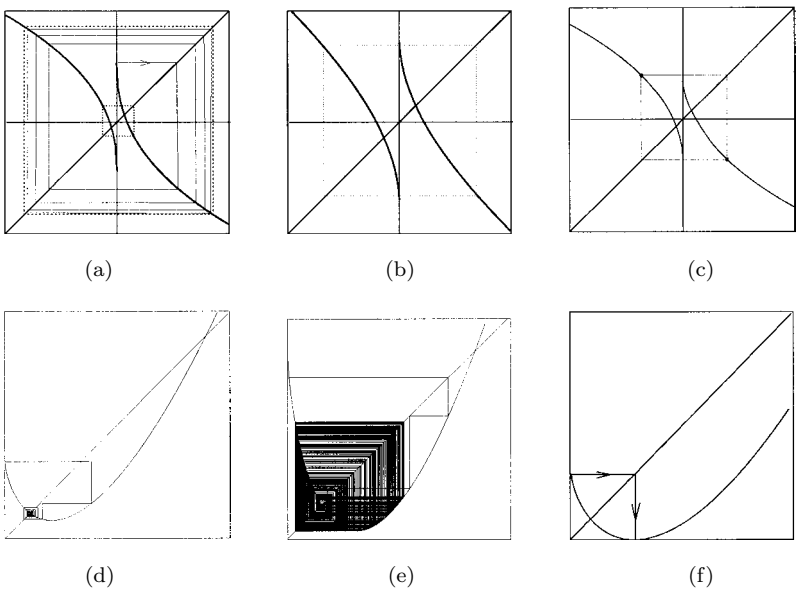

Fig. C.7.12. Transformations of the map (C.7.4) near $A \leq 0$.

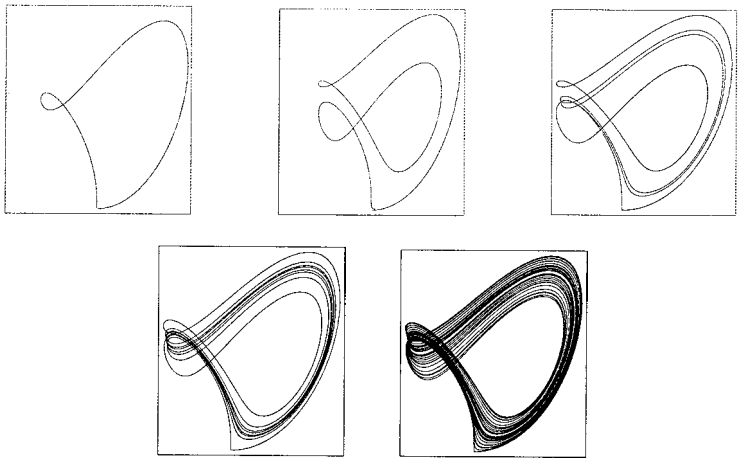

Fig. C.7.13. Homoclinic doubling cascade in the Shimizu-Morioka model, as the parameter a varies ($b = 0.40$). Using the *shooting* approach, find the corresponding values of parameter a.

cascades (Figs. C.7.12(c) and C.7.11(e)) similar to those that appear in the study of the purely quadratic map in Sec. C.11. The contrast is the infinite derivative at the discontinuity point that guarantees strong expansion near the origin.

The period-doubling cascade is closely related here to the homoclinic doubling cascade [71, 120, 126], see Fig. C.7.13.

The two-dimensional map has the shape of a distinguishable "hook" for the parameter values along the curve $H8$ in the region $A < 0$, as shown in Fig. C.7.10. In fact, this observation suggests the simplest recipe for computing the orientation of the homoclinic loop; namely, having chosen a point on the cross-section close to the stable manifold and computing the corresponding trajectory, one verifies if the initial and the final points of the trajectory lie on the same side from W^s on the cross-section. If this is the case, then $A > 0$, and $A < 0$ otherwise. The initial point should be reasonably close to W^s because when A changes its sign one more time and becomes positive again, the loop becomes twice twisted and so forth. Figure C.7.7 shows two such secondary bifurcation curves which originate from the point $A = 0$ and end up spiraling to two T-points in the (a, b)-parameter plane (examine the fine structure of T-point in [35, 174]). Such codimension-two point (approximately $a \simeq 0.781, b \simeq 0.39$ in Fig. C.7.7) corresponds to a heteroclinic cycle involving the saddle at the origin and the non-trivial saddle-foci. It follows from [35] that near the primary T-point there is an accumulating series of similar ones that lie within a sector bounded by the bifurcation curves corresponding to homoclinics and heteroclinics to these saddle-foci. This, in part, explains why the separatrix value A alters its sign here, and as a result, the loops change orientation (remember the 2D Poincaré map near a saddle-focus).

C.7.#86. Assume there is a homoclinic loop to a saddle-focus in the Shimizu-Morioka model (like a T-point). Without computing the characteristic exponent of the saddle-focus, what can we say about the local structure: is it trivial (one periodic orbit), or complex (infinitely many periodic orbits)? □

The classical Lorenz equation

$$\begin{aligned} \dot{x} &= -\sigma(x - y)\,, \\ \dot{y} &= rx - y - xz\,, \\ \dot{z} &= -\frac{8}{3}z + xy\,. \end{aligned} \tag{C.7.5}$$

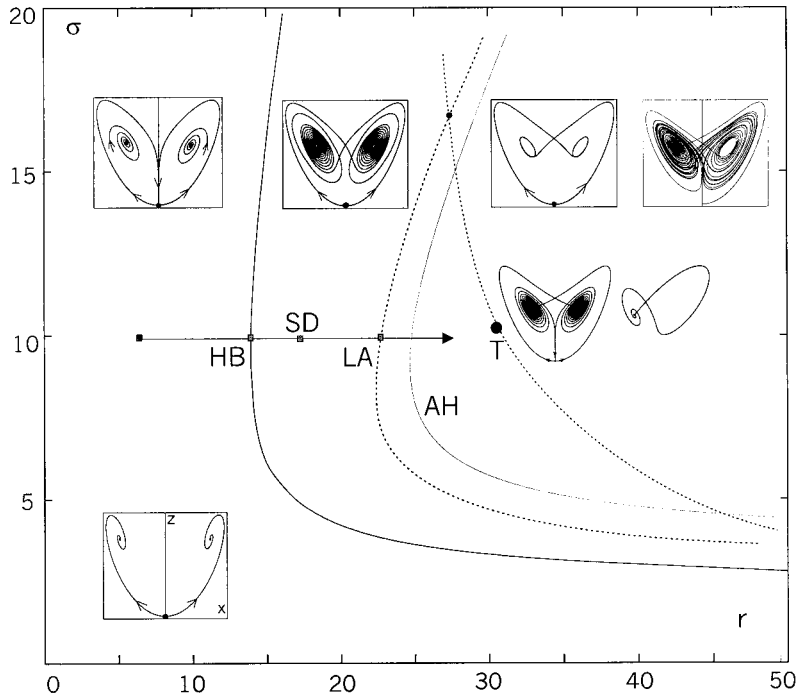

Fig. C.7.14. Famous path to the Lorenz attractor. The T-point is located at ($r \simeq 30.4$, $\sigma \simeq 10.2, b = 8/3$).

A fragment of its (r, σ) bifurcation diagram is shown in Fig. C.7.14. Detect the points where the path $\sigma = 10$ intersect the curve HB of the homoclinic butterfly and the curve LA on which the one-dimensional separatrices of the saddle tend to the saddle periodic orbits. Find the point on the curve LA above which the Lorenz attractor does not arise upon crossing LA towards larger values of r. The dashed line passing through the T-point in Fig. C.7.14 corresponds to the moment of the creation of the hooks in the two-dimensional Poincaré map when the separatrix value varishes: $A = 0$ (see discussion on the Shimizu-Morioka model). □

We have seen that homoclinic bifurcations in symmetric systems have much in common. Let us describe next the universal scenario of the formation of a homoclinic loop to a saddle-focus in a "typical" system. In particular, this mechanism works adequately in the Rössler model, in the new Lorenz models, in the normal form (C.2.27), and many others.

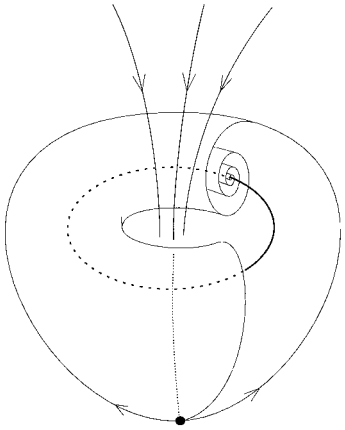

Fig. C.7.15. An attracting whirlpool.

The first step on the route to such a homoclinic bifurcation is a super-critical Andronov-Hopf bifurcation: the stable equilibrium states losses its stability and becomes a saddle-focus. The edge of its two-dimensional unstable manifold is the new-born stable periodic orbit. Next, let a real leading multiplier of the stable periodic orbit coalesce with the other one after which they become a complex conjugate pair remaining inside the unit circle. Then, the unstable manifold of the saddle-focus starts winding to the stable periodic orbit thereby forming an attractive "cup" or "a whirl-pool", as shown in Fig. C.7.15. As a parameter of the system varies further, the sizes of the scrolls increase, and eventually the unstable manifold of the saddle-focus touches its stable manifold. Usually, this homoclinic bifurcation follows the preceding stability-loss bifurcations of the periodic orbit via either a flip- or a torus-bifurcation. Moreover, if the saddle value is positive at the saddle-focus, then the whirlpool will contain an attracting set of non-trivial structure.

Let us visualize these steps using the example of the new Lorenz model [128]

$$\begin{aligned} \dot{x} &= -y^2 - z^2 - ax + aF\,, \\ \dot{y} &= xy - bxz - y + G\,, \\ \dot{z} &= bxy + xz - z\,, \end{aligned} \tag{C.7.6}$$

where (F, G) are control parameters and $(a = 1/4, b = 4.0)$ (see Fig. C.7.16).

The new Lorenz model is very rich in the sense of bifurcations. One of them is a non-transverse homoclinic saddle-node bifurcation. In Sec. C.2, we have

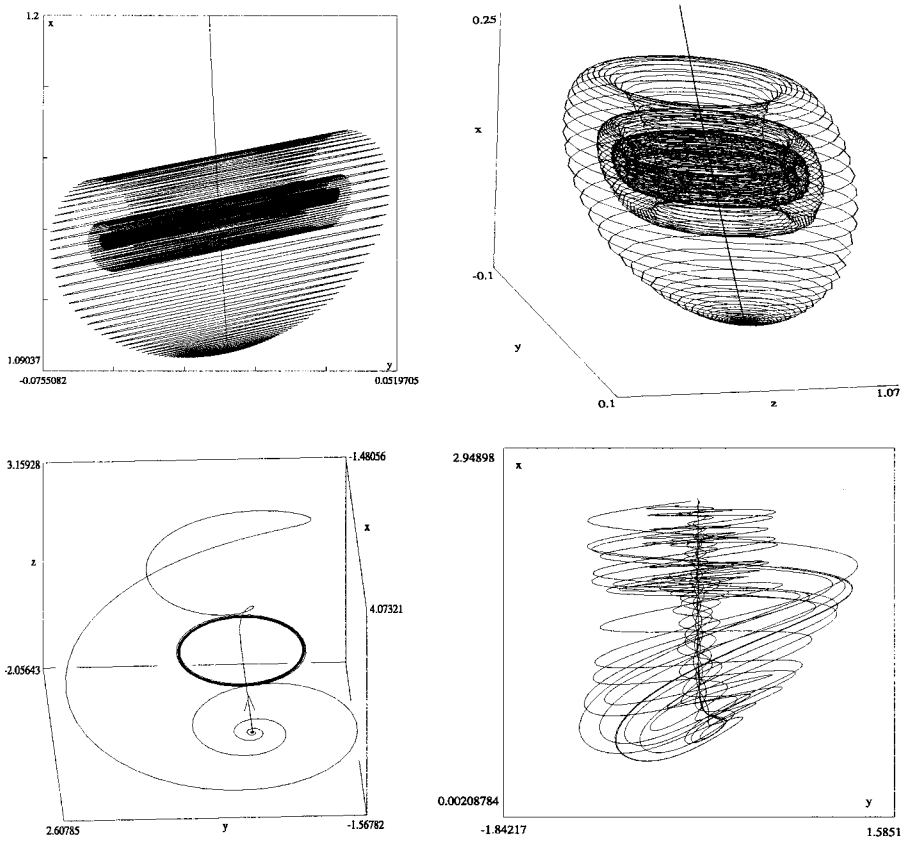

Fig. C.7.16. Creation of a whirlpool in the new Lorenz system.

already found the regular saddle-node bifurcation curve SN. Figure C.7.17 is the enlargement of the bifurcation diagram of the system near the upper branch of SN, compare with Figs. C.6.10 and C.2.4. This branch corresponds to a structurally unstable equilibrium state with one zero characteristic exponent, the other two have a negative real part. To the left of SN, this critical equilibrium disappears, whereas to the right of SN it splits into two: a stable one and and a saddle-focus (2,1). The curve H_1 corresponds to the homoclinic loop of the saddle-focus. The points where H_1 merges with SN correspond to the non-transverse homoclinic saddle-node bifurcations of codimension two.

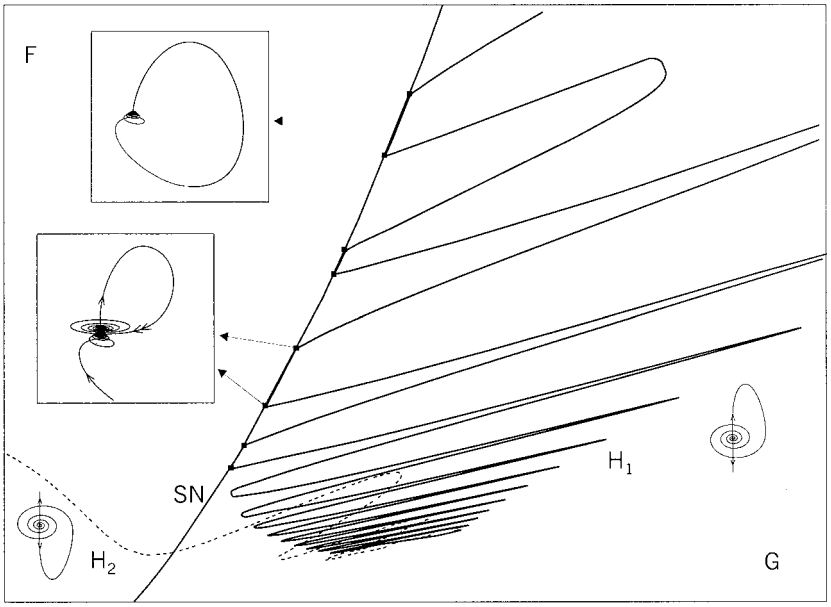

Fig. C.7.17. Enlargement of the bifurcation diagram in Fig. C.6.10. The marked points correspond to the non-transverse homoclinic saddle-node bifurcation.

At such a point the unstable manifold of the saddle-node returns to the equilibrium state along the strongly stable manifold. The rest of the curve SN is a bifurcation surface of codimension-one broken by these points into alternating intervals of two types. Bifurcation sequences on the route from the right to the left over these intervals differ significantly. In the first case, this is a plain saddle-node bifurcation: two equilibrium states coalesce and vanish. A point on the second type segments corresponds to the saddle-node equilibrium state with a homoclinic orbit which becomes an attractive limit cycle after the saddle-node point disappears on the left of SN. It is curious to note that this bifurcation sequence is reversible: having crossed over SN from the left to the right, the stability of the periodic orbit returns to the attractive equilibrium state. In this connection, see the discussion on "safe" and "dangerous" bifurcations in Chap. 14. □

Let us complete this section by an illustration corresponding to the homoclinic butterfly of the saddle-focus in the four-dimensional case. Let us consider

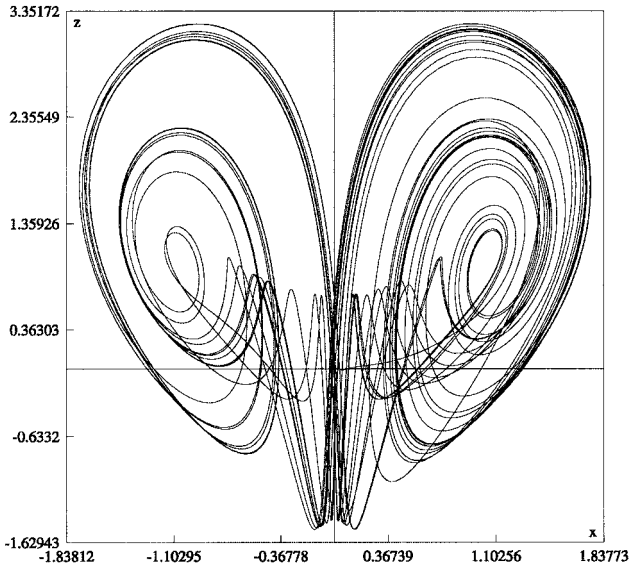

Fig. C.7.18. Homoclinic explosion caused by a homoclinic butterfly to a saddle-focus in system (C.7.7) at $a = 2, b = 0.5, \mu = 1.2$.

a four-dimensional perturbation of the Lorenz equation

$$\begin{aligned} \dot{x} &= -10(x - y)\,, \\ \dot{y} &= rx - y - xz\,, \\ \dot{z} &= -\frac{8}{3}z + \mu w + xy\,, \\ \dot{w} &= -\frac{8}{3}w - \mu z\,, \end{aligned}$$

and that of the Shimizu-Morioka model

$$\begin{aligned} \dot{x} &= y\,, \\ \dot{y} &= -ay + x - xz\,, \\ \dot{z} &= w\,, \\ \dot{w} &= -bw - \mu z + x^2\,, \end{aligned} \tag{C.7.7}$$

where a new parameter $\mu \geq 0$ is introduced so that the saddle equilibrium state at the origin restricted to the (z, w)-subspace becomes a stable focus.

C.7.#87. Find the stable, strongly stable and unstable linear subspaces of the equilibria at the origin. Detect numerically the primary homoclinic loops to the origin ($\mu = 0$ is a good initial guess). Classify them in terms of a homoclinic butterfly or a figure-eight. What are the first and the second saddle values at homoclinic bifurcations? What can you say about the dimensions of the stable and unstable manifolds of the periodic orbits that appear through a homoclinic explosion in both models? Construct the Poincaré maps. □

Index — Parts I & II

α-limit, 401, 413, 426, 449, 689, 733
α-limit point, 14
α-limit set, 14
γ-norm, 289, 306, 318
γ'-norm, 310, 318
γ-stable set, 315, 320
λ-lemma, 160, 161, 423, 426
τ-antiperiodic, 201, 320
τ-periodic, 320
ω-limit, 400, 413, 426, 436, 447, 679, 688, 732
ω-limit heteroclinic cycle, 15
ω-limit homoclinic cycle, 15
ω-limit point, 13, 14, 243
ω-limit set, 732
Ω-limit set, 813
Ω-moduli, 443

a center, 59, 402, 403, 404, 472, 474, 518, 611
a cusp, 550, 556, 557, 633, 835, 836
a canonical normal form, 696
a heteroclinic trajectory, 348, 416, 424
a homoclinic-8, 766, 767, 903
a homoclinic-8 of a saddle-focus, 772
a Klein bottle, 258, 637, 653, 655, 666, 668
a positive semi-trajectory, 6, 64, 400
a saddle-node, 61, 431, 460, 483, 525, 542, 564, 588, 629, 637, 639, 651, 759, 802
a scheme, 18, 396, 430, 439
a separatrix, 18, 29, 396, 431, 500, 516, 525, 645, 761
a strange attractor, 12, 24, 411, 412, 685, 751, 911
a strongly stable manifold, 431, 453, 478, 483, 485, 648, 725
a weak focus, 432, 470, 516, 801
absorbing domain, 12
admissible pair, 769
Afraimovich and Shilnikov theorem, 426
algebraic automorphism of a torus, 257
almost periodic motions, 404, 406, 408, 409
an area preserving map, 854
an asymptotic normal form, 858, 866, 869, 871
an attracting whirlpool, 921
an averaged system, 845
analytic manifold, 453, 472, 485, 490
analytical invariant manifold, 79
Andronov and Leontovich theorem, 700, 707
Andronov, 105, 106
Andronov-Hopf bifurcation, 598, 600, 825, 830, 833, 838, 840, 888
Andronov-Pontryagin system, 424
Andronov-Pontryagin theorem, 394, 395, 419, 430, 433
Andronov's setup, 444, 446, 450, 534
Andronov-Vitt, 203
annulus, 242

annulus principle, 235, 242, 255, 615, 616, 622
antiperiodic, 201
antiperiodic functions, 259
area preserving map, 854
Arnold tongue, 629
associated motion, 4
asymptotic representation, 557
asymptotic normal form, 858, 866, 869, 871
asymptotical phase, 204
asymptotically one-side stable, 688
asymptotically orbitally stable periodic trajectory, 204
asymptotically stable, 44, 454, 455, 472, 479, 480, 485, 490, 496, 511, 519, 522, 881
attracting cloud, 805
attracting whirlpool, 921
attraction basin, 413, 414, 417, 583, 584, 599, 604, 618, 620, 805, 906
attractive, 484, 522, 524, 556, 614, 733
attractor, 12, 671, 677
autonomous equation, 681
autonomous form, 657, 682
autonomous normal forms, 218
autonomous system, 1, 238, 311, 506, 618
averaged system, 845
averaging theorem, 848

ball, 238
Banach principle of contraction mappings, 223, 245, 261, 305, 643, 683, 707
Banach space, 231, 245, 394, 435, 438
Banach submanifold, 445
base, 279
basic concepts, 1
basic kinds of saddle equilibria, 83, 84
beat modulation, 630, 645
Belitskii theorem, 213
bi-asymptotic manifold, 675
bi-asymptotical trajectory, 104, 214, 433, 529
bifurcating point, 462,
bifurcation, 429, 435, 437, 444, 450, 537, 558, 559, 687, 700, 708, 712
bifurcation diagram, 568, 569, 595
bifurcation of a homoclinic loop, 748, 750, 761
bifurcation of a separatrix loop, 712, 713
bifurcation of a limit cycle, 643
bifurcation of codimension-k, 536
bifurcation of codimension-one, 662
bifurcation of codimension-two, 748, 749
bifurcation of resonant periodic orbit, 623
bifurcation of saddle-node fixed point, 564
bifurcation of saddle-node limit cycle, 566
bifurcation of the fixed point, 569, 572, 575, 577
bifurcation of the heteroclinic cycle, 765
bifurcation of the homoclinic-8, 765, 768
bifurcation parameter value, 444
bifurcation point, 557
bifurcation set, 444, 536, 557, 596, 771, 773
bifurcation surface of codimension-k, 536
bifurcation surface, 535, 536, 556, 587
bifurcation theory, 325
bifurcation unfolding, 607, 608, 619, 753
big lobe condition, 662, 663, 672
bi-infinite trajectory, 8
binary tree, 767

Birkhoff's theorem, 6, 10, 403, 413
birth of invariant torus, 611, 618, 623, 633, 803
birth of periodic orbit, 631, 720, 721, 731, 733, 868
blue sky catastrophe, 273, 475, 637, 669, 670, 680, 802, 804, 809, 897, 899
Bogdanov-Takens bifurcation, 894
Bogdanov-Takens normal form, 876, 902
Bogdanov-Takens point, 710
border saddle equilibrium state, 649
Borel lemma, 103
boundary system, 438
boundary value problem, 86, 91, 154, 155, 184, 185, 286, 289, 293, 339
Brauer's criterion, 238
breaking point, 633

canonical normal form, 696
Cantor pencil, 773
Cantor set, 16, 407, 408
cascade, 7
cell, 18
center, 59, 402, 403, 404, 472, 474, 518, 611
center manifold, 269, 282, 325, 326, 348, 446, 452, 458, 462, 472, 488, 531, 560, 599, 651, 861, 879
center manifold theorem, 271, 275, 276
center stable, 282
center stable manifold, 281, 282, 330, 331
center unstable manifold, 282, 284, 330, 333, 350
center unstable manifold theorem, 281
chain, 423, 426
chain rule, 796
change of time, 5
change of variables, 103, 137, 211, 276
chaos, 422, 430, 633, 634, 662
chaotic behavior, 673, 883, 885
characteristic equation, 23, 195, 270
characteristic exponents, 23, 38, 197, 199, 202, 204, 270, 331, 352, 538, 598
characteristic roots, 195
Cherry flow, 769, 770
Chua's circuit, 24, 824, 826, 831, 833, 856, 858, 860, 862, 874, 876, 878, 893, 904-907, 909, 911
circle diffeomorphisms, 264
circle map, 632, 855, 856
classification of center motions, 404
clockwise-right angled spiral, 118
closed convex set, 225, 228
closed convex subset, 252
closed invariant curve, 651
closing lemma, 411
codimension one, 435, 440, 446, 538, 597, 662
codimension two, 535, 688
completely degenerate fixed point, 466, 488, 492
completely unstable, 205, 458, 516, 525
completely unstable equilibrium state, 83, 102, 525
completely unstable fixed point, 127
completely unstable periodic trajectory, 205
complex, 483, 497
complex (degenerate) saddle, 485
complex dynamics, 412, 422, 427, 437, 439, 736, 742, 750
complex saddle-focus, 470, 472, 485
complex stable (weak) focus, 497
complex-conjugate multipliers, 611
complex-conjugate, 598
concentric circumferences, 59
contraction map, 242

contraction mapping principle, 683
contraction mappings, 223
conventionally stable invariant manifold, 322
conventionally stable manifold, 310, 313, 317
conventionally stable or γ-stable, 303
conventionally unstable invariant manifold, 322
conventionally unstable manifold, 313
convex hull, 101
counter-clockwise concentric circle, 60
counter-clockwise spiral, 28, 31
coupled map, 241
covering, 264
criterion of chaos, 422
critical case, 270, 451, 452, 458, 465, 477, 531, 804
critical equilibrium state, 452, 456, 532
critical fixed point, 478, 485, 515, 527
critical periodic orbit, 532
critical saddle, 486
cross form, 227, 228, 243, 252, 422
cross-section, 5, 112, 241
curvilinear triangle, 49
cusp, 550, 556, 557, 633, 835, 836
cusp bifurcation, 550, 633
cusp edge, 556, 557, 835, 836
cycle, 7, 14, 423
cyclic variable, 236

dangerous boundaries, 799, 804, 808, 810, 812, 880
dangerous point on the stability boundary, 805
dangerous stability boundary, 811, 812
degeneracy, 873
degenerate, 452, 462, 464
degenerate case, 124
degenerate equilibria, 452, 483
degenerate fixed point, 483
degenerate map, 123, 124
degenerate saddle-node, 649
Denjoy theorem, 265
dense diffeomorphism, 266
dense rough diffeomorfism, 398
devil staircase, 267, 856
devil's wheel, 817
dicritical node, 26
diffeomorphic, 413
diffeomorphism, 7, 115, 129, 211, 236, 242 , 398, 417, 422, 438, 478, 597, 666, 702, 739
dimension of manifold, 65
discrete dynamical system, 7
dissipative system, 403
double circuit separatrix loop, 787
double cycle, 607
double homoclinic loop, 759, 762, 775, 916
double limit cycles, 717
double separatrix loop, 718, 719, 787
double-scroll attractor, 24
double-scroll Chua's attractor, 909, 911
Duffing equation, 236
Dulac form, 103, 106
Dulac sequence, 699, 713
Dulac theorem, 101, 102
dwelling time, 643
dynamical systems, 6
Dynamically definite boundaries, 811, 812, 814, 816
dynamically indefinite boundary, 814

eigen-direction, 327, 328
eigenspace, 328
eigen-subspace, 73
eigenvalues, 23, 38, 115, 125, 126, 199, 270, 328, 414, 418, 432, 537, 579, 598
elliptic sectors, 528, 529
embedded map into the flow, 681, 682
embedding, 685

empirical chaotic character, 406
entire trajectory, 4, 6
equilibria, 429, 548
equilibrium point, 426, 430
equilibrium state of the saddle type, 45
equilibrium state, 3, 14, 21, 44, 56, 78, 270, 272, 280, 315, 395, 404, 416, 446, 454, 458, 464, 524, 598, 607, 633, 637, 677, 708, 808
equimorphism, 264
equivalent trajectory, 18
essential map, 656, 658, 663, 804
Euclidean norm, 42
Euclidean space, 231
exponential, 37
exponentially asymptotically stable equilibrium state, 44
exponentially completely unstable equilibrium state, 45, 78
exponentially completely unstable fixed point, 141
exponentially stable equilibrium state, 69
exponentially stable fixed point, 119
exponentially stable solution, 202
exponentially unstable, 45
exponents, 598
extended, 128
extended phase space, 2
extended stable eigenspace, 330, 352
extended stable eigen-subspace, 154
extended stable invariant subspace, 46, 128
extended stable manifold, 84, 154, 329, 330, 746
extended stable subspace, 56
extended unstable eigen-subspace, 154
extended unstable invariant subspace, 46, 128
extended unstable manifold, 84, 154, 331, 332
extended unstable subspace, 49, 50, 56
extra degeneracy, 871

families, 534
family of maps, 611
Farey tree, 767
fast periodic orbit, 678
fast system, 677
fast-slow system, 680
Feigenbaum multiplier, 883
figure-eight, 350
finitely-smooth change of variables, 103
finite-parameter family, 105, 106, 214, 216
first critical case, 458, 480
first Lyapunov value, 538, 587, 618, 763, 877, 879, 891
first separatrix value, 695
first type stability boundary, 803
fixed point, 114, 115, 125, 245, 418, 422, 478, 497, 519, 541, 610, 620
flight time, 659, 682, 684, 691
Floquet multipliers, 195
Floquet theorem, 198
foci, 838
focus equilibrium state, 74, 76
focus fixed point, 140, 238
focus, 74, 140, 825
fold bifurcation, 801, 803, 813
foliation of neighbourhood, 446
foliation, 279, 282, 453
formal change of variables, 218
formal series, 101
Fourier series, 407
fractal, 407
Franklin-Markov theorem, 409
frequency regime, 633
frequency spectrum, 634
fundamental matrix, 195

Gavrilov-Guckenheimer bifurcation, 835

general, 328
general case theorem, 284
general position, 532, 535, 539, 546
global, 325
global bifurcation, 325, 637
global map, 335, 641, 646, 689, 694, 702, 739, 760
global phase portrait, 526
global saddle-node bifurcation, 658
global stable, 79
global stable invariant manifold, 79
global unstable, 79
global unstable invariant manifold, 79
global unstable manifold, 651
globally dichotomic system, 287, 288, 302, 315, 509
gluing bifurcation, 912
gluing term, 770, 891
governing parameter, 533
Grobman-Hartman theorem, 61, 79, 95, 129, 132
group property, 2

Hadamard's theorem, 142
half-plane, 413
helicoids form, 740
Henon map, 884, 887
heteroclinic 397, 415, 424, 496, 520
heteroclinic connection, 778, 787, 896
heteroclinic contour, 348
heteroclinic cycle, 325, 348, 352, 437, 519, 777, 786, 789
heteroclinic point, 426
heteroclinic trajectory, 348, 416
hierarchy of non-leading manifolds, 73, 140
high-dimensional linear maps, 125
high-dimensional, 37
Hilbert's 16-th problem, 112
Hindmarsh-Rose model, 839, 899
holomorphic integral, 472
homeomorphic, 264, 411, 414, 485, 500
homeomorphic to a Möbius band, 811
homeomorphism, 6, 17, 59, 129, 207, 395, 411
homoclinic, 415
homoclinic bifurcations, 637, 688, 901, 911
homoclinic butterfly, 350, 351, 750, 773, 924
homoclinic cycles, 325
homoclinic doubling cascade, 918
homoclinic figure-eight, 350, 351, 355
homoclinic loop $\Gamma(\varepsilon)$, 801
homoclinic loop to a saddle focus, 736
homoclinic loops, 104, 325–327, 330, 334, 355, 397, 446, 475, 637, 646, 687, 720, 734, 760, 766, 906
homoclinic orbit, 413
homoclinic tangency, 438
homoclinic to saddle foci, 107
homoclinic to saddle, 107
homoclinic trajectory, 9, 214, 327, 330, 416, 424, 634, 638
homoclinic-8, 766, 767, 903
homoclinic-8 connection, 766, 767, 903
homoclinic-8 connection of a saddle-focus, 772
Homogeneous polynomial, 96, 97, 209
Homogeneous system, 222
horizontal strip, 420

identity map, 124, 259
inclination-flip bifurcation, 749, 753
infinite set of resonances, 108
infinitely degenerate equilibrium state, 465
infinitely degenerate fixed point, 488, 492
integral curve, 2, 238
integrating a system, 13
internal bifurcation, 438
intersect transversely, 416, 419
invariance of a set, 8
invariance of the manifold, 137

invariant, 9, 282, 747
invariant center local manifold, 274
invariant center manifold, 271, 282
invariant center stable manifold, 281, 284
invariant circle, 123
invariant curve, 260, 614, 618, 621, 623, 629, 634, 644, 661, 888, 893
invariant extended stable manifold, 328
invariant foliation, 271, 278, 302, 310
invariant leading manifold, 77
invariant manifold, 64, 79, 135, 142, 147, 154, 248, 280, 413, 415, 453, 464, 483, 500, 510, 521, 653, 677
invariant non-leading manifold, 69
invariant set, 9, 12, 402
invariant stable, 584
invariant subspace, 44, 126
invariant surface, 611
invariant tori, 235
invariant torus, 236, 239, 242, 243, 256, 258, 263, 406, 449, 611, 618, 623, 633, 649, 801, 809, 852
inverse map, 171, 253
irregular case, 822
isolated equilibrium state, 21

Jacobian matrix, 21, 117, 189, 216, 829, 831
Jordan basis, 39, 138, 456
Jordan block, 40
Jordan form, 104, 125, 199, 641
jumping direction, 170

Khorozov-Takens normal form, 860, 862, 874, 902, 905
Klein bottle, 258, 637, 653, 655, 666, 668
k-parameter family, 536
Kroneker-Capelli theorem, 842

Lagrange method, 842
Lagrangian equation, 429
Lamerey diagram, 116, 480, 490, 561, 578, 581, 588, 705, 756
Lamerey spiral, 116, 118, 491, 583
Lamerey stair, 116, 117, 130
Landau-Hopf scenario, 633
leading axis, 118
leading characteristic exponents, 74
leading coordinates, 83
leading direction, 25, 31, 120, 137
leading eigenvalues, 168, 183, 275
leading invariant, 126
leading invariant manifold, 141
leading invariant subspace, 44, 128
leading local manifold, 77
leading manifold, 65
leading multipliers, 126, 140
leading plane, 32
leading saddle invariant subspace, 128
leading saddle submanifold, 154
leading saddle subspace, 46, 126
leading stable invariant submanifold, 154
leading stable, 84
leading subspace, 45, 73
leading unstable eigen-space, 84
leading unstable invariant submanifold, 154
leaf of the foliation, 279
leaf of the strong stable foliation, 354
Leontovich theorem, 713
Leontovich, 105, 106, 325
Leontovich-Mayer theorem, 435
lifting, 264
limit cycle, 16, 111, 396, 435, 473, 484, 521, 607, 700, 712, 714, 771, 874
limit-quasiperiodic, 404, 407
linear form, 101, 103, 212
linear map, 115, 116, 134, 229
linear systems, 24, 37
linearized map, 114

linearized system, 21, 22, 24
Lipschitz condition, 142, 232, 245
Lipschitz curve, 624
Lipschitz function, 245, 248
Lipschitz invariant manifold, 248
local bifurcations, 271, 445, 531, 641
local case, 269
local center manifold, 276, 284
local extended stable manifold, 337
local instability, 483
local invariant manifold, 317
local map, 335, 337, 641, 646, 689, 698, 702, 738, 760
local stable invariant manifold, 509
local stable manifold, 64, 80, 132
local theory, 19
local unstable manifold, 64, 80, 132, 483
locally invariant set, 70
locally reduced system, 283, 285
locally straightened center manifold, 653
locally topologically equivalent periodic trajectory, 135
locally topologically equivalent system, 63, 65
logarithmic spirals, 53, 123
logistic map, 881, 884
loops, 325
Lorenz attractor, 24, 752, 915, 920
Lorenz equation, 750, 826, 831, 868, 919
lose of cycle's skin, 808, 809
lose of smoothness, 534, 617, 634
lose of stability, 452, 584, 594, 609, 816, 912
Lyapunov (focal) value, 800
Lyapunov exponents, 104, 197, 199
Lyapunov function, 455, 475, 479, 496, 512, 519, 524, 622, 874
Lyapunov stable, 410, 454, 455, 472, 479
Lyapunov surfaces, 203
Lyapunov theorem, 199, 202
Lyapunov value, 431, 433, 452, 459, 469, 480, 490, 496, 497, 538, 599, 608, 632, 718, 763

Maier theorem, 266
main stability boundary, 802
manifold, 71, 747
map, 170, 182, 641
Markov theorem, 410
Mathieu equation, 853
maximal chain, 424
maximal open set, 270
maximal rank, 535
Mayer's theorem, 398
Medvedev's construction, 897
Medvedev's example, 669
metric, 398
m-fan, 500
minimal set, 10, 14, 241, 265, 405
Möbius band, 207, 414, 490, 584, 707, 719, 808
Möbius manifold, 414
Möbius strip, 587
moduli, 440, 442
Morse-Smale class, 438, 445, 767
Morse-Smale diffeomorfism, 417, 426, 439
Morse-Smale flows, 417, 427
Morse-Smale systems, 413, 417, 419, 422, 437
motions, 404
multi-dimensional system, 437
multiple limit cycle, 609
multiplier +1, 559
multiplier -1, 578, 595, 604
multipliers (complex-conjugate), 476
multipliers, 112, 115, 125, 127, 204, 219, 261, 414, 476, 602
mutual intersection, 449

natural code, 767
negative Poisson stable point, 9, 401

negative semi-trajectory, 6, 64
Newhouse regions, 489
nil-manifold, 409
node (−), 140
node (+), 140
node, 825
node equilibria, 911
node equilibrium state, 74
node fixed point, 140
node point, 629
node region, 62, 649
non-autonomous system, 236, 310, 504, 509, 522, 587
non-degeneracy assumptions, 725, 760, 788
non-degenerate bifurcation, 763
non-degenerate homoclinic loop, 761
non-homogeneous boundary value problem, 93
non-homogeneous system, 93
non-homotopic diffeomorphism, 256
non-leading axis, 119
non-leading direction, 25, 32, 56
non-leading invariant manifold, 137
non-leading invariant subspace, 76, 126, 128
non-leading local manifold, 77
non-leading manifold, 65, 69, 70, 74, 76, 82, 137, 316, 638
non-leading multipliers, 126
non-leading plane, 31
non-leading stable invariant manifold, 154
non-leading subspace, 45, 73
non-leading unstable invariant manifold, 154
non-leading unstable sub-manifold, 327
non-leading, 44, 84, 126
non-local, 325
non-local center manifold, 325
non-orientable case, 707, 708
non-orientable circle map, 258
non-orientable homoclinic butterfly, 775
non-orientable homoclinic loop, 783
non-orientable homoclinic-8, 776
non-orientable Lorenz attractor, 917
non-orientable separatrix loop, 707
non-orientable surface, 717
non-periodic trajectory, 124
non-quasiperiodic motion, 404
non-resonant, 432, 436, 496, 499, 515, 579, 612
non-resonant case, 496
non-resonant eigenvalues, 101
non-resonant function, 106, 215
non-rigorous methods, 444
non-rough equilibrium state, 544
non-rough system, 397, 412, 429, 446, 451
non-roughness system, 429, 439
non-singular Jacobian matrix, 117
non-singular map, 132
non-smooth Klein bottle, 669
non-smooth unstable manifold, 352
non-transverse homoclinic orbit, 439
non-transverse intersection, 446
non-trivial attractor, 449
non-trivial equilibrium state, 602, 894
non-trivial fixed point, 602
non-trivial Jordan block, 25
non-trivial motions, 404
non-unique leading manifold, 79
non-uniqueness, 272
non-wandering orbit, 423
non-wandering point, 9, 399, 400, 402, 411, 417
non-wandering set, 265, 449
normal coordinates, 186, 188, 192, 201
normal form for the second critical case, 468, 469
normal form method, 276, 531
normal forms, 103, 857, 866, 912
not topologically equivalent system, 60

on-edge bifurcation, 646
on-edge homoclinic loop, 645, 646
one-dimensional Poincaré map, 744, 762
one-parameter family, 539, 604, 613, 623, 672
one-side stability, 688, 690
open region, 412
orbit superhomoclinic, 735
orbital normal form, 469, 470
orbital stability, 204
orbitally stable periodic trajectory, 204
orbit-flip bifurcation, 750, 753
orbit-flip homoclinic bifurcation, 759, 760
order of the resonance, 96, 209
ordinal number, 402
ordinary differential equations, 1
orientable case, 708
orientable circle diffeomorphism, 265
orientable curve, 6
orientable homoclinic-8, 777
oriented graph, 424
oscillatory regimes, 394
Ovsyannikov-Shilnikov theorem, 108

pair of complex-conjugate multipliers, 623
Palis and Smale theorem, 419
partial order, 100
period, 7, 111
period-doubling bifurcation (flip bifurcation), 801, 803, 808, 881, 894
period-doubling bifurcation, 587, 607, 668, 717, 759, 787, 803, 882
period-doubling cascade, 438, 884, 919
period-doubling of a fixed point, 757
periodic fixed point, 119
periodic orbits, 111, 396, 404, 416, 422, 475, 484, 498, 521, 621, 637, 720
periodic point, 111, 238
periodic regime, 629
periodic solutions, 111
periodic trajectory, 3, 4, 14, 111, 115, 135, 192, 195, 205, 272, 284, 475, 477
periodically forced self-oscillating systems, 235
persistence, 258
phase diagram, 424
phase portrait, 465, 517, 523, 528
phase space, 6, 401, 610
phase trajectory, 2,6
pitch-fork bifurcation, 462, 558, 859, 894
planar bifurcation, 542
Poincaré form, 103
Poincaré map, 112, 114, 119, 134, 172, 175, 262, 310, 334, 432, 475, 489, 584, 604, 618, 658, 667, 689, 807
Poincaré region, 101
Poincaré return time, 10, 14, 189
Poincaré rotation number, 265, 266
Poincaré rotation number, 265, 266, 442, 618, 624, 629, 653, 661, 768
Poincaré theorem, 101, 265
Poincaré, 101, 265
Poincaré-Bendixson theory, 397, 404
Poincaré-Dulac theorem, 212
Poisson stability, 411
Poisson-stable point, 401, 404
Poisson-stable trajectories, 9, 397, 401, 403, 410, 767
Poisson-stable, 9
polynomial change, 96, 100
positive Poisson-stable point, 9
positive semi-trajectory, 6, 64, 400
positively stable, 401
properly periodic motion, 404
pseudo-projection, 47
p-trajectory, 10, 401, 410, 413

Pugh theorem, 411
Pugh's closing lemma, 411

quadratic tangency, 441
qualitative integration, 12
qualitative investigation, 24
quasiminimal attractors, 770, 775
quasi-minimal set, 10, 14, 405, 767, 769
quasiperiodic, 618
quasiperiodic attractors, 770, 774
quasi-periodic flow, 11, 770
quasi-periodic function, 239
quasiperiodic motion, 404
quasiperiodic orbit, 618
quasiperiodic regime, 624, 629
quasi-periodic solution, 241
quasi-periodic trajectory, 11

real Jordan form, 125
recurrent trajectory, 10, 405
reduction principle, 658, 660, 682
reduction theorem, 277, 278, 531
regime, 430
regular case, 821
repelling, 458, 484, 487, 566, 620, 674, 747
repelling equilibrium state, 458, 532, 541
repelling fixed point, 482, 620
repelling periodic trajectory, 205
repelling zone, 886, 896
representative point, 4
rescaling of time, 5, 186, 187
resonance relation, 95, 96, 209
resonances, 696
resonant (hyper) plane, 101
resonant case, 497
resonant fixed point, 503, 511, 528
resonant periodic orbits, 536, 618, 623
resonant polynomial, 104
resonant relations, 494
resonant set, 96
resonant torus, 626
resonant wedges, 625, 629
resonant zone, 624, 629, 634, 661
reverse period-doubling bifurcation, 759
reversion of time, 34, 281
Riemannian surface, 270
rigid generation, 603
rigid loss of stability, 600, 615, 804, 806
Rössler system, 838, 904
rotation number, 265, 769
rotation of the vector field, 396
rough, 24, 115
rough cycle, 394
rough diffeomorfism, 398
rough equilibria, 438, 554
rough equilibrium states, 395, 826
rough fixed point, 578
rough focus, 603
rough periodic trajectory, 115
rough saddle, 458, 486
rough stability, 454, 469, 485
rough stable periodic orbit, 660
rough systems, 394, 398, 419, 429
rough unstable cycle, 485
roughness/structural stability, 395, 398, 399, 412
route to the blue sky catastrophe, 676
Routh-Hurwitz criterion, 23, 24, 820, 829
Routh-Hurwitz determinant, 451, 477, 802
Routh-Hurwitz matrix, 821

saddle, 28, 34, 46, 78, 119, 128, 395, 413, 426, 507, 514, 584, 637, 745, 770, 823
saddle equilibrium state, 24, 28, 34, 46, 57, 79, 357
saddle equilibrium, 687, 788

saddle fixed point, 119, 121, 122, 128, 141, 142, 153, 154, 168, 439, 517, 519, 522
saddle in the first case, 745
saddle index, 105, 691, 706
saddle map, 160, 169, 228, 230, 420, 729
saddle periodic orbit, 604, 663, 748
saddle periodic trajectories, 111, 201, 207, 208, 516
saddle point, 526
saddle region, 62
saddle type, 45
saddle value, 105, 690, 696, 712, 717, 825
saddle with 2m separatrices, 500
saddle-foci, 169, 447, 781, 830
saddle-focus (1,2), 46
saddle-focus (2,1), 46
saddle-focus (2,2), 46
saddle-focus, 437, 443, 446, 498, 603, 618, 674, 687, 736, 745, 770, 841
saddle-focus equilibrium state, 34, 35, 46, 53, 58, 84, 104
saddle-focus fixed point, 128
saddle-focus in the second case, 745
saddle-node, 61, 431, 460, 483, 525, 542, 564, 588, 629, 637, 639, 651, 759, 802
saddle-node bifurcation of a fixed point, 757, 763, 812
saddle-node bifurcation of periodic orbit, 567
saddle-node equilibrium state, 61, 73, 638, 647, 674
saddle-node fixed point, 650, 673, 763, 888
saddle-node periodic orbit, 655, 666, 681, 801
safe boundary, 804, 810
safe point on the stability boundary, 804
safe stability boundary, 802, 807, 816
safe, 799
schematic portrait, 18
scheme, 18, 396, 430, 439
Schwarzian derivative, 881
second critical case, 465, 471, 489
second Lyapunov value, 619
self oscillations, 394, 430, 603
self-limit, 410, 413
self-limited trajectory, 14
self-limiting manifold, 740
semi-orientable homoclinic butterfly, 774
semi-orientable homoclinic-8, 776
semi-stable, 433, 434, 484, 548, 590, 607, 881
semi-stable curve, 622
semi-stable cycle, 566, 674, 685
semi-stable equilibrium state, 556
semi-trajectories, 14, 399, 480, 497
separatrices, 396, 431, 500, 516, 525, 645, 761
separatrix, 18, 29, 396, 431, 500, 516, 525, 645, 761
separatrix loop, 105, 435, 688, 694, 700, 712, 761, 900
separatrix value, 771
set(minimal), 10, 14, 241, 245, 405
shape of a roulette, 54
shift map, 853, 901
Shilnikov condition, 742
Shilnikov theorem, 721, 748
Shimizu-Morioka model, 826, 837, 840, 858, 866, 895, 911
shortened normal form, 110
Siegel region, 101, 102, 103
simple dynamics, 412, 437, 736, 742
simple equilibrium state, 808
simple homoclinic loop, 762
simple leading eigenvalues, 183, 184
simple saddle-node, 431, 460, 651, 671, 681, 709, 716
single valued inverse map, 253

single-circuit homoclinic loop, 758
singularly perturbed system, 675
sink, 64
skeleton, 18
Smale horseshoe, 741, 885
small denominators problem, 102
small lobe condition, 662, 669
smooth annulus map, 631
smooth attractive invariant curve, 762
smooth attractive invariant manifold, 677, 762
smooth conjugacy theorem, 276
smooth diffeomorphism, 114
smooth dynamical system, 8
smooth foliation, 280, 453
smooth invariant closed curve, 239
smooth invariant curve, 616, 620, 631
smooth invariant foliation, 282
smooth invariant manifold, 79, 84
smooth leading saddle manifold, 84
smooth manifold, 419, 653
smooth torus, 665
soft birth of an invariant torus, 809
soft generation of an invariant cycle, 614
soft loss of stability, 600, 803, 805
solid torus, 407, 662
solution, 1
special trajectory, 17, 769
spectrum, 142
spiral attractor, 24
S-property, 409
stability boundaries, 451, 475, 531, 579, 604, 799, 800, 832
stability in the sense of Lyapunov, 202, 203
stability of the torus, 262
stability region, 270
stable complex equilibrium state, 469
stable eigen-subspace, 148
stable equilibrium state, 23, 65, 76, 126, 604, 677
stable fixed point, 614, 618, 648
stable focus, 600, 605
stable focus equilibrium state, 26, 32, 33, 45, 74, 76
stable focus fixed point, 123, 127
stable invariant curve, 618
stable invariant manifold, 132, 134, 142, 168, 261
stable invariant sub-manifold, 84
stable invariant subspace, 29, 46, 128
stable leading manifold, 128
stable leading subspace, 46
stable manifold, 161, 208, 414, 431, 446, 460, 485, 510, 605, 618, 634, 735
stable node (−), 127
stable node (+), 127
stable node equilibrium state, 25, 26, 27, 31, 33, 45, 75
stable node fixed point, 119, 120, 127
stable periodic orbit, 603, 629, 677
stable periodic trajectory, 111
stable solution, 202
stable subspace, 36, 119
stable topological node equilibrium state, 64
stable topological sink equilibrium state, 64
stable, 128
standard form, 453
stationary regime, 633
Sternberg theorem, 103, 212
straightening, 71, 162, 183, 278
strange attractor, 12, 24, 411, 412, 685, 751, 911
strong resonances, 500, 515, 612, 635
strong stability, 453, 460
strong stable foliation, 272, 279, 280, 284
strong stable invariant foliation, 272, 319
strong unstable invariant foliation, 282, 322

strongly resonant value, 499
strongly stable, 44, 126
strongly stable axis, 119
strongly stable invariant manifold, 137, 168, 280, 314
strongly stable invariant subspace, 126
strongly stable manifold, 431, 453, 478, 483, 485, 648, 725
strongly stable sub-manifold, 331
strongly unstable manifold, 746
strongly unstable sub-manifold, 327, 329
strong-stable foliation, 651, 662, 672
structural instability, 412, 435, 442, 446, 451, 556, 561, 632, 718
structural stability, 398, 419, 429, 446, 677, 719, 767, 843
structurally stable 24, 111, 115
structurally stable equilibrium state, 21, 24, 47, 56, 61, 63, 104, 262, 318
structurally stable fixed point, 133, 154, 168
structurally stable periodic point, 266
structurally stable periodic trajectories, 115, 135, 266
structurally stable saddle, 79
structurally unstable equilibrium point, 62, 109
structurally unstable, 284
subcritical Andronov-Hopf bifurcation, 605, 812, 880, 909
subcritical bifurcation, 600
sublinear estimate, 698
sub-manifolds, 84
supercritical Andronov-Hopf bifurcation, 603, 633, 674, 807, 891
supercritical bifurcation, 600
surfaces without contact, 456
swallowtail, 554, 633, 643
synchronization, 264, 430, 630, 645
systems of first degree of non-roughness, 430

tangential manifold, 84
the Bogdanov-Takens normal form, 820
the breakdown of the invariant manifold, 662
the disappearance of the saddle-node equilibrium, 640
the Duffing equation, 820
the essential map, 657
the first separatrix value, 695
the flight time function, 659
the Khorozov-Takens normal form, 820
the third critical case, 493
the uniqueness of the limit cycle, 712
time-reverse system, 5
topological classification, 56
topological conjugacy, 128, 129, 132, 169
topological equivalence, 394, 398, 440, 442, 446, 536
topological invariant, 430, 441
topological node, 134
topological saddles, 64, 134
topological type, 63, 133, 207, 414
topologically conjugate, 442
topologically conjugate fixed points, 133
topologically conjugate Poincaré map, 135
topologically eigenvalent system, 17, 59, 61, 96, 135
torus, 397, 618, 626, 627, 635, 665, 769, 887
trajectory, 7
trajectories (equivalent), 18
trajectory of the Poincaré map, 114
trajectory Poisson-stable, 9
trajectory special, 17
transcritical bifurcation, 558, 559

transfinite ordinal number, 402
transient regime, 801
transversality conditions, 354, 739, 746
transverse curve, 534
transverse family, 533, 537, 558, 561, 579, 608
transverse homoclinic trajectory, 422
triangular form, 272, 278
trigonometric Fourier series, 406
triple instability, 869
trivial resonance, 494, 497
truncated normal form, 110
turbulence, 633
twins, 405
two degeneracy regime, 645
two-dimensional invariant torus, 258
two-dimensional Poincaré map, 119
two-parameter family, 604, 633, 672
two-way heteroclinic connection, 782
types of the principal stability boundary, 803

unattainable from one side, 436
unique fixed point, 223, 225, 230, 247
unique invariant manifold, 73, 253
unique solution, 155, 245, 289
uniquely defined center manifold, 276
uniqueness, 712
unstable, 128
unstable complex focus, 469, 499
unstable direction, 121
unstable eigen-subspace, 148
unstable equilibrium state, 558
unstable fixed point, 116, 614, 620
unstable focus, 709
unstable focus equilibrium state, 30, 31, 34, 45, 78, 123
unstable focus fixed point, 123, 128
unstable heteroclinic cycle, 440
unstable invariant manifold, 132, 142, 261
unstable invariant sub-manifold, 84
unstable invariant subspace, 30, 46, 128
unstable Lamerey spiral, 118
unstable leading multipliers, 183
unstable manifold, 161, 182, 418, 446, 485, 603, 618, 634, 670, 734
unstable node equilibrium state, 30, 34, 45, 78, 119
unstable node fixed point, 119, 128
unstable non-leading manifold, 128
unstable non-leading subspace, 46
unstable separatrices, 507, 700, 814
unstable subspace, 36, 119
unstable topological node equilibrium state, 64
unstable topological source equilibrium state, 64
van der Pol equation, 236, 267, 630, 643, 820, 849, 901
variational equation, 2, 91, 92, 194
velocity field, 7
versal families, 445, 534, 536
vertical strip, 420

wandering point, 8, 399, 400, 405
wandering trajectory, 399
weak focus, 432, 470, 516, 801
weak resonance, 104, 493, 499, 515, 527, 634
weak saddle-focus, 497
weak, 406, 497
wedge, 551
Weierstrass's method, 270
Wietorius-van Danzig solenoid, 407, 408
Wronsky formula, 197

zebra pattern, 51
zero saddle value, 712

Bibliography

[*] This bibliography does not pretend to be complete and includes only references directly related to the content of this book. Besides, the references to some books that are particularly pertinent to the subject of this book are marked with an asterisk $*$.

[1] Afraimovich, V. S., Bykov, V. V. and Shilnikov, L. P. [1977] "The Origin and structure of Lorenz attractor," *Sov. Phys. Dokl.* **22**(5), 253–255.

[2] Afraimovich, V. S. and Shilnikov, L. P. [1973] "On critical sets of Morse–Smale systems," *Trans. Moscow Math. Soc.* **28**, 1761–1765.

[3] Afraimovich, V. S. and Shilnikov, L. P. [1974] "On some global bifurcations connected with the disappearance of fixed point of a saddle-node type," *Soviet Math. Dokl.* **15**, 1761–1765.

[4] Afraimovich, V. S. and Shilnikov, L. P. [1974] "On small periodic perturbations of autonomous systems," *Doclady AN SSSR* **5**, 734–742.

[5] Afraimovich, V. S. and Shilnikov, L. P. [1977] "The annulus principle and problems on interaction of two self-oscillation systems," *Prikladnaja Matematika i Mehanika* **41**, 618–627.

[6] Afraimovich, V. S. and Shilnikov, L. P. [1982] "On a bifurcation of codimension-one leading to the appearance of a countable set of tori," *Soviet Math. Dokl.* **25**, 101–105.

[7] Afraimovich, V. S. and Shilnikov, L. P. [1991] "Invariant tori, their breakdown and stochasticity," *Amer. Math. Soc. Transl.* **149**, 201–211.

[8] Andronov, A. A. [1933] "Mathematical problems of the theory of self-oscillations," in *All-Union Conference on Auto-oscillations*, November 1933 (GTTI: Moscow-Leningrad), 32–71.

[9] Andronov, A. A. and Leontovich, E. A. [1937] "Some cases of the dependence of the limit cycles upon parameters," *Uchenye zapiski Gorkovskogo Universiteta* **6**, 3–24.

[10] Andronov, A. A. and Leontovich, E. A. [1968] "Dynamical systems of first degree of roughness on the plane," *Am Math. Soc., Transl., II, Ser.* **75**, 149–199.

[11] * Andronov, A. A., Leontovich, E. A., Gordon, I. E. and Maier, A. G. [1971] *The Theory of Bifurcations of Dynamical Systems on a Plane* (Israel program of scientific translations, Jerusalem).

[12] * Andronov, A. A., Leontovich, E. A., Gordon, I. E. and Maier, A. G. [1973] *The Theory of Dynamical Systems on a Plane* (Israel program of scientific translations, Jerusalem).

[13] Andronov, A. A. and Pontryagin, L. S. [1937] "Systèmes grossières," *Dokl. Acad. Nauk SSSR* **14**(5), 247–251.

[14] Andronov, A. A. and Vitt, A. A. [1930] "Zur Theorie des Mitmehmens von van der Pol," *Archiv für Elektrotechnik*, Bd. XXIV, 99.

[15] Andronov, A. A. and Vitt, A. A. [1933] "On Lyapunov stability," *Zhurnal Eksperimental'noi i Teoreticheskoi Fisiki* **5**.

[16] Anosov, D. V., Bronshtejn, I. U., Aranson, S. Kh. and Grines, V. Z. [1988] *Smooth Dynamical Systems*, *Dynamical Systems I*, Encyclopedia of Mathematics Science I (Springer-Verlag: New York), 149–233.

[17] * Andronov, A. A., Vitt, A. A. and Khaikin, S. E. [1966] *Theory of Oscillations* (Pergamon Press: Oxford).

[18] Arneodo, A., Coullet, P., Spiegel, E. and Tresser, C. [1981] "Asymptotic chaos," *Physica* **D14**, 327–347.

[19] Arnold, V. I. [1973] "Lectures on bifurcations and versal families," *Recrs. Math. Surv.* **27**(5), 54–123.

[20] * Arnold, V. I. [1982] *Geometrical Methods in the Theory of Ordinary Differential Equations* (Springer-Verlag: New York).

[21] * Arnold, V. I., Afraimovich, V. S., Ilyashenko, Y. S. and Shilnikov, L. P. [1994] *Bifurcation Theory*, Dynamical Systems V. Encyclopaedia of Mathematical Sciences (Springer-Verlag: New York).

[22] Arnold, V. I. and Ilyashenko, Y. S. [1985] *Ordinary Differential Equations*, Dynamical Systems I. Encyclopaedia of Mathematical Sciences (Springer-Verlag: New York).

[23] Auslander, L., Green, L. and Hahn, F. [1963] "Flows on homogeneous spaces," *Annals of Mathematics Studies* **53** (Princeton University Press: Princeton, N.J.).

[24] * Bautin, N. N. [1949] *Behavior of Dynamical Systems near the Boundaries of Stability Regions* (OGIZ GOSTEHIZDAT: Leningrad).

[25] * Bautin, N. N. and Leontovich, E. A. [1976] *Methods and Rules for the Qualitative Study of Dynamical Systems of the Plane* (Nauka: Moscow).

[26] Bautin, N. N. and Shilnikov, L. P. [1980] "Suplement I: Safe and dangerous boundaries of stability regions," *The Hopf Bifurcation and Its Applications*, Russian translation of the book by Marsden, J. E. and McCracken, M. (Mir: Moscow).

[27] Belitskii, G. R. [1979] *Normal Forms, Invariants, and Local Mappings* (Naukova Dumka: Kiev).

[28] Belogui, J. A. [1981] *Module de estabilidade para campos vetoriais em variedades tridimensionais* (Ph.D. Thesis, I.M.P.A., Brazil).

[29] Belyakov, L. A. [1974] "A case of the degeneration of a periodic motion with homoclinic curves," *Math. Zametki* **15**, 336–341; [1980] "The bifurcation set in a system with a homoclinic saddle curve," *ibid.* **28**, 910–916; [1984] "Bifurcation of systems with homoclinic curve of a saddle-focus with saddle quantity zero," *ibid.* **36**, 838-843.

[30] Bendixson, J. [1901] "Sur les courbes definies par les equations differentielles," *Acta Math.* **24**.

[31] Birkhoff, G. D. [1927] "Dynamical systems," *Amer. Math. Soc., Colloquium Publications* **9**.

[32] Birkhoff, G. D. [1935] "Nouvelles recherche sur les systèmes dynamiques," *Memorie Pont Acad. Sci. Novi Lyncaei* **53**(1), 85–216.

[33] Bogdanov, R. I. [1975] "Versal deformations of a singular point on the plane in the case of zero eigenvalues," *Functional Analysis and Its Applications* **9**(2), 144–145.

[34] Bykov, V. V. [1978] "On the structure of a neighborhood of a separatrix contour with a saddle-focus," in *Methods of Qualitative Theory of Differential Equation* (Gorky: Gorky State University), 3–32; [1980] "On bifurcations of dynamical systems with a separatrix contour containing a saddle-focus," *ibid.* 44–72; [1988] "On the birth of a non-trivial hyperbolic set from a contour formed by separatrices of a saddle," *ibid.* 22–32.

[35] Bykov, V. V. [1993] "The bifurcations of separatrix contours and chaos," *Physica* **D62**, 290–299.

[36] Cartwright, M. L. and Littlewood, J. E. [1945] "On nonlinear differential equations of the second order, I: The equation $\ddot{y} + k(1 - y^2)\dot{y} + y = b\,\lambda\,k\cos(\lambda t + a)$, k large," *J. Lond. Math. Soc.* **20**, 180–189.

[37] Chenciner, A. [1981] "Courbes fermées invariantes non-normalement hyperboliques au voisinage d'une bifurcation de Hopf dégénerée de diffeomorphismes $\mathbb{R}^2$," *Comptes Rendus Acad. Sci. 292, Ser.* **1**, 507–510.

[38] Chow, S.-N., Deng, B. and Fiedler, B. [1990] "Homoclinic bifurcations of resonant eigenvalues," *J. Dyn. Diff. Eq.* **2**(2), 177–245.

[39] * Chow, S.-N. and Hale, J. [1982] *Methods of Bifurcation Theory* (Springer-Verlag: New York).

[40] * Chow, S.-N., Li, C. and Wang, D. [1994] *Normal Forms and Bifurcations of Planar Vector Fields* (Cambridge University Press: Cambridge).

[41] Chua, L. O. [1998] *CNN: A Paradigm for Complexity* (World Scientific: Singapore).

[42] de Melo, W. [1980] "Moduli of stability of two-dimensional diffeomorphisms," *Topology* **19**, 9–21.

[43] de Melo, W. and van Streen, S. J. [1987] "Diffeomorphisms on surfaces with finite number of moduli," *Erg. Theory Dynam. Systems* **7**, 415–462.

[44] Deng, B. [1993] "Homoclinic twisting bifurcations and cusp horseshoe maps," *J. Dyn. Diff. Eq.* **5**, 417–467.

[45] Diaz, L., Rocha, J. and Viana, M. [1996] "Strange attractors in saddle-node cycles: prevalence and globality," *Invent. Math.* **125**, 37–74.

[46] Doedel, E. [1997] "Nonlinear numerics," *Int. J. Bif. Chaos* **7**(9–10), 2127–2143.

[47] Dulac, H. [1923] "Sur les cycles limites," *Bull. Soc. Math. France* **51**, 45–188.

[48] Fenichel, N. [1971] "Persistence and smoothness of invariant manifolds for flows," *Indiana Univ. Math. J.* **21**, 193–226.

[49] Fink, A. M. [1974] *Almost Periodic Differential Equations*, Lecture Notes in Mathematics **377** (Springer-Verlag: Berlin, New York).

[50] Gambaudo, J. M., Glendinning, P. and Tresser, C. [1988] "The gluing bifurcation. I: Symbolic dynamics of the closed curves," *Nonlinearity* **1**(1), 203–214.

[51] Gavrilov, N. K. [1978] "On some bifurcations of an equilibrium state with one zero and a pair of purely imaginary roots," in *Methods of Qualitative Theory of Differential Equations* (Gorky State University: Gorky); [1987] "On bifurcations of equilibrium with one zero and pair of pure imaginary eigenvalues and additional degeneracy," *ibid.* 43–51.

[52] Gavrilov, N. K. and Roshchin, N. V. [1983] "On the stability of an equilibrium with one zero and a pair of pure imaginary eigenvalues," in *Methods of Qualitative Theory of Differential Equations* Leontovich–Andronova, ed., (Gorky State University: Gorky), 41–49.

[53] Gavrilov, N. K. and Shilnikov, A. L. [1996] "On a blue sky catastrophe model," Proc. Int. Conf. *Comtemp. Problems of Dynamical Systems Theory*, ed. Lerman, L. (Nizhny Novgorod State University: Nizhny Novgorod). [1999] "An Example of blue sky catastrophe," in *Ams Transl. Series II.* "Methods of qualitative theory of differential equations and related topics." (AMS, Providence, Rhode Island).

[54] Gavrilov, N. K. and Shilnikov, L. P. [1972] "On three-dimensional dynamical systems close to systems with a structurally unstable homoclinic curve I," *Math. USSR Sbornik* **88**(44), 467–485.

[55] Gavrilov, N. K. and Shilnikov, L. P. [1973] "On three-dimensional dynamical systems close to systems with a structurally unstable homoclinic curve II," *ibid.* **90**(1), 139–156.

[56] * Golubitsky, M. and Schaeffer, D. [1985] *Singularities and Groups in Bifurcation Theory I* (Springer-Verlag: New York).

[57] * Golubitsky, M., Stewart, I. and Schaeffer, D. [1988] *Singularities and Groups in Bifurcation Theory II* (Springer-Verlag: New York).

[58] Gonchenko, S. V. and Shilnikov, L. P. [1990] "Invariants of Ω-conjugacy of diffeomorphisms with a structurally unstable homoclinic trajectory," *Ukrainian Math. J.* **42**(2), 134–140.

[59] Gonchenko, S. V. and Shilnikov, L. P. [1993] "On moduli of systems with a structurally unstable homoclinic Poincaré curve," *Russian Acad. Sci. Izv. Math.* **41**(3), 417–445.

[60] Gonchenko, S. V., Turaev, D. V. and Shilnikov, L. P. [1993a] "On models with non-rough Poincaré homoclinic curves," *Physica* **D62**, 1–14.

[61] Gonchenko, S. V., Turaev, D. V. and Shilnikov, L. P. [1993b] "Dynamical phenomena in multi-dimensional systems with a structurally unstable homoclinic Poincaré curve," *Russian Acad. Sci. Dokl. Math.* **47**(3), 410–415.

[62] Gonchenko, S. V., Shilnikov, L. P. and Turaev, D. V. [1996] "Dynamical phenomena in systems with structurally unstable Poincaré homoclinic orbits," *Interdisc. J. Chaos* **6**(1), 1–17.

[63] Gonchenko, S. V., Sten'kin. O. V. and Turaev, D. V. [1996] "Complexity of homoclinic bifurcations and Ω-moduli," *Int. J. Bifurcation & Chaos* **6**(6), 969–989.

[64] * Guckenheimer, J. and Holmes, P. [1983] *Nonlinear Oscillations, Dynamical Systems, and Bifurcations of Vector Fields* (Springer-Verlag: New York), Series title: Applied Mathematical Sciences **42**.

[65] Guimond, L. S. [1999] "Homoclinic loop bifurcations on a Möbius band," *Nonlinearity* **12**(1), 59–78.

[66] Halanay, A. [1966] *Differential Equations; Stability, Oscillations* (Academic Press: New York) Series title: Mathematics in Science and Engineering **23**.

[67] Hale, J. and Kocak, H. [1991] *Dynamics and Bifurcations* (Springer-Verlag: New York).

[68] Hermann, M. [1971] "Mesure de Lebesgue et nombre de rotation," *Proc. Symp. Geometry Topology*, Lecture Notes in Mathematics, Vol. 597 (Springer-Verlag: New York), 371–295.

[69] Homburg, A. J. [1996] "Global aspects of homoclinic bifurcations of vector fields," *Memoirs of the A.M.S.* **578**.

[70] Homburg, A. J., Kokubu, H. and Krupa, M. [1994] "The cusp horseshoe and its bifurcations in the unfolding of an inclination flip homoclinic orbit," *Ergod. Th. Dynam. Syst.* **14**, 667–693.

[71] Homburg, A. J., Kokubu, H. and Naudot, V. [1997] "Homoclinic-doubling cascades," preprint.

[72] Homburg, A. J. and Krauskopf, B. [1998] "Resonant homoclinic flip bifurcations," preprint, Free University-Berlin.

[73] Ilyashenko, Yu. S. and Yakovenko, S. Yu. [1991] "Finite-smooth normal forms of local families of diffeomorphisms and vector fields," *Uspechi Mat. Nauk*, Vol. 46, **1**(277), 1–39.

[74] Ilyashenko, Yu. S. and Yakovenko, S. Yu. [1993] "Nonlinear Stokes phenomena in smooth classification problems," *Adv. Soviet Math.*, Vol. 14, 235–287.

[75] Khazin, L. G. and Shnol, E. E. [1991] *Stability of Critical Equilibrium States* (Manchester University Press).

[76] Khibnik, A. I, Kuznetsov, Y. A., Levitin, V. V. and Nikolaev, E. V. [1993] "Continuation techniques and interactive software for bifurcation analysis of ODE's and iterated maps," *Physica* **D62**(1–4), 360–371.

[77] Kisaka, M., Kokubu, H. and Oka H. [1993] "Bifurcations to N-homoclinic orbits and N-periodic orbits in vector fields," *J. Dyn. Diff. Eq.* **5**, 305–357.

[78] Kokubu, H., Komuro, M. and Oka, H. [1996] "Multiple homoclinic bifurcations from orbit flip. I. Successive homoclinic-doublings," *Int. J. Bif. Chaos* **6**, 833–850.

[79] Kokubu, H. and Naudot, V. [1997] "Existence of infinitely many homoclinic-doubling bifurcations from some codimension-three homoclinic orbits," *J. Dyn. Diff. Eq.* **9**, 445–462.

[80] Krauskopf, B. [1994] "Bifurcation sequences at 1:4 resonance: An inventory," *Nonlinearity* **7**(3), 1073–1091.

[81] Krylov, N. M. and Bogolyubov, N. N. [1947] *Introduction to Nonlinear Mechanics* (Princeton University Press: Princeton).

[82] * Kuznetsov, Yu. A. [1998] *Elements of Applied Bifurcation Theory* (Springer-Verlag: New York).

[83] Kuznetsov, Yu. A. and Levitin, V. V. [1996] "CONTENT: A multiplatform environment for analyzing dynamical systems" (Centrum voor Wiskunde en Informatica, Amsterdam), ftp.cwi.nl/pub/CONTENT.

[84] Levitan, B. M. and Zhikov, V. V. [1982] *Almost Periodic Functions and Differential Equations* (Cambridge University Press: Cambridge [Cambridgeshire]; New York).

[85] Leontovich, E. A. [1951] "On birth of limit cycles from separatrices," *DAN SSSR* **74**4, 641–644.

[86] Li, W. and Zhang, Z. F. [1991] "The "blue sky catastrophe" on closed surfaces," *Adv. Series Dynam. Syst.* **9** (World Scientific, River Edge, N.J.), 316–332.

[87] Lorenz, E. N. [1963] "Deterministic non-periodic flow," *J. Atmos. Sci.* **20**, 130–141.

[88] Lukyanov, V. [1982] "On bifurcations of dynamical systems with a separatrix loop to a saddle-node," *Diff. Eq.* (*Russian*) **58**, 1493–1506.

[89] Lyapunov, A. M. [1950] "Problème général de la stabilité du mouvement," *Ann. de la Faculté des Sciences de Toulouse* **9**, 203–474.

[90] Lyapunov, A. M. [1966] *Stability of Motion* (Academic Press: New York).

[91] Malkin, I. G. [1952] *Theory of Stability of Motion* (Washington, D. C., United States Atomic Energy Commission, Series title: Translation series: AEC-tr-3352).

[92] Markov, A. A. [1933] "Stabilitat im Liapunoffschen Sinne und Fastperiodizitat," *Math. Zeitschr.* **36**.

[93] Mayer, A. G. [1943] "On center trajectories and a Birkhoff problem," *Mat. Sbornik* **12**(1).

[94] Meyer, K. R. [1968] "Energy functions for Morse–Smale systems," *Anter. J. Math.* **90**(4), 1031–1040.

[95] Medvedev, V. S. [1980] "On a new type of bifurcations on manifolds," *Mat. Sbornik* **113**, 487–492.

[96] Naudot, V. [1996] "Bifurcations homoclines des champs de vecteurs en dimension trois," thesis, l'Université de Bourgogne, Dijon.

[97] Newhouse, S., Palis, J. and Takens, F. [1983] "Bifurcations and stability of families of diffeomorphisms," *Publ. Math. IHES* **57**, 5–71.

[98] * Nemytskii, V. V. and Stepanov, V. V. [1960] *Qualitative Theory of Differential Equations* (Princeton, N.J., Princeton University Press. Series title: Princeton Mathematical Series **22**).

[99] Nozdracheva, V. P. [1982] "Bifurcation of a noncoarse separatrix loop," *Differ. Equations* **18**, 1098–1104.

[100] Ovsyannikov, I. M. and Shilnikov, L. P. [1987] "On systems with a saddle-focus homoclinic curve," *Math. USSR Sb.* **58**, 557–574.

[101] Ovsyannikov, I. M. and Shilnikov, L. P. [1992] "Systems with a homoclinic curve of multi-dimensional saddle-focus type, and spiral chaos," *Math. USSR Sb.* **73**, 415–443.

[102] Palis, J. [1969] "On Morse–Smale dynamical systems," *Topology* **4**, 385–404.

[103] Palis, J. [1978] "A differentiable invariant of topological conjugacies and moduli of stability," *Asterisque* **51**, 335–346.

[104] Palis, J. and de Melo, W. [1982] *Geometric Theory of Dynamical Systems. An Introduction* (Springer-Verlag: New York).

[105] Palis, J. and Pugh, C. [1975] "Fifty problems in dynamical systems," *Lecture Notes in Mathematics* Vol. 486, 34–353.

[106] Palis, J. and Smale, S. [1969] "Structural stability theorem," preprint.

[107] Peixoto, M. M. [1962] "Structural stability on two-dimensional manifolds," *Topology* **1**, 101–120.

[108] Poincaré, H. [1903] "Sur l'equilibre d'une masses fluide animés d'un mouvement de rotation," *Acta Mathematica* **7**.

[109] Poincaré, H. [1885] "Sur les courbes définies par des équations différentielles," *J. de Math. Pures et Appl.* **1**, 167–244.

[110] Poincaré, H. [1903] *Figures d'equilibre d'une masse fluide* (Paris).

[111] Poincaré, H. [1921] "Analyse des travans de Henri Poincaré faite par luimeme," *Acta Mathematica* **38**, 36–135.

[112] Pontryagin, L. S. [1933] "Les fonctions presque périodiques et l'analysis situs," *C.R. Acad. Sci.* **196**(17), 1201–1203.

[113] Pugh, C. C. [1967] "The closing lemma," *Amer. J. Math.* **89**, 956–1009.

[114] Robinson, C. [1989] "Homoclinic bifurcation to a transitive attractor of Lorenz type," *Nonlinearity* **2**, 495–518.

[115] Robinson, C. [1992] "Homoclinic bifurcation to a transitive attractor of Lorenz type II," *SIAM J. Math. Anal.* **23**, 1255–1268.

[116] Roussarie, R. [1986] "On the number of limit cycles which appear by perturbation of separatrix loop of planar vector fields," *Bol. Soc. Math. Brasil* **17**(2), 67–101.

[117] Rychlik, M. R. [1990] "Lorenz attractors through Sil'nikov-type bifurcation. Part I," *Ergod. Th. Dynam. Syst.* **10**, 793–821.

[118] Sacker, R. [1964] "On invariant surfaces and bifurcations of periodic solutions of ordinary differential equations," *IMM-NUY* **333**, New York State University.

[119] Sanstede, B. [1993] "Verzweigungstheorie homokliner Verdopplungen," Ph.D. Thesis, Free University of Berlin, Institut für Angewandte Analysis und Stochastic, Report No. 7, Berlin.

[120] Sanstede, B. [1995] "Center manifold for homoclinic solutions," *Weierstrass Inst. Appl. Analysis Stochastic*, preprint N 186.

[121] Shashkov, M. V. [1994] "Bifurcations of separatrix contours," Ph.D. Thesis, Nizhny Novgorod State University.

[122] Shashkov, M. V. [1992] "On bifurcations of separatrix contours with two saddles," *Int. J. Bif. Chaos* **2**(4), 911–914.

[123] Shashkov, M. V. [1992] "On the bifurcations of separatrix contours on two-dimensional surfaces. I," *Selecta Math. Sovietica* **11**(4), 341–353.

[124] Shashkov, M. V. [1994] "On the bifurcations of separatrix contours on two-dimensional surfaces. II," *ibid.* **13**(2), 175–182.

[125] Shashkov, M. V. and Turaev, D. V. [1996] "On the complex bifurcation set for a system with simple dynamics," *Int. J. Bif. Chaos* **6**(5), 949–968.

[126] Shilnikov, A. L. [1990] "Qualitative and numerical analysis of Lorenz-like systems," Ph.D Thesis, Gorky State University.

[127] Shilnikov, A. L. [1993] "Bifurcations of the Lorenz attractors in the Morioka–Shimizu model," *Physica* **D62**, 338–346.

[128] Shilnikov, A. L., Nicolis, G. and Nicolis, C. [1995] "Bifurcation and predictability analysis of a low-order atmospheric circulation model," *Int. J. Bif. Chaos* **5**(6), 1701–1711.

[129] Shilnikov, A. L., Shilnikov, L. P. and Turaev, D. V. [1993] "Normal forms and Lorenz attractors," *Int. J. Bif. Chaos* **1**(4), 1123–1139.

[130] Shilnikov, L. P. [1963] "Some cases of generation of periodic motion from singular trajectories," *Math. USSR Sbornik* **61**(103), 443–466.

[131] Shilnikov, L. P. [1965] "A case of the existence of a denumerable set of periodic motions," *Sov. Math. Dokl.* **6**, 163–166.

[132] Shilnikov, L. P. [1967] "The existence of a denumerable set of periodic motions in four-dimensional space in an extended neighborhood of a saddle-focus," *Soviet Math. Dokl.* **8**(1), 54–58.

[133] Shilnikov, L. P. [1967] "On a Poincaré-Birkhoff problem," *Math. USSR Sbornik* **3**, 415–443.

[134] Shilnikov, L. P. [1968] "On the generation of periodic motions from trajectories doubly asymptotic to an equilibrium state of saddle type," *Math. USSR Sbornik* **6**, 427–437.

[135] Shilnikov, L. P. [1969] "On a new type of bifurcation of multi-dimensional dynamical systems," *Soviet Math. Dokl.* **10**, 1368–1371.

[136] Shilnikov, L. P. [1970] "A contribution to the problem of the structure of an extended neighborhood of a rough equilibrium state of saddle-focus type," *Math. USSR Sbornik* **10**, 91–102.

[137] Shilnikov, L. P. [1975] "Theory of the bifurcations of dynamical systems," *Math. Physics* **20**, 674–676.

[138] Shilnikov, L. P. [1981] "The bifurcation theory and quasihyperbolic attractors," *Uspehi Mat. Nauk* **36**, 240–241.

[139] Shilnikov, L. P. and Turaev, D. V. [1997] "Simple bifurcations leading to hyperbolic attractors," *Computers Math. Applic.* **34**(2–4), 173–193.

[140] Shilnikov, L. P. and Turaev, D. V. [2000] "A new simple bifurcation of a periodic orbit of blue sky catastrophe type," in AMS Transl. Series II. "Methods of qualitative theory of differential equations and related topics" (AMS, Rhode Island, Providence).

[141] Simonov, A. A. [1978] "An investigation of bifurcations in some dynamical systems by the methods of symbolics dynamics," *Sov. Math. Dokl.*, **19**, 759–763.

[142] Smale, S. [1960] "Morse inequalities for a dynamical system," *Bull. Amer. Math. Soc.* **66**, 43–49.

[143] Smale, S. [1963] "Diffeomorphisms with many periodic points," in *Diff. Combin. Topology*, ed. S. Cairus (Princeton University Press: Princeton), 63–86.

[144] Sotomayor, J. [1971] "Generic bifurcations of dynamical systems," in *Dynamical Systems Proc. Symp. Univ. Bahia*, Salvador, 561-582, Zbl.296.58007.

[145] Sotomayor, J. [1971] "Structural stability and bifurcation theory," in *Dynamical Systems Proc. Symp. Univ. Bahia*, Salvador, 549-560, Zbl.293.34081.

[146] Takens, F. [1974] "Singularities of vector fields," *Publ. Math. IHES* **43**, 47–100.

[147] Tresser, C. [1984] "About some theorems by L. P. Sil'nikov," *Ann. Inst. Henri Poincaré, Phys. Theor.* **40**, 441–461.

[148] Turaev, D. V. [1984] "On a case of bifurcations of a contour composed by two homoclinic curves of a saddle," in *Methods of Qualitative Theory of Differential Equations* (Gorky State University), 162–175.

[149] Turaev, D. V. [1991] "On bifurcations of dynamical systems with two homoclinic curves of the saddle," Ph.D. Thesis, Nizhny Novgorod State University.

[150] Turaev, D. V. [1996] "On dimension of nonlocal bifurcational problems," *Int. J. Bif. Chaos* **2**(4), 911–914.

[151] Turaev, D. V. and Shilnikov, L. P. [1987] "On bifurcations of a homoclinic "figure-eight" for a saddle with a negative saddle value," *Soviet Math. Dokl.* **44**(2), 422–426.

[152] Turaev, D. V. and Shilnikov, L. P. [1995] "On a blue sky catastrophe," *Soviet Math. Dokl.* **342**(5), 596–599.

[153] Turaev, D. V. and Shilnikov, L. P. [1998] "An example of a wild strange attractor," *Sbornik. Math.* **189**(2), 291–314.

[154] van der Pol, B. [1927] "Forced oscillations in a circuit with nonlinear resistance (receptance with reactive triode)," *London, Edinburgh and Dublin Phil. Mag.* **3**, 65–80 (Reprinted in Bellman and Kakaba [1964]).

[155] Van Strien, S. J. [1982] *On Parameter Families of Vector Fields. Bifurcations Near Saddle-connections*, Ph.D. Thesis, Utrecht University.

[156] * Wiggins, S. [1988] *Global Bifurcations and Chaos* (Springer-Verlag: New York).

[157] Eleonsky, V. M., Kulagin, N. E., Turaev, D. V. and Shilnikov, L. P. [1988] "On the classification of self-localized states of the electromagnetic field within nonlinear medium," DAN SSSR **309**(9) 898–852.

[158] Shashkov, M. [1999] "Impossibility of complete bifurcation description for some classes of systems with simple dynamics", Abstracts of Int. Conference, *Equadiff 99* (Berlin), 22.

[159] Shilnikov, L. P., Turaev, D. V. [1997] "Superhomoclinic orbits and multipulse homoclinic loops in Hamiltonion systems with discrete symmetries", Regular and Chaotic Dynamics **2**(3/4) 126–138.

[160] ∗ Ilyashenno, Y. Li, Weigu [1999] Nonlocal bifurcations. *Math. Surveys and Monographs* **66** (AMS, Rhode Island, Providence).

[161] Afraimovich, V., Bykov, V. V. and Shilnikov L. P. [1983] "On attracting structurally unstable sets of Lorenz attrcator type", *Trans. Moscow. Math. Soc.* **44**, 150–213.

[162] Arneodo, A. Couller, P. H. and Spiegel, E. A. [1985] "The dynamics of triple convection", *Geophys. Astrophys. Fluid Dynamics* **31**, 1–48.

[163] Arneodo, A. Coulle r, P. H., Spiegel, E. A. and Tresser, C. [1985] "Asymptotic chaos", *Physica* **14D**, 327–347.

[164] Back, A., Guckenheimer, J., Myers, M. R., Wicklin, F. J. and P. A. Worfolk [1992] "DsTool: Computer assisted exploration of dynamical systems", *Notices Amer. Math. Soc.* **39**(4), 303–309; ftp://cam.cornell.edu/pub/dstool/.

[165] Bautin, N. N. [1984] *Behavior of Dynamical Systems near the Boundaries of Stability Regions* (Nauka: Moscow).

[166] Belykh, V. N. [1980] Qualitative methods of the theory of nonlinear oscillations of concentrated systems, Gorky State Univerosity press: Gorky.

[167] Byragov, V. S. [1987] "Bifurcations in a two-parameter family of conservative mappings that are close to the Henon mapping", in *Methods of the Qualitative Theory of Differential Equations* (Gorky: Gorky State Univ. Press), 10–24.

[168] Bykov, V. V. [1998] "On bifurcations leading to chaos in Chua's circuit", *Int. J. Bifurcation & Chaos* **8**(4), 685–699.

[169] Bykov, V. V. and Shilnikov, A. L. [1992] "On boundaries of the region of existence of the Lorenz attractor", *Selecta Math. Sovietica* **11**(4), 375–382.

[170] Feigenbaum, M. [1978] "Quantative universality for a class of nonlinear transformations", *J. Statist. Phys.* **19**, 25–52.

[171] Gaspard, P. [1993] "Local birth of homoclinic chaos", *Physica* **D62**, 94–122.

[172] Gaspard, P. and Nicolis, G. [1983] "What can we learn from homoclinic orbits in chaotic dynamics?" *J. Stat. Phys.* **27**(1), 499–518.

[173] Glendenning, P. and Sparrow, C. [1984] "Local and global behavior near homoclinic orbits", *J. Stat. Phys.* **35**, 645–696.

[174] Glendenning, P. and Sparrow, C. [1985] "T-point: a codimension-two heteroclinic bifurcation", *J. Stat. Phys.* **43**, 479–488.

[175] Gonchenko, S. V. and Gonchenko, V. S. [2000] "On Andronov-Hopf bifurcations of two-dimensional diffeomorphisms with homoclinic tangencies", Preprint No. 556, WIAS, Berlin.

[176] Gonchenko, S. V. and Komlev, Yu. A [1988] "Bifurcations and chaos in a cubic map of the plane", in *Methods of Qualitative Theory of Diff. Equations* (Gorky University Press: Gorky), 33–39.

[177] Hindmarsh, J. L. and Rose, R. M. [1984] "A model of neuronal bursting using three cioupled first order differential equations", *Proc. R. Soc. Lond.* **B221**, 87–102.

[178] Khibnik, A. I., Kuznetsov, Yu. A., Levitin, V. V. and Nikolaev, E. V. [1993] "Continuation techniques and interactive software for bifurcation analysis of ODEs and iterated maps", *Physica* **62D**, 360–371.

[179] Khibnik, A. I., Roose, D. and Chua, L. O. [1993] "On periodic orbits and homoclinic bifurcations in Chua's circuit with smooth nonlinearity", *Int. J. Bifurcation & Chaos* **3**(2), 363–384.

[180] Krauskopf, B. and Osinga H. M. [1999] "Investigating torus bifurcations in the forced Van der Pol oscillator", in *Numerical Methods for Bifurcation Problems and Large-Scale Dynamical Systems* eds. E. J. Doedel, L. S. Tuckerman, IMA Volumes in Mathematics and its Applications **119**, Springer-Verlag, to appear.

[181] Osinga H. M. [1999] "Non-orientable manifolds of periodic orbits", *Proceedings of Equadiff 99*, Berlin, to appear.

[182] Kuznetsov, Yu. A. [1998] "CONTENT — integrated environment for analysis of dynamical systems Tutorial", Ecole Normale Superieure de Lyon, Rapport de Recherche UPMA-98-224; ftp://ftp.cwi.nl/pub/CONTENT.

[183] Lorenz, E. N. [1984] "Irregularity: A fundumental property of the athmosphere", *Tellus* **A36**, 98–110.

[184] Mira, C. [1987] *Chaotic Dynamics: From the One-dimensional Endomorphism to the Two-Dimensional Diffeomorphism.* (World Scientific: Singapore-New Jersey-Hong Kong).

[185] Pisarevskii, V., Shilnikov, A. L. and Turaev, D. V. [1998] "Asymptotic normal forms for equilibria with a triplet of zero charactersitic exponents in systems with symmetry", *Regular and Chaotic Dynamics* **3**(1), 19–27.

[186] Roschin, N. V. [1978] "Unsafe stability boundaries of the Lorenz model", *J. Appl. Math. Mech.* **42**(5), 1038–1041.

[187] Rucklidge, A. M. [1994] "Chaos in magnetoconvection", *Nonlinearity* **7**, 1565–1591.

[188] Rössler, O. [1976] "An equation for continuous chaos", *Phys. Lett.* **57A**, 397–398.

[189] Shilnikov, A. L. and Shilnikov, L. P. [1991] "On the nonsymmetric Lorenz model", *Int. J. Bifurcation & Chaos* **1**(4), 773–776.

[190] Shimizu, T. and Morioka, N. [1980] "On the bifurcation of a symmetric limit cycle to an asymmetric one in a simple model", *Phys. Lett.* **76A**, 201–204.

[191] Vladimirov A. G. and Volkov, D. Yu. [1993] *Optics Commun.* **100**, 351–360.